Mississippi Valley Division

US Army Corps of Engineers®

Mississippi River and Tributaries Flowline Assessment: Mississippi River Sedimentation Report

MRG&P Report No. 24; Volume 4 • December 2018

MRG&P
Mississippi River Geomorphology & Potamology Program

Report prepared for the Mississippi River Commission

Mississippi River Geomorphology &
Potamology (MRG&P) Program

MRG&P Report No. 24; Volume 4
December 2018

Mississippi River and Tributaries Flowline Assessment: Mississippi River Sedimentation Report

Ronald R. Copeland

Mississippi Valley Division
U.S. Army Corps of Engineers
1400 Walnut Street
Vicksburg, MS 39180

Report 4 of a series

Prepared for U.S. Army Corps of Engineers, Mississippi Valley Division
1400 Walnut Street
Vicksburg, Mississippi 39180

Under Project 449963, “Mississippi River and Tributaries Flowline Assessment”

Abstract

A numerical sedimentation model assessment was conducted to determine the effects of long-term sedimentation processes on the Project Design Flood (PDF) flowline for the Mississippi River. The assessment reach was between Pilots Station, which is located at the end of Southwest Pass in Louisiana, and Cairo, IL, which is located at the confluence of the Ohio River. In addition, the assessment determined the effects of scour and deposition, which occur during the passage of the PDF hydrograph, on maximum water-surface elevations. The HEC-6T numerical sedimentation model was used in this assessment.

The assessment identified a long-term degradation trend between Helena, AR, and Cairo, IL, and a long-term aggradation trend between Helena, AR, and Red River Landing, Louisiana. The numerical model was used to evaluate the effects of several driving variables on the long-term sedimentation trends. These variables included the effects of floods, sediment inflow, dikes, historical cutoffs, sea-level rise, and subsidence.

The assessment results provide 50-year increases in PDF water-surface elevations attributed to sedimentation in the Mississippi River. These results are to be added to water-surface elevations calculated using an unsteady flow HEC-RAS model that uses current surveys to define the HEC-RAS geometry.

Contents

Figures and Tables

Figures

Tables

Preface

The research documented in this report was conducted as part of the "Mississippi River and Tributaries Flowline Assessment"; Project 449963. The report is published through the Mississippi River Geomorphology and Potamology Program, which is sponsored by Headquarters, U.S. Army Corps of Engineers (USACE) and managed by the USACE Mississippi Valley Division (MVD) in Vicksburg, MS. The MVD Commander was MG Richard G. Kaiser. The MVD Director of Programs was Mr. Jim Bodron.

Unit Conversion Factors

Multiply	By	To Obtain
acres	4,046.873	square meters
cubic feet	0.02831685	cubic meters
cubic yards	0.7645549	cubic meters
degrees Fahrenheit	(F-32)/1.8	degrees Celsius
feet	0.3048	meters
inches	0.0254	meters
miles (U.S. statute)	1,609.347	meters
square feet	0.09290304	square meters
square miles	2.589998 E+06	square meters

1 Introduction

Objective

The primary purpose of this assessment was to determine the long-term effects of sedimentation processes on the Project Design Flood (PDF) flowline for the Mississippi River between Venice, LA, at River Mile (RM) 10.7 and the confluence of the Ohio River at RM 953.8, near Cairo, IL. In addition, the assessment determined the effects of scour and deposition, which occur during the passage of the PDF hydrograph, on maximum water-surface elevations. The HEC-6T numerical sedimentation model was used in this assessment, as were location labels in terms of 1962 RMs.

This report is one part of the overall MR&T Flowline Assessment Project. Table 1 lists the series of reports associated with the overall project, with this report listed in bold font.

Table 1. List of reports included in the overall project.

Report Name	Description
Executive Summary	The Executive Summary briefly summarizes the important information from the entire project assessment.
Main Report	The Main Report summarizes the results in each of the aspects of the entire project assessment and shows the combined effects of the PDF event scenarios.
Hydrology Report	The Hydrology Report assesses the flow of water arriving to the MR&T System during the PDF event scenarios.
Hydraulics Report	The Hydraulics Report assesses the water surface elevations in the Mississippi and Atchafalaya rivers during the PDF event scenarios.
Mississippi River Sedimentation Report	The Mississippi River Sedimentation Report assesses how the next 50 years of sedimentation are expected to change the Mississippi River channel; these changes would impact the water surface elevations expected during the PDF event in the future.
Atchafalaya River Sedimentation Report	The Atchafalaya River Sedimentation Report assesses how the next 50 years of sedimentation are expected to change the Atchafalaya River channel; these changes would impact the water surface elevations expected during the PDF event in the future.

Approach

The numerical model was also used to evaluate specific geomorphic variables to determine which are the most significant in forming the future character of the Mississippi River. The numerical model makes it possible to evaluate the effect of a single independent driving variable by varying that variable in the model and holding all others constant. Historical data mask the effect of individual variables because the driving variables act together at the same time. Effects evaluated included a significant reduction in sediment supply, dikes, cutoffs, sea-level rise, and subsidence.

Background

The Regional Model of the Mississippi River between Pilots Station (RM 18) and Cairo, IL, was used as the starting point in developing the Flowline Model. The Regional Model was completed in 2011 and is documented in a report entitled *Numerical Sedimentation Investigation, Mississippi River, Cairo to Pilots Station,* which is still under review. The cross-section geometry for the Regional Model was taken from 1988–1992 hydrographic surveys. The Regional Model had been calibrated to 2002 conditions (11 years). Modifications were made to the Regional Model to incorporate additional data collected after completion of the original study. Most notably, the new data included (1) flow diversion measurements at several distributaries downstream from New Orleans, LA, (2) flow diversion measurements from the controlled levee breach during the 2011 flood at Bird's Point, which is located at the head of the New Madrid Floodway, and (3) water-surface elevations from the 2011 flood. Enhancements from recent HEC-6T numerical model studies of the Mississippi River were also incorporated. The Regional Model was verified by simulating an additional 11 years through 2013.

The Flowline Model assessment simulated the 1991–2013 hydrograph to obtain an existing condition. These 2013 calculated conditions were then written to a new HEC-6T geometry and sediment file that was used as the initial condition for future predictions. Using the calculated 2013 geometry, the project flood peak water-surface elevations were determined using steady state discharges in the numerical model. Then, using the 2013 geometry for the initial condition, a 50-year hydrograph, followed by a steady-state run with the PDF peak discharges, was simulated. The difference in these two calculated water-surface elevations was taken to be

the difference in water-surface elevations due to sedimentation in the 50-year period.

The sedimentation assessment and the estimated 2016 PDF hydrograph assessment were conducted at the same time. To meet schedules, it was necessary to conduct the sediment assessment sensitivity analysis and geomorphic analysis using the 1955 PDF peak discharges. Initial results reported in this report relate to the 1955 PDF. Final results of water-surface differences relate to the estimated 2016 PDF.

2 Numerical Model Description

HEC-6T description

The HEC-6T one-dimensional (1D) numerical sedimentation model was used in this assessment (Thomas 2016). Thomas initiated development of this computer program at the U.S. Army Engineer District, Little Rock, in 1967. Further development at the U.S. Army Engineer Hydrologic Engineering Center by Thomas produced the widely used HEC-6 generalized computer program for calculating scour and deposition in rivers and reservoirs. Additional modification and enhancement to the basic program by Thomas and his associates at the U.S. Army Engineer Research and Development Center (ERDC) led to the HEC-6W program. The HEC-6T program used in this assessment is the product of additional modification and enhancement conducted by Thomas at Mobile Boundary Hydraulics (MBH) PLLC. Version H6TV51425eR_J01_160512 was used to make calculations in this assessment. The model is proprietary and can be obtained from MBH.

The HEC-6T program produces a 1D model that simulates the response of the riverbed profile to sediment inflow, bed-material gradation, and hydraulic parameters. The model simulates a series of steady-state discharge events, their effects on the sediment transport capacity at cross sections, and the resulting degradation or aggradation. The program calculates hydraulic parameters using a standard-step backwater method.

HEC-6T is a state-of-the-art program for use in mobile bed channels. The numerical model computations account for all the basic processes of sedimentation: erosion, entrainment, transportation, deposition, and compaction of the bed for the range of particle sizes found in the Mississippi River. The model calculates aggradation and degradation of the streambed profile over the course of a hydrologic event. It does not simulate bank erosion or natural adjustments in channel widths. When applied by experts using good engineering judgment, the HEC-6T program will provide good insight into the behavior of mobile bed rivers. Additional guidance related to model calibration, application, and interpretation can be found in the following references: *Sedimentation in Stream Networks* (Thomas 2016); *Chapter 14 - Computational Modeling of Sedimentation Processes* (Thomas and Chang 2008); and *Guidelines for the Calibration and Application of Computer Program HEC-6* (USACE-HEC 1992).

Model network

The New Orleans, Vicksburg, Memphis, and St. Louis Districts were each responsible for developing the Regional Model in their respective reaches of responsibility along the Mississippi River. The model's geometry is broken into 25 segments as shown in the network schematics in Figure 1 and Figure 2. The number of cross sections in each segment and the description of the segment boundaries are listed in Table 2.

Table 2. Description of HEC-6T segments.

Segment	Number of Cross Sections	Average Distance between Cross Sections (miles)	Description	1962 River Miles (RM)
1	133	2.0	Mississippi River - Pilots Station to Profit Island	-18.0 to 246.3
2	6	1.0	Mississippi River - Main Channel - Profit Island	246.9 to 251.8
3	6	0.4	Mississippi River - Chute Channel - Profit Island	246.8 to 248.6
4	27	2.0	Mississippi River - Profit Island to Tarbert Landing	253.0 to 306.3
5	72	1.8	Mississippi River - Tarbert Landing to Yazoo River	306.3 to 437.3
6	3	7.6	Yazoo River	1.5 to 16.7
7	81	1.8	Mississippi River - Yazoo River to Arkansas River	438.4 to 580.8
8	19	1.6	Arkansas River	0.6 to 29.0
9	9	2.2	Mississippi River - Arkansas River to White River	580.8 to 598.0
10	69	1.5	White River	0.0 to 100.0
11	45	1.6	Mississippi River - White River to St. Francis River	600.1 to 672.6
12	19	1.0	St. Francis River	0.5 to 17.7
13	38	2.7	Mississippi River - St. Francis River to Hatchie River	674.7 to 772.8
14	3	1.0	Hatchie River	0.1 to 2.0
15	18	2.7	Mississippi River - Hatchie River to Obion River	774.0 to 819.4
16	3	1.0	Obion River	0.1 to 2.0

Segment	Number of Cross Sections	Average Distance between Cross Sections (miles)	Description	1962 River Miles (RM)
17	35	2.6	Mississippi River - Obion River to Island 8	820.0 to 910.0
18	5	1.0	Mississippi River - East Loop Island 8	910.5 to 914.6
19	5	1.0	Mississippi River - West Loop Island 8	910.5 to 914.6
20	9	1.9	Mississippi River - Island 8 to Wolf Island	915.6 to 930.8
21	3	1.5	Mississippi River - East Loop Wolf Island	931.5 to 934.4
22	3	1.5	Mississippi River - West Loop Wolf Island	931.5 to 934.4
23	8	2.7	Mississippi River - Wolf Island to Cairo	934.4 to 953.0
24	37	1.0	Ohio River – Cairo to Metropolis	953.0 to 990.0
25	46	2.4	Upper Mississippi River - Cairo to Chester	0.8 to 109.9

Figure 1. Schematic of HEC-6T stream network in New Orleans and Vicksburg Districts.

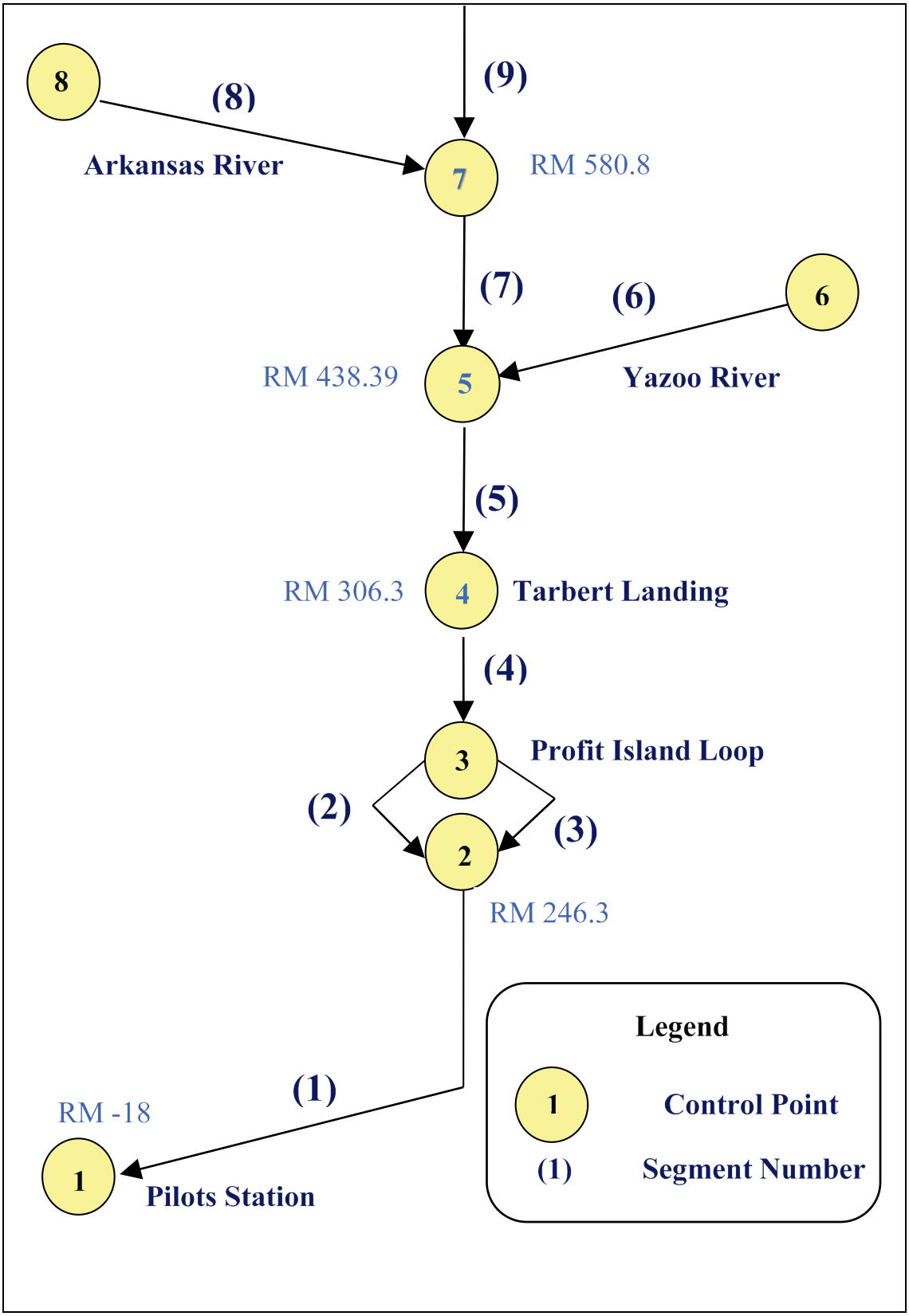

Figure 2. Schematic of HEC-6T stream network in Memphis and St. Louis Districts.

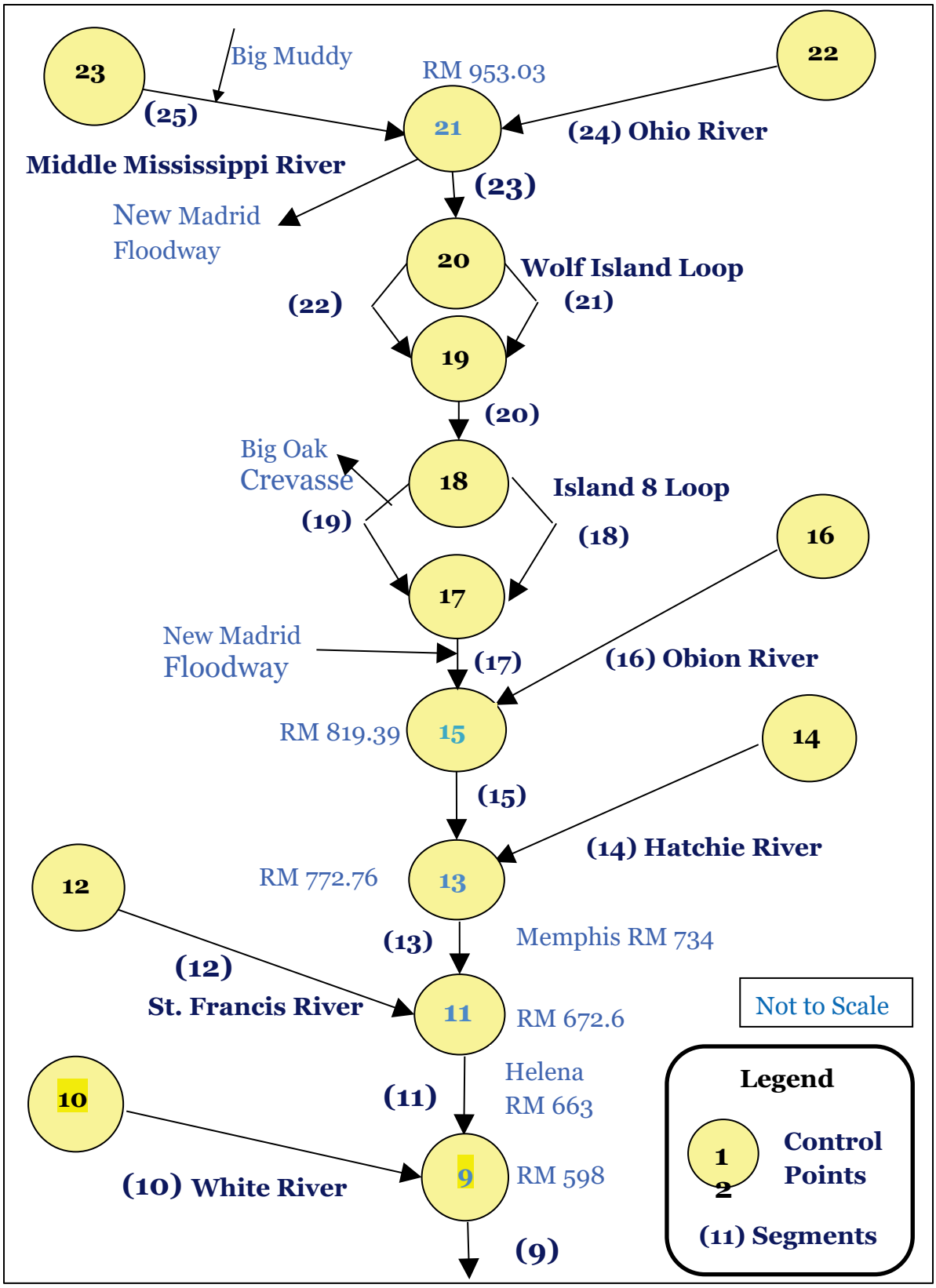

Channel geometry regional model

The cross-section geometry in the Regional HEC-6T model was developed from hydrographic survey data taken between 1988 and 1992. Survey datum was NGVD 1929. The hydrographic surveys were conducted at different times in the different districts. Even in the same district, surveys were taken in a sporadic pattern. One of the consequences of this anomaly is that direct comparisons between historical surveys at individual cross sections or even short reaches may be misleading. This factor makes model calibration to changes in surveyed bed volumes difficult and most likely unreliable.

Dike fields were included in the model by modifying hydrographic survey cross sections so that the projection of dike crest elevations obstructed conveyance in the channel. The Regional Model included dike fields constructed prior to 1992.

The cross sections are coded from left to right looking downstream and generally have reach lengths of 2 to 4 miles. Some cross-section distances are less than a half-mile in more complex areas of the river such as bends, dike fields, and crossings. Some cross section reach lengths are greater than 4 miles in reaches where it was difficult to find a representative cross section for 1D flow.

Reach lengths for the channel were measured between the thalwegs for each cross section. Reach lengths for the overbanks were measured from two-thirds of the length of the overbank between each cross section.

More detailed information about the survey data used to develop the cross sections in the Regional Model is provided in the Regional Model report, which is still under review.

Channel geometry flowline model

The geometry in this Flowline Model was updated to include additional features from recent studies. These studies had used the Regional Model as a starting point. The new models had an upstream boundary at Tarbert Landing (RM 306.3) and were developed to evaluate specific engineering designs. The Myrtle Grove study was conducted by Thomas (2012), for the State of Louisiana, and evaluated sedimentation issues related to a proposed diversion at Myrtle Grove. Another HEC-6T model was

developed by U.S. Army Corps of Engineers (USACE) ERDC (Sharp et al. 2013) to study sedimentation effects of the West Bay Diversion. This model used the Myrtle Grove study as a starting point. A third study was the *Mississippi River Hydrodynamic and Delta Management Study*[1]. The third study was the most recent, and the HEC-6T input file from that study (LMR1_FWOP_NRC1_Final_R19) was used as the primary reference for incorporating new information into the HEC-6T Flowline Model. These updates included (1) additional cross sections to reduce reach lengths, (2) revised diversion percentages at existing distributaries based on recent measurements, and (3) new diversions opened or discovered since completion of the Regional Model study (West Bay and Fort St. Philip).

The LMR1_FWOP_NRC1Final_R19 model included both datum and subsidence adjustments. The 1992 hydrographic survey geometry had been adjusted to NAVD88, and subsidence was calculated as the simulation progressed. These adjustments were not incorporated into the Flowline Model, which is based on the NGVD29 datum. The effect of subsidence was evaluated with the Flowline Model as part of the sensitivity analysis.

To facilitate the separation of South Pass and Pass a Loutre in the Flowline Model, cross sections at Head of Passes were modified. Cross sections -0.90, -0.50, and -0.01 were added to those used in the Regional Model using geometry from LMR1_FWOP_NRC1_Final_R19. Cross section -0.70 was removed from the Regional Model. The added cross sections were revised so that Regional Model dredging depths were retained.

Cross sections 10.7 and 11.5, from LMR1_FWOP_NRC1_Final_R19 were added to the Flowline Model. This was done to include the Venice gage and the Above-Venice discharge range in the model. Cross section 10.7 excluded dredging, which is consistent with the Regional Model. At RM 11.5, the bed sediment reservoir depth was changed to 1 foot (ft) from 0 ft to be consistent with other cross sections in the Regional Model.

Cross sections 18, 20, 27.8, 28.8, and 30.8 from LMR1_FWOP_NRC1_Final_R19 were added to the Flowline Model. This was done to reduce excessive distance between cross sections. The bed

[1] Thomas, William A., Michael J. Trawle, and Ronnie E. Heath. In preparation. *Executive Summary: Mississippi River Hydrodynamic and Delta Management Study, HEC-6T One-Dimensional Model Study*. Vicksburg, MS: U.S. Army Engineer Research and Development Center.

sediment reservoir depth was changed to 1 ft from 0 ft to be consistent with other cross sections in the Regional Model.

Cross sections 50.2, 51.6, 58.8, and 61.30 from LMR1_FWOP_NRC1_Final_R19 were added to the Flowline Model. This was done to reduce excessive distance between cross sections. At 50.2 and 51.5, the bed sediment reservoir depth was changed to 1 ft from 0 ft to be consistent with other cross sections in the Regional Model. The bed sediment reservoir depth of 5 ft at cross sections 58.8 and 61.8, from LMR1_FWOP_NRC1_Final_R19 Model, was used in the Flowline Model.

The Medora Dikes (RM 211-RM 213) are treated differently in the Regional Model and LMR1_FWOP_NRC1_Final_R19. The Regional Model inserts the dike geometry and assumes that the area between the dikes will be filled with sediment. Erosion and deposition are allowed only from the end of the dike to the opposite bank. LMR1_FWOP_NRC1_Final_R19 uses the geometry from before the dikes were built, allows deposition/erosion across the entire cross section, and dredges the channel between the end of the dike and the opposite bank. This works if there is no calculated erosion in the dike field below the crest elevation at any discharge. The Regional Model approach was retained in the Flowline Model.

The Redeye Dikes (RM 223–RM 225) are treated the same in both the Regional Model and LMR1_FWOP_NRC1_Final_R19. Deposition/erosion is confined to the channel between the end of the dike and the opposite bank. The LMR1_FWOP_NRC1_Final_R19 model included dredging.

Recent HEC-6T enhancements made it possible to change model geometry as the numerical simulation progressed. With this addition to the program, it was possible to add dikes during the 1992–2012 simulation as they were constructed. The locations of HEC-6T cross sections that are affected by dikes are listed in Table 3 through Table 5. Dikes listed in the tables with an absence of notation in the “Notes” column were in place in the initial 1992 geometry. If the dikes were raised, extended, or modified in some way, the year that the modifications were made is listed in the “Notes” column. If a dike was constructed between the years 1992–2012, the construction year is listed in the table. Plans were unavailable for a few dikes, and their notation is “Not in Model.” The 50-year projections were made with dikes constructed up to 2012.

Table 3. Dikes in New Orleans District Pilots Station (RM 18.) to Union Point (RM 326).

Cross Section	Dike Field	Descending River Bank	Constructed
-18.0	Southwest Pass	Left and Right	1908-1923
-16.5	Southwest Pass	Left and Right	1908-1923
-14.7	Southwest Pass	Left and Right	1908-1923
-13.3	Southwest Pass	Left and Right	1908-1923
-11.9	Southwest Pass	Left and Right	1908-1923
-10.7	Southwest Pass	Left and Right	1908-1923
-9.3	Southwest Pass	Right	1908-1923
-7.7	Southwest Pass	Right	1908-1923
-5.8	Southwest Pass	Right	1908-1923
-1.9	Southwest Pass	Right	1908-1923
211.6	Medora Dikes		1999
212	Medora Dikes		1999
212.2	Medora Dikes		1999
223.0	Red Eye Dikes		1994
224.1	Red Eye Dikes		1994
224.4	Red Eye Dikes		1994
297.45	Smithland Dikes		1990-1996
298.1	Smithland Dikes		1990-1996
298.9	Smithland Dikes		1990-1996
299.5	Smithland Dikes		1990-1996
300.3	Smithland Dikes		1990-1996

Table 4. Dikes in Vicksburg District Union Point (RM 326) to Rosedale (RM 592).

Cross Section	Dike Field	Descending River Bank	Notes
330.61	Jackson Point	Left	
337.00	Fritz Island	Right	
339.02	Buck Island	Left	Constructed 1994
346.81	Esperance Point	Right	1997 Modifications
349.00	Opposite Warnicott Landing	Left	Constructed 1995
351.12	Opposite Warnicott Landing	Left	1995 Modifications
352.98	Opposite Warnicott Landing	Left	
357.00	Natchez Island	Right	1991 and 1994 Modifications
357.00	Chute Blocked by Carthage Point Dikes	Left	Constructed 1994
358.63	Carthage Point	Left	Constructed 1992
358.63	Natchez Island	Right	
369.00	Opposite Riffle Point	Left	Constructed 1997
374.59	Chute Restricted by Waterproof Bar Dikes	Right	
377.00	Chute Restricted by Waterproof Bar Dikes	Right	
378.59	Waterproof Bar	Right	Modifications 1994
385.01	Spithead Towhead	Left	Modifications 1994
387.41	Chute Restricted by Browns Field Dikes	Right	
389.01	Cottage Bed	Left	
389.01	Browns Field	Right	
391.40	Chute Restricted by Browns Field Dikes	Right	
393.00	Bondurant	Right	Modifications 1991
394.61	Bondurant Towhead	Right	
398.80	Below Grand Gulf	Left	
401.21	Downstream from Coffee Point	Right	Constructed 1995
402.80	Coffee Point	Right	1995 Modifications
405.18	Upstream from Coffee Point	Right	1995 Modifications
407.62	Yucatan Cutoff Restricted by Closure Dike	Right	
409.03	Yucatan Cutoff Restricted by Closure Dike	Right	
411.2	Upstream from Yucatan	Right	Constructed 2013 – not in model
415.00	Togo Island	Left	
419.40	Newtown Bend	Right	Constructed 1995
422.41	Diamond Cutoff	Left	Constructed 1996

Cross Section	Dike Field	Descending River Bank	Notes
427.40	Below Racetrack	Left	Constructed 1997
429.20	Below Racetrack	Left	1996 Modifications
431.00	Below Racetrack	Left	1996 Modifications
432.00	Racetrack	Right	Constructed 1995
433.00	Racetrack	Right	Constructed 1996
438.39	Chute Restricted by Upstream Dikes	Right	
440.80	False Point	Right	2004 Modifications
447.20	Marshall Point Cutoff	Right	
448.79	Forest Home Towhead	Left	1997 Modifications
451.20	Forest Home Towhead	Left	1994 Modifications
453.01	Forest Home Towhead	Left	Constructed 1997
457.21	Below Belle Island	Left	Constructed 2010
460.80	Willow Cutoff	Right	
463.20	Willow Cutoff	Right	Constructed 1999
464.79	Tennessee Bar	Left	Constructed 2000
467.20	Tennessee Bar	Left	Constructed 1994
468.97	Arcadia Point	Left	
470.13	Arcadia Point	Left	2010 Modifications – not in model
470.13	Cottonwood	Right	
471.40	Arcadia Point	Left	2009 Modifications
477.20	Point Lookout	Right	
478.00	Point Lookout	Right	
481.06	Ajax Bar	Left	
483.00	Ajax Bar	Left	1997 Modifications
484.80	Ben Lomond	Left	
486.40	Ben Lomond	Left	
487.80	Ben Lomond	Left	
489.00	Ben Lomond	Left	2007 Modifications - not in model
490.80	Baleshed Landing	Left	2003 Modifications - not in model
492.69	Baleshed Landing	Left	1997 Modifications
494.59	Baleshed Landing	Left	
495.59	Cutoff Restricted by Wilson Point Dike 3-R	Right	
497.20	Cutoff Restricted by Wilson Point Dike 3-R	Right	

Cross Section	Dike Field	Descending River Bank	Notes
499.59	Wilson Point	Right	
502.80	Corregidor	Left	
504.66	Corregidor	Left	
507.29	Chute Restricted by Cracraft Dike	Right	
509.20	Cracraft	Right	
509.20	Caroline	Left	
510.00	Cracraft	Right	
512.80	Leota	Left	
512.80	Cracraft	Right	
515.03	Leota	Left	
515.03	Chute Restricted by Island 86 Dikes	Right	
516.60	Chute Restricted by Island 86 Dikes	Right	
518.21	Chute Restricted by Island 86 Dikes	Right	
518.21	Island 86	Right	1994 Modifications
521.19	Chute Restricted by Island 86 Dikes	Right	
522.76	Seven Oaks	Right	
524.40	Seven Oaks	Right	
524.40	Walnut Point	Left	2003 Modifications-not in model
526.00	Cutoff Restricted by Refuge Dikes	Left	
526.00	Anconia Chute Dike	Right	1997 Modifications
527.80	Cutoff Restricted by Refuge Dikes	Left	
529.20	Refuge	Left	
532.20	Island 84	Left	
532.20	Vaucluse Bendway Weirs	Right	Constructed 2001 – not in model
533.13	Island 84	Left	1994 Modifications
533.13	Vaucluse Bendway Weirs	Right	Constructed 2001 – not in model
535.17	Longitudinal Dikes	Right	Removed 1993
535.17	Warfield Point	Left	Constructed 1995
535.17	Island 84	Left	Constructed 1994
537.25	Leland Bar	Right	
538.56	Leland Bar	Right	
540.38	Leland Neck	Left	
540.38	Tarpley Cutoff Dikes	Right	2008 Modifications

Cross Section	Dike Field	Descending River Bank	Notes
543.21	Island 82 – Miller Bend	Right	
544.72	Island 82 – Miller Bend	Right/Left	
546.83	Ashbrook- Miller Bend	Right/Left	
549.00	Ashbrook Cutoff	Left	
560.00	Chute Restricted by Chicot Landing Dikes	Right	
562.40	Chute Restricted by Chicot Landing Dikes	Right	
565.19	Chute Restricted by Chicot Landing Dikes	Right	
569.03	Chute Restricted by Catfish Point Dikes	Left	
576.21	Chute Restricted by Below Prentiss Dikes	Left	
578.80	Below Prentiss	Left	1995 Modifications
584.86	Malone Field	Right	
589.07	Terrene	Left	
590.40	Terrene	Left	2003 Modifications
591.99	Montgomery Point Towhead	Right	2002 Modifications

Table 5. Dikes in Memphis District Rosedale (RM 592) to Cairo (RM 954).

Cross Section	Dike Field	Descending River Bank	Notes
600.10	Smith Point	Left	
602.95	Henrico	Right	1991 Modifications
604.92	Island 70	Left	Constructed 1993
606.00	Island 70	Left	
607.17	Island 70	Left	
610.94	Below Knowlton	Right	
613.60	Below Knowlton	Right	
614.58	Below Knowlton	Right	
616.07	Below Knowlton	Right	
621.03	Island 67	Left	
623.12	Below Ludlow	Left	
627.10	Sunflower	Left	
631.05	Rescue Landing	Left	Constructed 1996
637.91	Island 62	Right	
637.91	Chute Restricted by Closure Dike	Left	
639.73	Island 62	Right	
648.47	Kangaroo Point	Right	
649.00	Kangaroo Point	Right	1998 Modifications
651.91	Friars Point	Left	
654.23	Chute Restricted by Upstream Dike	Right	1998 Modification
656.21	Montezuma Towhead	Right	1999 Modifications
658.06	Montezuma Bar	Left	
666.01	Chute Restricted by Closure Dike	Right	
666.01	Prairie Point	Right	
667.00	Chute Restricted by Closure Dike	Right	
667.00	Prairie Point	Right	
668.22	Prairie Point	Right	
668.22	Flower Lake	Left	
670.00	St. Francis Towhead	Left	
676.20	Below Walnut Bend	Right	1997 Modifications
681.00	Bordeaux Point	Left	1993 Modifications
681.00	Walnut Bend	Right	Constructed 1997

Cross Section	Dike Field	Descending River Bank	Notes
682.06	Walnut Bend	Right	Constructed 1997
682.06	Bordeaux Point	Left	1993 Modifications
691.40	Chute Restricted by Commerce Dike	Left	
692.43	Commerce	Left	
696.80	Porter Lake	Right	2004 Modifications
700.28	Porter Lake	Right	
702.30	Porter Lake	Right	
704.08	Pickett	Left	1997 Modifications
704.08	Seypple	Right	Constructed 1997
707.79	Norfolk-Star	Left	Constructed 2008
707.79	Cat Island	Right	Constructed 2009
710.60	Cat Island	Right	2002 Modifications
711.00	Cat Island	Right	2002 Modifications
719.67	Armstrong	Right	
723.85	Dismal Point	Right	
726.67	Dismal Point	Right	Constructed 1998
735.90	Hopefield Point	Right	
736.48	Hopefield Point	Right	Constructed 1992
737.00	Robinson Crusoe	Right	
738.00	Robinson Crusoe	Right	
738.95	Robinson Crusoe	Right	
738.95	Loosahatchie Bar	Right	
740.00	Robinson Crusoe	Right	
740.00	Sycamore Chute	Right	Constructed 1994
741.00	Above Loosahatchie	Left	1994 Modifications
741.00	Sycamore Chute	Right	Constructed 1994
744.98	Randolph Point	Left	
748.94	Poker Point	Right	1994 Modifications
748.95	Shelby Forrest	Left	Constructed 1997
752.98	Corona Bar	Right	
756.97	Densford	Left	2014 Modifications - not in model
766.90	Below Richardson Landing	Left	
770.60	Randolph	Left	Constructed 2005

Cross Section	Dike Field	Descending River Bank	Notes
770.60	Lookout Bar	Right	2007 Modifications
772.76	Lookout Bar	Right	Constructed 2002
772.76	Lookout Bar	Right	2007 Modifications
774.00	Hatchie	Left	Constructed 2003
774.00	Sunrise Towhead	Right	Constructed 2006
783.50	Plum Point	Left	
784.00	Plum Point	Left	1994 Modifications
788.13	Keyes Point	Left	1995 Modifications - not in model
788.13	Island 30	Right	Constructed 1995
790.00	Keyes Point	Left	
792.10	Keyes Point	Left	
792.10	Kat Aubrey	Right	
796.01	Ashport Goldust	Right	
800.04	Forked Deer	Left	
803.84	Island 25	Right	
807.79	Nebraska Point	Left	
812.44	Below Tamm Bend	Left	
818.00	Wrights Point	Right	
819.39	Wrights Point	Right	
820.80	Wrights Point	Right	
823.46	Chute Restricted by Island 21 Dike	Left	
828.24	Head of Island 21	Left	1994 Modifications
831.72	Island 20	Right	1998 Modifications
835.86	Island 18 Towhead	Left	
839.82	Caruthersville - Linwood Bend	Right	
841.50	Tennemo	Left	
841.50	Caruthersville - Linwood Bend	Right	2004 Modifications
844.20	Caruthersville - Linwood Bend	Right	
846.40	Opposite Caruthersville	Left	
847.96	Sandy Hook Dike #2	Right	
851.97	Hathaway	Left	
851.97	Robinson Bayou	Right	
864.70	Below Cherokee	Left	

Cross Section	Dike Field	Descending River Bank	Notes
869.08	Steward Towhead	Right	1999 Modifications
872.40	Steward Towhead	Right	
873.04	Ruddles Point Dikes	Right	
874.20	Ruddles Point Dikes	Right	
880.00	Island 11	Right	
881.89	Island 11	Right	
885.40	Kentucky Point	Left	
886.40	Kentucky Point	Left	1993 and 2001 Modifications
887.20	Kentucky Point	Left	1993 and 2001 Modifications
888.20	Chute Restricted by Dike	Left	1993 and 2001 Modifications
895.00	Hotchkiss Bend	Right	
899.27	Donaldson Point	Right	Constructed 2004
899.27	Below Island 9	Left	2000 Modifications
903.45	Donaldson Point	Right	
905.60	Donaldson Point	Right	2003 Modifications
914.60	Below Island 7 and 8	Right	2003 Modifications
915.59	Below Island 7 and 8	Right	
925.00	Below Williams	Left	
927.50	Moore Island	Right	1997 and 2006 Modifications
934.40	Wolf Island Weir	Left	Constructed 1995
944.75	Island No. 1	Left	
944.75	Pritchard Dikes	Right	
947.40	Island No. 1	Left	
949.00	Island No. 1	Left	

Hydrographs

Discharge hydrographs are simulated in the numerical model by a series of steady-state events. The duration of each event is chosen such that the changes in bed elevation, due to deposition or scour, do not significantly change the hydraulic parameters during that event. In this assessment, computational time-steps of 1 day were used. A 1-day time-step is not necessary to meet the requirement of insignificant bed change but was chosen for convenience because available data were reported as mean daily flows.

The approach used in HEC-6T approximates unsteady flow by stepping through a time sequence of steady discharges. This method does not take into consideration flow routing or backwater storage effects, introducing the potential for timing issues in flow propagation through the model. Thus, HEC-6T may not be appropriate for predicting flood hydrographs and stages, but experience has shown that it is successful in predicting long-term sedimentation processes.

Reported daily discharges are available at several gages within the study area. Uncertainty is associated with the choice of discharge data for the inflow hydrograph because there are discrepancies in the reported data. Continuity of the discharge record is inconsistent with both time and distance. Discrepancies in reported average mean daily discharges, between October 1990 and September 2013, at various points on the Mississippi River, are shown in Table 6. The average mean daily discharges for the 23-year period, shown in Table 6, were calculated from U.S. Geological Survey (USGS) or USACE-reported mean daily discharge data. The 23-year mean daily discharge at Thebes on the Mississippi River above Cairo is approximately 4% greater than the combined mean daily discharges for the Mississippi River at Chester and from the Big Muddy River. Big Muddy discharges had to be estimated from upstream gages, and local inflow could account for some of the difference. The 23-year reported mean daily discharge at Hickman is approximately 3.5% less than the combined reported flow from the Ohio River and the Mississippi River at Thebes, minus the outflow at Birds Point. The Birds Point outflow was calculated in HEC-6T using a rating curve based on 2011 USGS measurements. The mean daily discharge was averaged over the 23-year period, recognizing that the only year with outflow at Birds Point was 2011. The 23-year reported mean daily discharge at Memphis is approximately 3.5% greater than the sum of the mean daily discharges from the Mississippi River at Hickman, the Obion and Hatchie Rivers, and the 2011 inflow from the New Madrid Floodway, minus the 2011 outflows at Big Oak Crevasse (Crevasse No. 1). The increase at Memphis tends to balance out the decrease at Hickman. There is approximately a 1% loss in mean daily discharge at Helena when compared to the sum of Memphis and St. Francis River flows. The 23-year mean daily discharge passing Arkansas City is approximately 1% less than the sum of the mean daily discharges from the Mississippi River at Helena and the White and Arkansas Rivers. There is approximately a 2.5% increase in mean daily discharge at Vicksburg when compared to the sum of Arkansas City and Yazoo River flows. This increase helps to balance out the decrease

recorded at Helena and Arkansas City. Flow past Vicksburg and Natchez is relatively consistent. The largest discrepancy is at the Old River Diversion Structure where the sum of reported discharges in the Old River Outflow Channel and in the Mississippi River at Tarbert Landing is approximately 4.5% higher than the reported discharge upstream at Natchez and Vicksburg.

Table 6. Reported 1991–2013 mean daily discharge passing Mississippi River and Tributary gages.

	Reported Average Annual Mean Daily Discharge 1000 cfs	Discrepancy with Reported Upstream Gage(s)		
		1000 cfs	%	Notes on Discrepancy Calculation
Chester	237.0			
Big Muddy River	0.8			
Thebes	246.9	9.1	3.83	Thebes = Chester + Big Muddy
Ohio River	298.0			
Birds Point Crevasse	0.5			Calculated from USGS measurements
Hickman	525.8	-18.6	-3.42	Hickman = Thebes + Ohio - Birds Point
Big Oak Crevasse	0.1			Calculated from USGS measurements
New Madrid Floodway	0.7			Calculated from USGS measurements
Obion River	3.4			
Hatchie River	3.7			
Memphis	553.2	19.7	3.69	Memphis = Hickman – Big Oak + New Madrid + Obion + Hatchie
St. Francis River	6.3			
Helena	554.0	-5.5	-0.98	Helena = Memphis + St. Francis
White River	30.3			
Arkansas River	49.8			
Arkansas City	627.1	-7.0	-1.10	Arkansas City = Helena + White + Arkansas
Yazoo River	18.1			
Vicksburg	661.1	15.9	2.46	Vicksburg = Arkansas City + Yazoo
Natchez	662.2	1.1	0.17	Natchez = Vicksburg
Old River Outflow	159.3			
Tarbert Landing	533.2	30.3	4.58	Tarbert Landing = Natchez – Old River Outflow
Total		45.0		

The discrepancies between reported discharges are not consistent annually. As shown in Table 7, there is an annual variation in the discrepancies between Natchez and Old River and Vicksburg and Natchez. The differences between Vicksburg and Natchez are insignificant, but the differences between Natchez and Old River are puzzling. These discrepancies at Old River produce a conundrum with respect to determining a hydrograph for the HEC-6T model.

Table 7. Annual discrepancy in recorded discharges at gages.

Water Year	Mean Annual Flow (cfs)		Discrepancy	Mean Annual Flow (cfs)	Discrepancy
	Tarbert+C39*	Natchez	Natchez/ Tarbert+C39	Vicksburg	Vicksburg/Natchez
1991	775,973	710,782	8.4%	720,087	-1.3%
1992	567,992	544,152	4.2%	548,801	-0.9%
1993	950,403	872,373	8.2%	886,602	-1.6%
1994	817,121	807,858	1.1%	809,301	-0.2%
1995	672,033	629,302	6.4%	612,695	2.6%
1996	673,667	585,902	13.0%	587,385	-0.3%
1997	849,170	749,047	11.8%	751,032	-0.3%
1998	752,027	679,636	9.6%	679,671	0.0%
1999	700,016	638,434	8.8%	638,328	0.0%
2000	426,175	427,524	-0.3%	416,737	2.5%
2001	555,901	523,638	5.8%	519,355	0.8%
2002	695,422	651,952	6.3%	665,697	-2.1%
2003	649,492	605,962	6.7%	616,508	-1.7%
2004	685,139	635,481	7.2%	645,596	-1.6%
2005	701,797	676,948	3.5%	682,081	-0.8%
2006	406,762	403,920	0.7%	396,292	1.9%
2007	616,545	638,307	-3.5%	630,790	1.2%
2008	846,169	804,268	5.0%	799,308	0.6%
2009	695,614	696,099	-0.1%	672,233	3.4%
2010	875,167	885,645	-1.2%	878,661	0.8%
2011	799,482	795,681	0.5%	801,581	-0.7%

Water Year	Mean Annual Flow (cfs)		Discrepancy	Mean Annual Flow (cfs)	Discrepancy
	Tarbert+C39*	Natchez	Natchez/ Tarbert+C39	Vicksburg	Vicksburg/Natchez
2012	540,380	563,048	-4.2%	559,203	0.7%
2013	673,517	704,731	-4.6%	687,531	2.4%

*C39 = Old River Outflow Channel

The HEC-6T hydrographs used in the Flowline Assessment were based on data from upstream boundary gages and did not include adjustments to tributary inflows to match downstream gages. This approach maintains the beneficial effect of simulating the correct timing of tributary contributions but does not account for differences in measured discharges in upstream and downstream gages. (A more detailed discussion of attempts to reproduce recorded discharges at gages in the Memphis District by adjusting tributary inflows is discussed in the Regional Model Report.)

Lag was not accounted for in the HEC-6T inflow hydrograph. Ignoring lag was deemed a reasonable simplification because tributary inflow downstream from Cairo is a minor fraction of the total inflow from the Ohio and Middle Mississippi Rivers. Differences in reported and calculated average mean daily discharges between 1991 and 2013 are listed in Table 8. Calculated discharges for the Old River Outflow Channel and Tarbert Landing are about 6% less than the reported discharges. This is consistent with comparisons of the reported gage data differences between Natchez and Tarbert Landing.

Table 8. Difference in reported and calculated average mean daily discharge passing Mississippi River gages, 1991–2013.

	Reported Average Mean Daily Discharge 1000 cfs	Calculated Average Mean Daily Discharge 1000 cfs	Difference as a Percentage of Calculated
Thebes	246.9	244.4	-1.01
Hickman	525.8	541.1	+2.90
Memphis	553.2	548.7	-0.81
Helena	554.0	554.8	+0.14
Arkansas City	627.1	635.0	+1.26
Vicksburg	661.1	653.1	-1.22

	Reported Average Mean Daily Discharge 1000 cfs	Calculated Average Mean Daily Discharge 1000 cfs	Difference as a Percentage of Calculated
Natchez	662.2	653.1	-1.39
Old River Outflow	159.3	150.0	-6.20
Tarbert Landing	533.2	503.1	-5.98

The Flowline Model hydrograph incorporates additional discharge data that became available after completion of the Regional Model study. New data were available for the Yazoo, Arkansas, White, St. Francis, Hatchie, and Obion Rivers.

Middle Mississippi River

The inflow boundary conditions for the Middle Mississippi River hydrographs were determined from USGS gages Mississippi River at Chester, IL (07020500), located at RM 109; Mississippi River at Thebes, IL (07022000), located at RM 43; and Big Muddy River at Plumfield, IL (05597000). Data were available at all three gages between 1 Oct 1987 and 30 Sep 2014. One would expect the sum of Plumfield and Chester discharges to equal the Thebes discharge. However, due to unsteady flow effects, storage, downstream contributions from the watersheds, and measurement errors, this is not the case. Therefore, a systematic method was adopted to assign upstream boundary conditions. The Flowline Model used the same methodology that was used in the Regional Model. Mean daily inflow from the Big Muddy was taken to be the difference in the reported discharges at Thebes and Chester or the reported discharge at Plumfield if the Thebes minus Chester difference was less than the reported value at Plumfield. The reported discharge at Chester was compared to the difference in the reported discharge at Thebes and the adopted Big Muddy discharge. The maximum of these was adopted for the upstream boundary. This methodology tends to maximize the discharge from the gage data.

Ohio River

The inflow boundary conditions for the Ohio River hydrograph were determined from the USGS gage Ohio River at Metropolis, IL (03611500), located at Ohio RM 943 (approximately 38 miles upstream from the Mississippi River confluence). Data were available at Metropolis between 1 Oct 87 and 30 Sep 2014.

Yazoo River

The Yazoo River hydrograph was developed using data from the USACE gage Yazoo River at Greenwood at RM 166, and USGS gages, Yazoo River at Redwood (07288800) at RM 16.7 and Yazoo River below Steele Bayou near Long Lake (07288955) at RM 9.5. Calculated mean daily discharges for the Yazoo River between 1 Oct 1987 and 30 Sep 1995 were estimated by correlation to the Greenwood gage. An average ratio of Steel Bayou to Greenwood mean daily discharges was determined using the 1995–2003 record. During this time period, daily discharges were reported at both gages. The correlation ratio was 1.7144. Mean daily discharges for the Yazoo River between 1 Oct 1995 and 30 Sep 2011 were taken from reported data at the Steel Bayou gage. No correlation to Greenwood was necessary for this time period. Mean daily discharges for the Yazoo River between 1 Oct 2011 and 22 Mar 2014 were taken from reported data at the Redwood gage. No correlation to Greenwood was necessary for this time period. Linear interpolation was used to determine discharge for days with missing data. The maximum data gap at Steele Bayou was 5 days and at Redwood the maximum data gap was 4 days.

Arkansas River

The hydrograph for the Arkansas River was determined using data from the USGS gage Murray Dam near Little Rock (07263450), located at RM 141.5, and the USACE (D02) gage at Dam No. 2, which is located at approximate RM 33. The drainage area above the Murray Dam gage is 158,138 square miles, and above the Dam No. 2 gage the drainage area is 160,475 square miles, so there is negligible local inflow. It was determined that the smallest standard deviation in the mean daily flow ratios of the two gages data occurred when Murray Dam flows were lagged one day. Daily data were available at the USGS gage between 2 Jul 1969 and 30 Sep 2014. Daily data were available at the USACE gage between 2 Jul 1969 and 31 Aug 2012, with some daily data missing. No data were available at Dam No. 2 after 31 Aug 2012. The HEC-6T hydrograph for the Arkansas River was based primarily on the Dam No. 2 data, with the Murray Dam data and linear interpolation used to fill data gaps. The maximum data gap at Dam No. 2 that was filled by linear interpolation was only 7 days. This corresponds to approximately 0.98% of the hydrograph at Dam No. 2. When gate closures at Dam No. 2 caused a severe discontinuity in the mean daily discharge from one day to the next, the gage data were modified to reduce the chance of inducing

numerical instabilities to the numerical solution. The smoothing was achieved by a combination of linear regression across days when flow was significantly reduced and transferring lagged discharges from the Murray Dam gage. These smoothing modifications were associated with low flow events and did not significantly affect the total runoff. These modifications resulted in a change in total runoff of less than 0.1%. Modifications are documented in Arkansas River.xlsx. Possible effects of hydropower operations were not considered.

The hydrograph at Dam No. 2 after 31 Aug 2012 was estimated using Murray Dam flows increased by a constant ratio. The ratio was determined by dividing the runoff from the Arkansas River at Dam No.2 between 2 Jul 1969 and 31 Aug 2012, by the runoff from the Arkansas River at Murray Dam for the same time period. The Dam No. 2 data included the previously described data gap filling adjustments.

White River

The White River inflow hydrograph was based on calculated mean daily discharge data from USACE data, in Hydrologic Engineering Center Data Storage System (HEC-DSS) format, for the gage White River at Clarendon (WR116), located at RM 99.1. Data were available from this gage between 1 Oct 1987 and 31 Dec 2014. Linear interpolation was used to determine discharge for days with missing data. The maximum data gap at Clarendon was 7 days.

St. Francis River

The St. Francis River inflow hydrograph was based on calculated mean daily discharge data from USACE DSS data for the gage St. Francis River at Riverfront, located at RM 58.0. Data were available from this gage between 1 Oct 1987 and 31 Dec 2011. Discharges on days with missing data were determined using linear interpolation. The maximum data gap at Riverfront was 38 days. Calculated mean daily discharges for the St. Francis River between 1 Jan 2012 and 30 Sep 2014 were estimated by correlation to the USACE Hatchie River at Rialto gage. An average ratio of Riverfront to Rialto mean daily discharges was determined using the 1988–2011 record. During this time period, daily discharges were reported at both gages. The correlation equation was Riverfront = Hatchie * 1.731.

Hatchie and Obion Rivers

The Hatchie River inflow hydrograph was based on calculated mean daily discharge data from the USACE DSS gage at Rialto, TN (HA 116), located at RM 34.0. USACE data were available between 1 Oct 1987 and 31 Dec 2014. Discharges on days with missing data were determined using linear interpolation or data from the USGS gage at Rialto, TN (07030050). The maximum data gap at Rialto was 15 days. Most of the days with missing data were between June and December 2001.

The Obion River inflow hydrograph was based on calculated mean daily discharges from USACE DSS gage Obion River at Bogota, TN (OB 113), located at RM 36.7 and Obion River at Obion (OB112), located at RM 62.4. At Bogota, data were available from 1 Oct 1987 through 31 Dec 2014. Discharges on days with missing data were determined using linear interpolation or were correlated to USACE DSS data from the At-Obion gage. The correlation required that At-Obion data were available for the days when data were missing at the Bogota gage. A correlation ratio was then computed using the known average ratio of measured data from the day preceding and the day following the missing data. Some days with missing data in the DSS file, where linear interpolation was inappropriate, and At-Obion data were unavailable, were supplied by Memphis District. The maximum data gap filled by linear interpolation was 15 days. The maximum data gap filled by correlation to the At-Obion gage was 74 days. The maximum data gap filled by Memphis District was 15 months.

50-year hydrograph

The projected 50-year hydrograph was developed from historical data. The 1991–2013 hydrograph was followed by the 1988–2014 hydrograph. The 2011 high water hydrograph occurred two times during the 50-year simulation. The 1988–2014 hydrographs at Memphis, Vicksburg, and Tarbert Landing are shown in Figure 3.

Figure 3. 1988–2014 hydrographs.

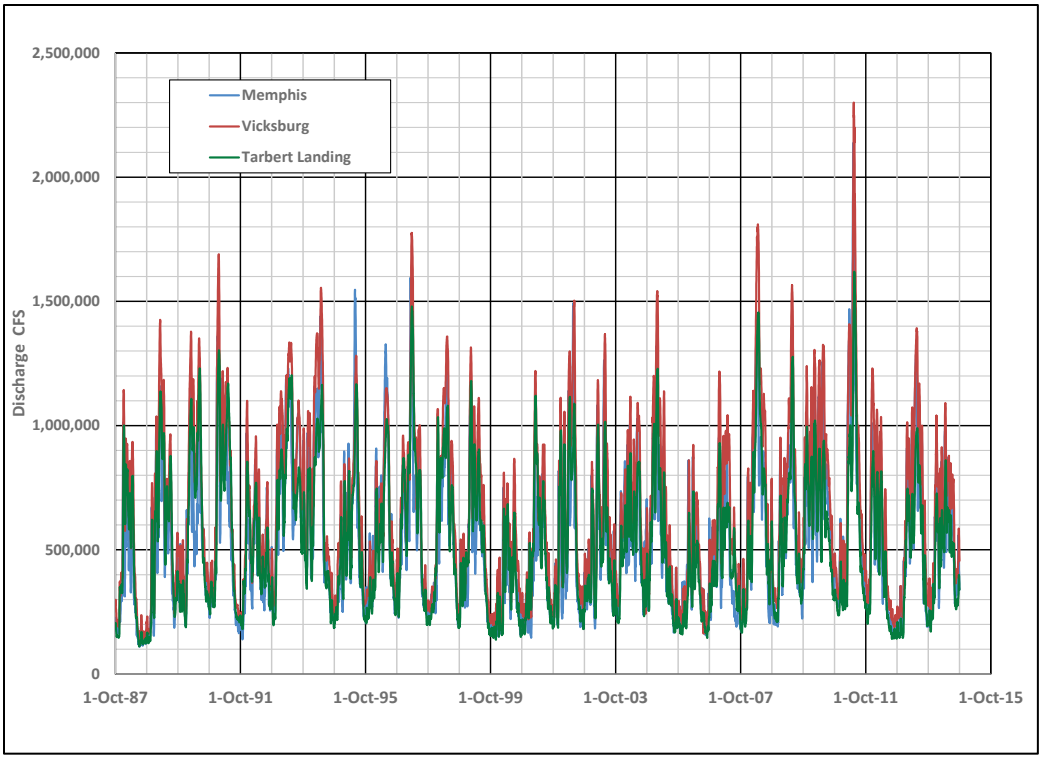

Project Design hydrograph

Peak discharges for the 1955 PDF, labeled 58A-EN, were used initially to calculate the difference in peak water-surface elevations due to 50 years of sedimentation processes in the Mississippi River between Pilots Station and Cairo. The hydrograph from this flood was used to calculate differences in water-surface elevations due to sedimentation processes during the passage of a major flood. The 1955 PDF peaks were also used to evaluate the influence of various geomorphic driving variables on Mississippi River geomorphic trends.

The PDF hydrograph was in the process of being evaluated during the early stages of the sedimentation assessment. Peak discharges are significantly greater with the estimated 2016 PDF. Peak discharges for the 1955 and estimated 2016 PDFs are compared in Table 9. The estimated 2016 PDF peaks were used to re-calculate the difference in peak water-surface elevations due to 50 years of sedimentation processes. However, the PDF estimate was not used to re-evaluate geomorphic trends.

Table 9. HEC-6T PDF peak discharge.

	1962 RM	Design 1955 PDF 1000 cfs	HEC-6T 1955 PDF 1000 cfs	HEC-6T 2016 Estimated PDF 1000 cfs
Middle Mississippi River	953.0	240	142	422
Ohio River	953.0	2,250	2,220	2,369
Below Cairo	953.0	2,362	2,362	2,791
Downstream from Birds Point	949.0	1,910	1,812	1,932
Downstream from New Madrid	889.0	2,410	2,362	2,819
Memphis	734.4	2,410	2,412	2,856
Helena	663.0	2,410	2,462	2,776
Arkansas City	554.1	2,890	2,892	3,250
Vicksburg	435.7	2,710	2,712	2,966
Coochie	317.3	2,720	2,712	2,966
Red River Landing	302.4	2,100	2,075	2,344
Downstream from Morganza	210.8	1,500	1,500	1,743
Downstream from Bonnet Carré	127.1	1,250	1,250	1,493
Above Venice	11.5		1,128	1,222
Above Head of Passes	0.7		648	695
Pilots Station	-18.0		273	289

Distributary flows at Fort St. Philip and downstream

Distributary flow distribution percentages used in the Regional Model were updated in the Flowline Model to incorporate additional data collected after completion of the Regional Model study. Significant data were collected in the distributaries below Venice, including the diversion at West Bay, which was opened in 2004 and was not included in the Regional Model. The distributary at Fort St. Philip (RM 20) was also added to the Flowline Model.

The distributary diversion reference stations on the Regional Model input file records were updated to the new HEC-6T usage. This makes the Flowline Model more consistent with LMR1_FWOP_NRC1_Final_R19.

The following paragraphs describe the development of distributary flow percentages used in the Flowline Model. For completeness, the descriptions include cases when the original Regional Model input was retained.

Distributary diversions in Southwest Pass

The Southwest Pass flow diversion percentages from the Regional Model were used in the Flowline Model. The flow percentage in Burrwood Bayou was based on nine measurements taken in 2003–2005. The data showed no apparent trend between the diversion percentage and the Southwest Pass discharge, so a constant value of 12% was used. The flow diversion percentages at the other distributaries were assumed to vary directly with the ratio of the width of each distributary gap to the width at Burrwood Bayou (continuity principle). Southwest Pass diversion percentages used in the Regional Model and the Flowline Model are listed in Table 10.

Table 10. Outflow from Southwest Pass distributaries percentage of discharge immediately upstream from diversion.

Distributary	1962 RM	Discharge Upstream from Distributary (cfs)			
		10,000	300,000	400,000	500,000
Burrwood Bayou	-14.4	12%	12%	12%	12%
Outlet W-2 and Overbank Flows	-9.8	7%	7%	10%	19%
Joseph Bayou	-4.5	12%	12%	12%	12%
Southwest Pass at Mile 3.0 West	-3.0	4%	4%	4%	4%

There are differences in the Southwest Pass diversion percentages used in the Regional Model and LMR1_FWOP_NRC1_Final_R19. At Burrwood Bayou, for instance, only 1% was diverted when the Southwest Pass discharge was less than 140,000 cfs and 12% when the discharge was greater than 180,000 cfs. The difference is not significant at Outlet W-2 where the lower diversion percentages only occur when Southwest Pass discharges are less than 20,000 cfs. The difference at Joseph Bayou is significant where the lower flow diversions occur when discharges are less than 200,000 cfs. Significant differences also occur at RM 3.0 for discharges less than 210,000 cfs. It is recommended that additional flow measurement programs be established to better define the outflow from distributaries and possible changes in outflow magnitudes with time.

South Pass and Pass a Loutre

Diverted flow out of South Pass and Pass a Loutre was separated in the Flowline Model to be consistent with the Myrtle Grove and LMR1_FWOP_NRC1_Final_R19 models. The index station for the Head of Passes distributaries was changed to Pilottown (RM 2.46).

Uncertainty related to the magnitude of flow distribution percentages out of Pass a Loutre and South Pass has been reduced as more flow measurements have been obtained. In the Regional Model, flow distribution percentages out of Pass a Loutre and South Pass were based on six measurements taken between 1996 and 2002. Flow distribution percentages in the Myrtle Grove and the LMR1_FWOP_NRC1_Final_R19 models were based on 36 data sets taken between 1979 and 2006. An additional 40 data sets, taken between 2007 and 2012, were used to develop flow distribution percentages for the Flowline Model. The data sets typically included measured discharges at Pilottown, Pass a Loutre, South Pass, and Southwest Pass. Data sets that failed a continuity test by more than 10% were excluded from the analysis. Comparisons of the assigned flow distributions used in the three models to measured combined discharges out of Pass a Loutre and South Pass are shown in Figure 4.

Figure 4. Combined diversion percentages at Pass a Loutre and South Pass used in the three model studies.

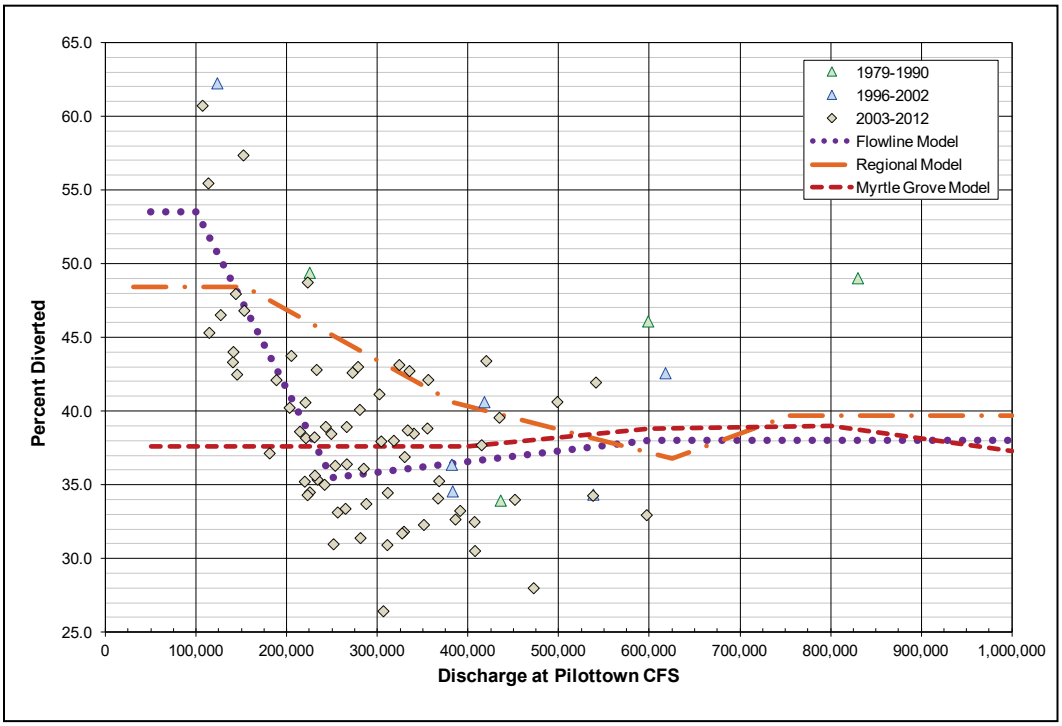

The Pass a Loutre and South Pass flow diversion percentages adopted for the Flowline Model were based on data collected between 1990 and 2012. Two linear regression curves were developed for both distributaries: one for data when the discharge at Pilottown was less than 250,000 cfs and the other for data when the discharge at Pilottown was greater than 250,000 cfs. Adopted flow distribution percentages are shown in Figure 5, Figure 6, and in Table 11. The flow diversion percentages were varied between a discharge range of 100,000 cfs and 600,000 cfs, which is within the range of data collected. Beyond these limits the flow diversion percentage was held constant rather than extrapolated.

The sediment diversion coefficients from the Regional Model were retained.

Table 10. Distributary outflow – Pass a Loutre and South Pass percentage of Pilottown discharge.

Distributary	1962 RM	Discharge at Pilottown (cfs)				
		50,000	100,000	250,000	600,000	1,000,000
South Pass	-0.01	26.5%	26.5%	18.0%	20.0%	20.0%
Pass a Loutre	.78	27.0%	27.0%	17.5%	18.0%	18.0%

Figure 5. Percent of Pilottown flow diverted at Pass a Loutre – variation with discharge 1990–2012.

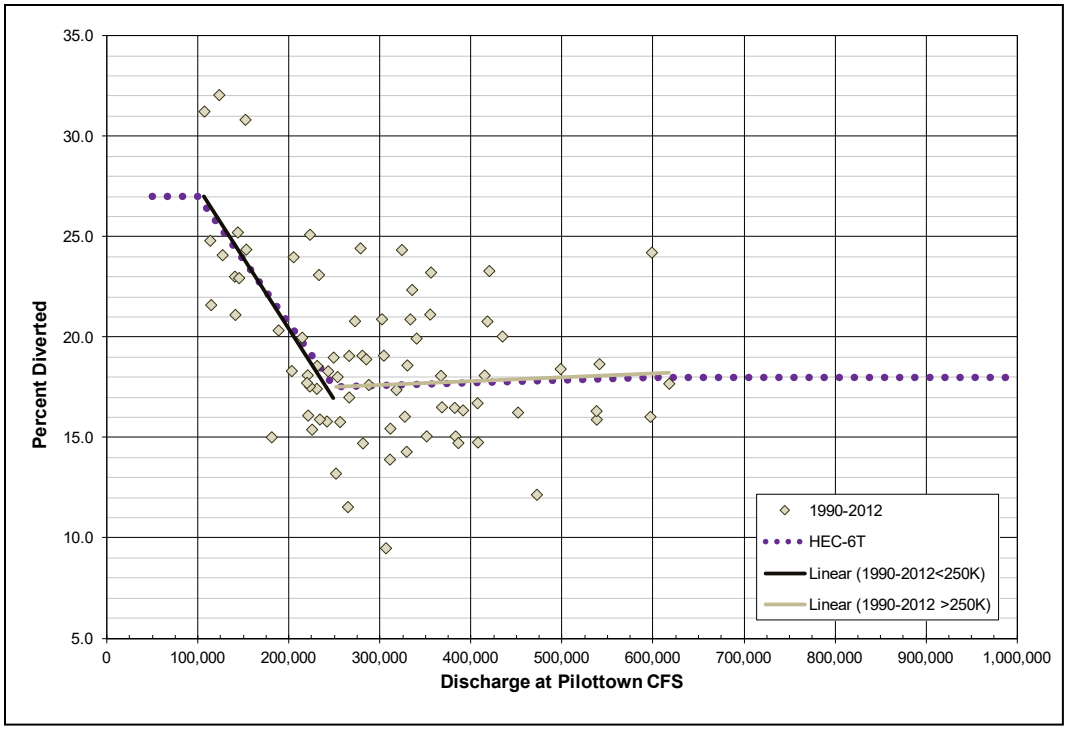

Figure 6. Percent of Pilottown flow diverted at South Pass – variation with discharge 1990–2012.

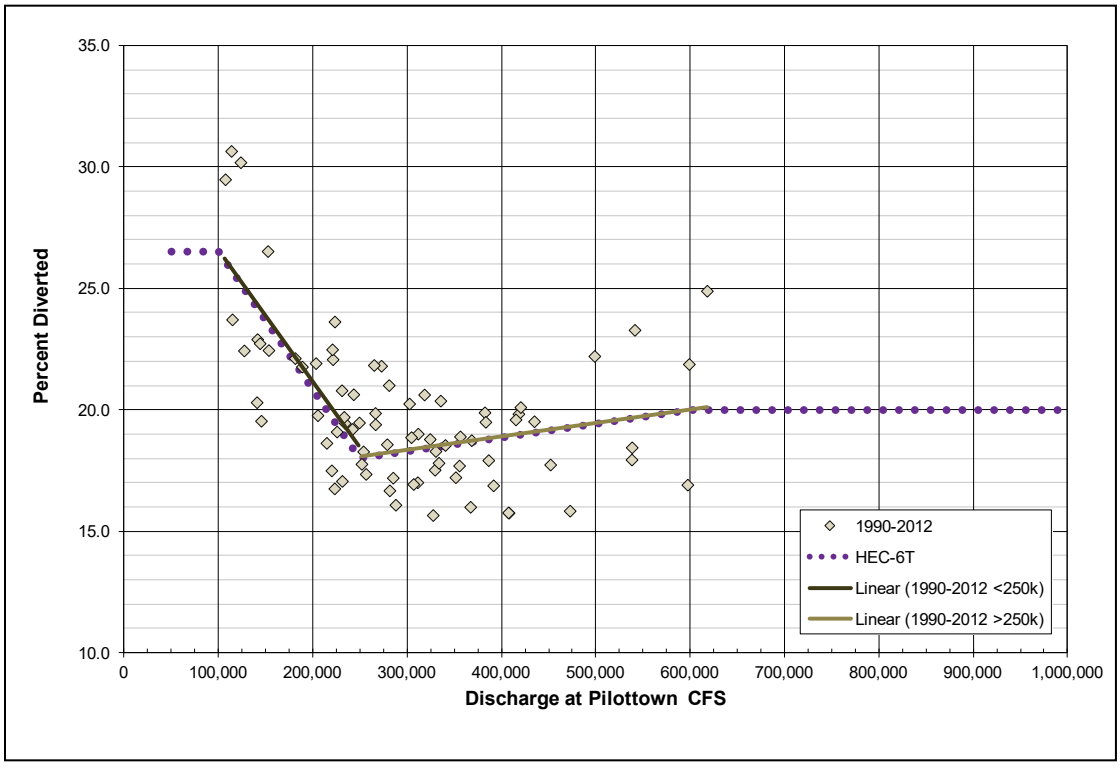

Cubits Gap

The Regional Model combined the distributary flows at Cubits Gap with overbank flows in the vicinity of Cubits Gap into a single outflow point. The Flowline Model separates outflow through Cubits Gap from overbank discharges that occur at high flow. This approach was adopted in the Myrtle Grove and the LMR1_FWOP_NRC1_Final_R19 models. The overbank flows are labeled as "Leaks." Diversion percentages for "Leaks" were incorporated from LMR1_FWOP_NRC1_Final_R19 at RM 2.46 (RM 1.97 in LMR1_FWOP_NRC1_Final_R19). These percentages were developed from a mass continuity analysis of measurements in the Mississippi River above Venice and at Pilottown and in the major diversions in between. The outflow at "Leaks" was assumed to be the missing variable that balanced the continuity equation. Overbank flow begins to occur at discharges above 600,000 cfs. The linear rating curve has a diversion percentage of 3.3% at 800,000 cfs and 10.9% at 1,000,000 cfs and above. The upstream cross section is the index station for "Leaks."

Measured diversion percentages for Cubits Gap were determined using 1991–2012 measurements in Cubits Gap and measurements upstream from Cubits Gap. After 2004, the discharge upstream from Cubits Gap was calculated by subtracting measured West Bay Diversion discharge from measured discharge in the Mississippi River above West Bay. Prior to 2004 the discharge upstream from Cubits Gap was calculated by subtracting the measured Grand Pass and Baptiste Collette discharges from the measured discharge in the Mississippi River at Above-Venice. Linear regression lines through the measured data (Figure 7 and Figure 8) indicate that there are no significant trends in the flow diversion percentage at Cubits Gap with either time or discharge. An average percentage of 17.4% was calculated from all the data, and a constant diversion percentage was used in the Flowline Model. This approach is different from that used in LMR1_FWOP_NRC1_Final_R19, which varied diversion percentage at Cubits Gap with discharge and used Above-Venice (RM 11.5) as the index station. LMR1_FWOP_NRC1_Final_R19 diversion percentages varied between 12.79% at 200,000 cfs and 16.56% at 1,000,000 cfs. (Note: comment in LMR1_FWOP_NRC1_Final_R19.T5 says that the index station was moved to Above Cubits Gap in November 2011; however, the HEC-6T input file indicates an index station at RM 11.5.)

Sediment diversion coefficients for “Leaks” were taken from LMR1_FWOP_NRC1_Final_R19. The sediment diversion coefficients at Cubits Gap were retained from the Regional Model.

Figure 7. Cubits Gap diversion percentages as a function of time.

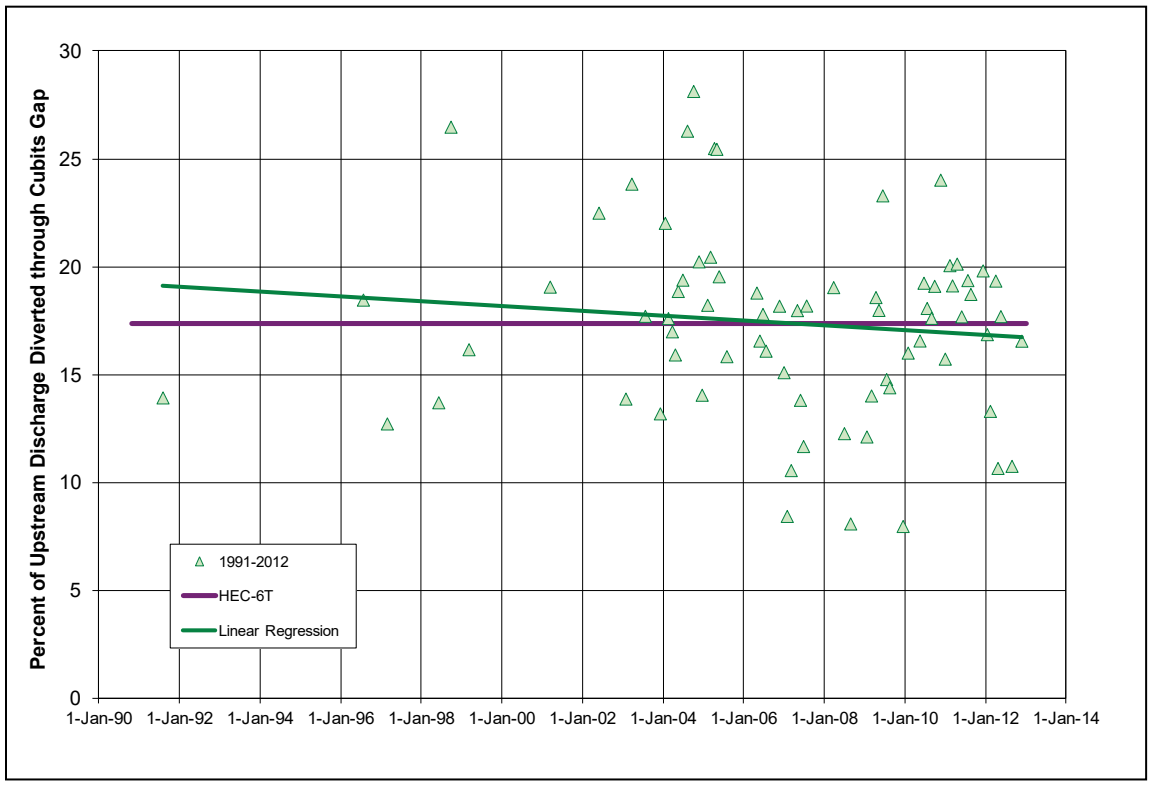

Figure 8. Cubits Gap diversion percentages as a function of Mississippi River discharge.

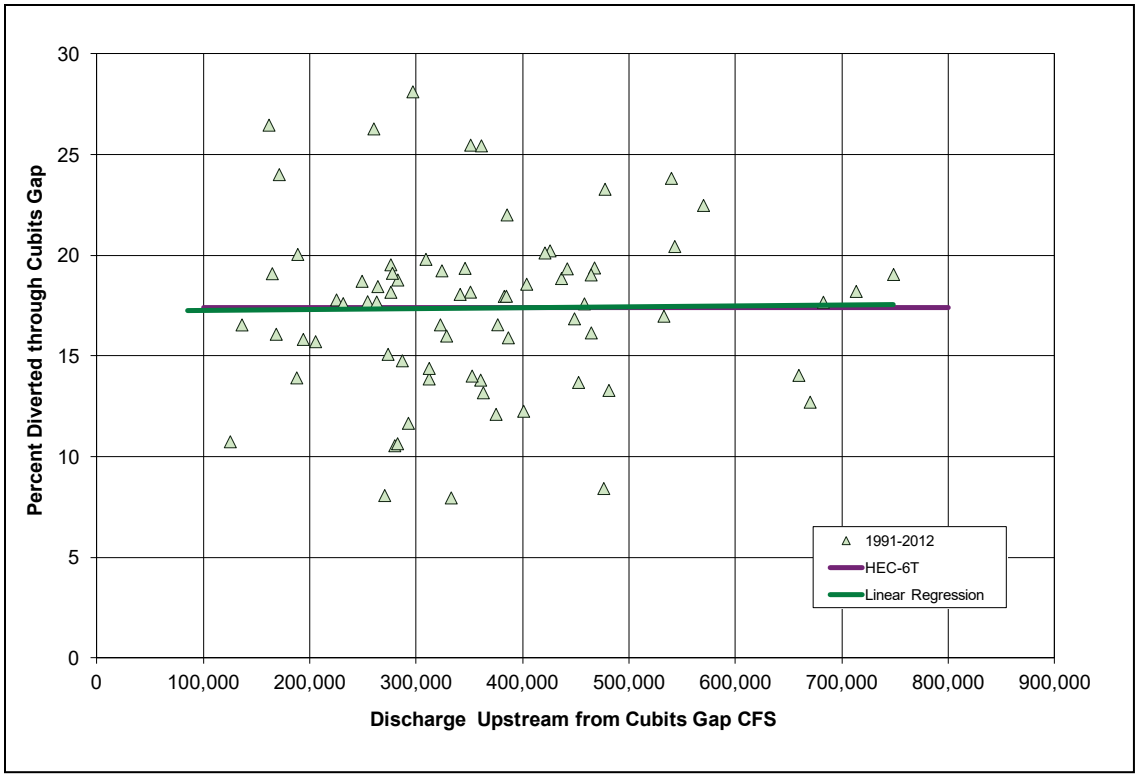

West Bay

The West Bay diversion was included in the Flowline Model. West Bay opened 26 Oct 03. The *LMR1_FWOP_NRC1_Final_R19* model used a constant value of 7% of the Above-Venice discharge for the diversion percentage at West Bay. However, this is inconsistent with 2003–2012 data. Using measured data through 2012, an average diversion percentage was calculated for each water year between 2004 and 2007, and an average diversion percentage was also calculated for 2008–2012. Measured data suggested that the water year boundaries should be modified somewhat to accommodate obvious discontinuities in the data. Adopted constant flow diversion percentages were added to the hydrograph and are shown in Table 12 and Figure 9. No significant relationship between Mississippi River discharge and the diversion percentage at West Bay was observed from the 2008–2012 data. The cross section upstream from West Bay was used as the index station.

In the absence of data, sediment diversion coefficients were adopted from *LMR1_FWOP_NRC1_Final_R19,* which were set equal to the river concentrations for all grain sizes less than 2 millimeters (mm).

Table 11. Distributary outflow - West Bay.

	Percentage of Mississippi River Discharge Upstream from West Bay.
Before 23 Oct 2004	0%
23Oct04–31Aug04	2.2%
1Sep04–30Sep05	5.3%
1Oct05–31Dec06	6.2%
1Jan07–30Sep07	8.2%
1Oct07–31Dec12	10.6%

Figure 9. Flow diversion percentages at West Bay 2004 – 2012.

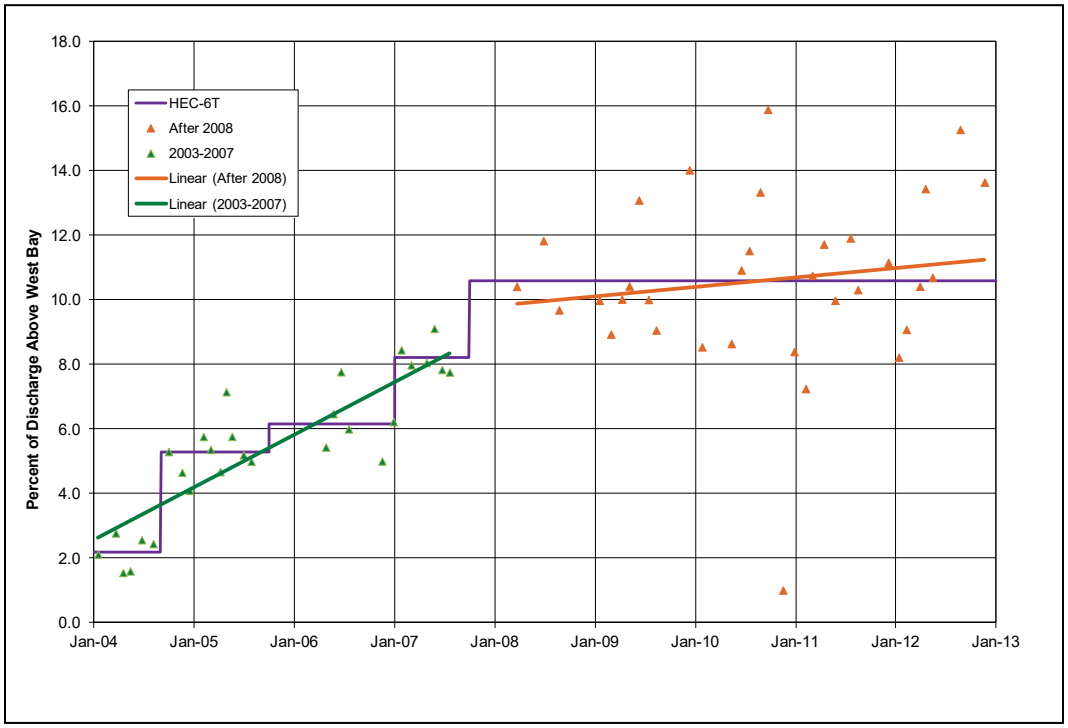

Grand Pass

The Grand Pass flow diversion percentages from the Regional Model were modified in the Flowline Model based on additional data collected after 2006. These are slightly different from those used in LMR1_FWOP_NRC1_Final_R19. The index station is the Above-Venice discharge range. A linear regression of all data collected between 1991 and 2012 was used to determine new flow diversion coefficients and is shown in Figure 10 and Table 13. The flow diversion percentages were varied between a discharge range of 200,000 cfs and 1,000,000 cfs, which is

within the range of data collected. Beyond these limits the flow diversion percentage was held constant rather than extrapolated.

Sediment diversion coefficients are the same in both models and reflect that the bed of Grand Pass is equal to the Mississippi River invert. The sediment diversion coefficients for all size classes in the distributary were arbitrarily assigned a value of 0.9.

Figure 10. Measured Above-Venice (RM 11.5) discharge in Grand Pass.

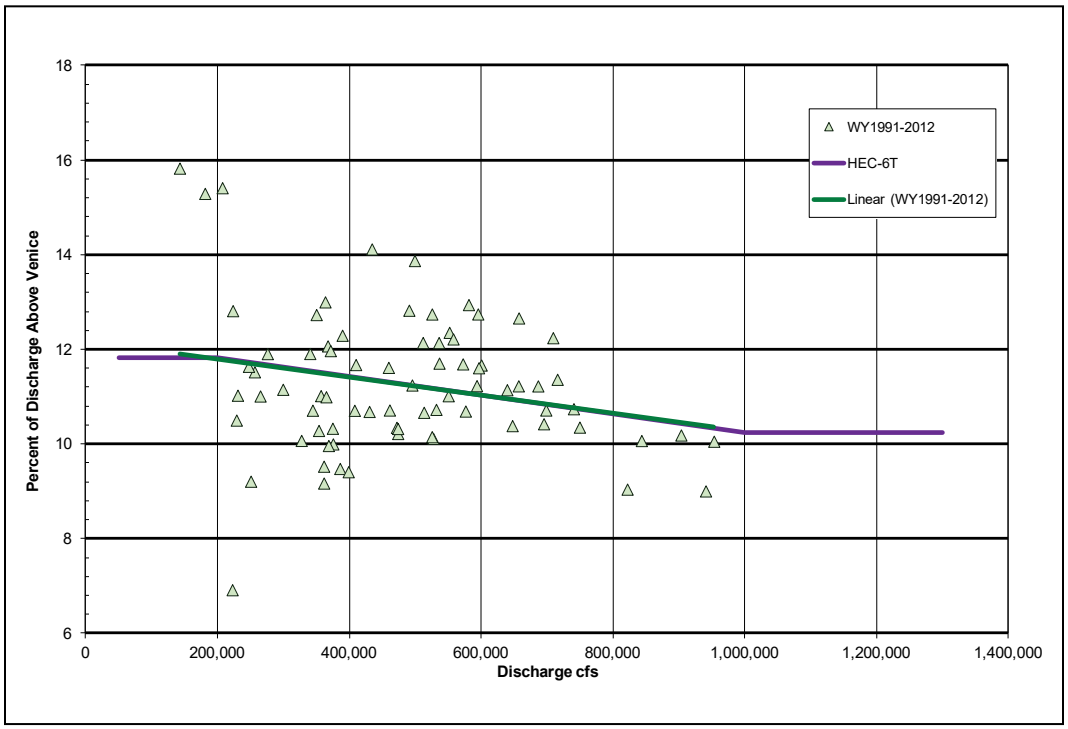

Table 12. Distributary outflow Grand Pass and Baptiste Collette (percentage of Above-Venice discharge).

Distributary	1962 RM	Discharge (cfs)				
		50,000	200,000	600,000	1,000,000	1,300,000
Grand Pass	10.4	11.8%	11.8%	11.0%	10.2%	10.2%
Baptiste Collette	11.4	10.5%	10.5%	11.0%	11.4%	11.4%

Baptiste Collette

The Baptiste Collette flow diversion percentage in the Regional Model was a constant 11% of the Above-Venice (RM 11.5) discharge. The Regional Model percentage was based on measurements taken between 1997 and 2006.

Additional measurements taken between 2006 and 2012 suggest a slight increase in flow diversion out of Baptiste Collette with discharge. A linear regression of all data collected between 1990 and 2012 was used to determine new flow diversion coefficients and is shown in Figure 11 and Table 13. The index station is the Above-Venice discharge range. The flow diversion percentages were varied between a discharge range of 200,000 cfs and 1,000,000 cfs, which is within the range of data collected. Beyond these limits the flow diversion percentage was held constant rather than extrapolated. The adopted flow diversion rating curve is slightly different from that used in LMR1_FWOP_NRC1_Final_R19.

Sediment diversion coefficients are the same in both the Regional Model and the LMR1_FWOP_NRC1_Final_R19 model for the significant grain sizes. However, for the coarser grain sizes LMR1_FWOP_NRC1_Final_R19 used sediment diversion coefficients of 0.9 whereas the Regional Model used zero. The Rouse (1937) equation was used to determine the concentration of sediment above the surveyed elevation of the diversion channel invert in the Regional Model, and the Regional Model sediment diversion coefficients were retained in the Flowline Model.

Figure 11. Measured Above-Venice discharge in Baptiste Collette.

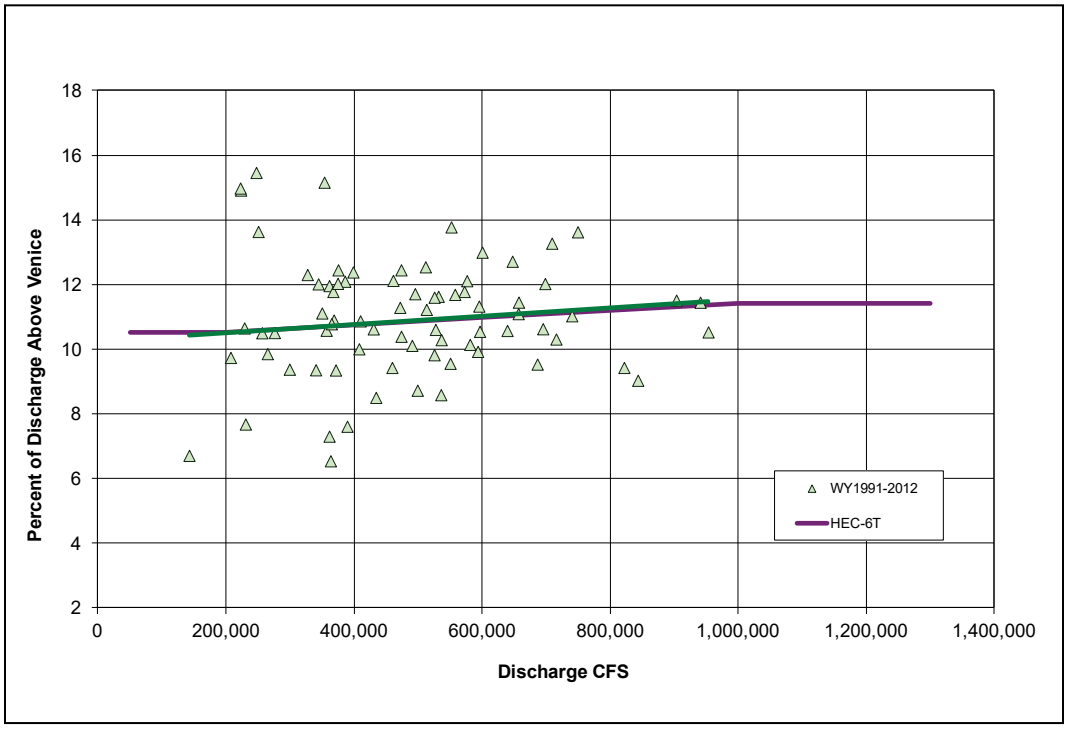

Fort St. Philip and Ostrica

The Fort St. Philip Diversion between RM 20 and RM 14 and the diversion below Ostrica Lock between RM 25 and RM 22 were included in the Flowline Model. The diversion percentages for Fort St. Philip were taken from LMR1_FWOP_NRC1_Final_R19 for Mississippi River discharges up to 800,000 cfs. These measurements were based on recent flow measurements. Measurements taken in 2016 by Louisiana's Water Institute were used for a Mississippi River discharge of 1,250,000 cfs. Without any available data, the diversion percentage was held constant for discharges exceeding 1,250,000 cfs. The only data available for Ostrica were the 2016 Water Institute measurements. The 2016 measured percentage at Ostrica was used in the model for a discharge of 1,250,000 cfs. The rating curve for lower discharges was determined using a ratio of maximum discharges at Fort St. Philip and Ostrica. Without any available data, the diversion percentage was held constant for discharges exceeding 1,250,000 cfs. Diversion percentages for Fort St. Philip and Ostrica are listed in Table 14.

The index station for these diversions is Myrtle Grove at RM 57. Using this index station should be revisited when more data become available—Belle Chasse may be a better choice since Belle Chasse data were used to estimate the diversion percentages at Fort St. Philip and Ostrica.

The sediment diversion coefficients from LMR1_FWOP_NRC1_Final_R19 were used in the Flowline Model.

Table 13. Distributary outflow at Fort St. Philip and Ostrica (percentage of discharge at Myrtle Grove [RM 57]).

Distributary	1962 RM	Discharge (cfs)				
		320,000	400,000	600,000	800,000	1,250,000
Fort St. Philip	20 to 14	0%	5.48%	8.04%	9.60%	10.84%
Ostrica	25 to 22	0%	1.57%	2.30%	2.75%	3.10%

Distributary flows upstream from Ostrica

Distributary flow distribution percentages used in the Regional Model were updated in the Flowline Model to incorporate additional data collected after completion of the Regional Model study. Outflows through the Davis Pond diversion structure (RM 118.4) opened in 2002 were added to the Flowline Model. Flow diversion percentages at Bonnet Carré

Spillway (RM 128) were modified in the Flowline Model to account for leaks identified during the 2011 flood. Overbank flow at Manchac Point (RM 221–RM 210.8) and Devil's Swamp (RM 244.2–RM 236) were included in the Flowline Model. Flood diversions at Birds Point (RM 951) were also added to the Flowline Model. Distributary diversion percentages at Bird's Point were determined from measured data collected by the USGS during the 2011 flood.

The following paragraphs describe the development of distributary flow percentages used in the Flowline Model. For completeness, the descriptions include cases when the original Region Model input was retained.

Bohemia Spillway

The Bohemia Spillway extends for 12 miles along the left descending bank of the Mississippi River between RM 33 and RM 45. It is a constructed feature of the MR&T, but it has not been maintained. Flow presently occurs over the spillway during flood flows. In the Regional Model study, New Orleans District (MVN) determined that flow over the spillway commenced when the Mississippi River flow exceeded 927,000 cfs. The maximum river flow approaching the Bohemia Spillway is 1,250,000 cfs. It is controlled by operations at Old River Control Complex, Morganza Control Structure, and Bonnet Carré Spillway. Therefore, the computation of outflows at the Bohemia Spillway was made for river flows between 927,000 cfs and 1,250,000 cfs.

Diversion percentages were calculated by MVN using the weir equation. The weir heights in these calculations were determined by superimposing the left outer-bank elevations over water surface profiles determined from stage gage records. The bank elevations were taken from the 1992 Hydrographic Survey provided by MVN[1]. Water surface profiles were determined from recorded stages at West Pointe a la Hache, Port Sulphur, and Empire. The profiles were taken on dates that correspond to discharges of 800,000 cfs, 1,000,000 cfs, and 1,250,000 cfs at Tarbert Landing. Discharges were calculated incrementally along the spillway using the equation $Q = CLH^{3/2}$, with C = 3.0. The calculated discharge for

[1] For more information, visit the following website: www.mvn.usace.army.mil/Missions/Engineering/Geospatial-Section/MRHB_Historic/MRHB_1992.

the project flood, 1,250,000 cfs, was approximately 50,000 cfs or 4% of the river discharge approaching RM 45.

There are four cross sections in the model for the spillway. These cross sections extend from RM 33 to RM 45. The 50,000 cfs was divided into four 1.0% diversions—one increment for each of the four cross sections.

The Regional Model diversion percentages at the Bohemia Spillway were retained in the Flowline Model.

Caernarvon Division Structure

The Caernarvon Diversion Structure is located at RM 81.4. Flow through the Caernarvon Diversion Structure is controlled and is not a unique function of Mississippi River discharge. Controlled conditions are not compatible with the HEC-6T option of assigning a percentage to determine the diversion discharge. However, for the systematic assessment purpose, the unique relationship is adequate. Flow through the diversion was calculated by MVN as a function of the Mississippi River stage, head loss through the structure with the gates open, and tailwater downstream from the structure. A maximum flow of 6,000 cfs was allowed. For studies relating to the operation of the Caernarvon Diversion Structure and its effect on downstream conditions and/or sediment delivery to the Gulf of Mexico, more detailed definition of diversion flows in the numerical model hydrograph would be required.

A tailwater rating curve for the structure was derived from stage-discharge gage data in the outflow channel from the period of record between January 2001 and December 2006 and is shown in Figure 12. Discharges ranged between 6,000 and 500 cfs. The stage data were converted from NAVD88 to NGVD29. Differential heads for 100% gate openings were determined from the discharge rating curve found in the Caernarvon Design Memorandum. The differential heads were added to values from a polynomial regression curve of the tailwater stage-discharge data to obtain a headwater stage-discharge rating curve through the structure.

A stage-discharge curve in the Mississippi River at the Caernarvon Diversion Structure was developed from January–December 2001 stage data at Algiers Lock and Braithwaite and January–December 2001 discharge data at Tarbert Landing. Trend lines were computed through each data set. The stage for the riverside at Caernarvon was interpolated

between those trend lines. The trend lines and the interpolated rating curve are shown in Figure 12. Maximum flow upstream from Caernarvon is 1,250,000 cfs and is controlled by operations at Old River Control Complex, Morganza Control Structure, and Bonnet Carré Spillway.

The Mississippi River discharges at Tarbert Landing that are required to achieve specified discharges through the Caernarvon Diversion Structure are shown in Table 15. Specified discharges through Caernarvon are in the first column. The headwater elevations required for those discharges are shown in the fourth column. The Mississippi River flows required to provide the headwater elevations were read from the interpolated rating curve in Figure 13 and recorded in the fifth column. For example, the headwater elevation required to provide a diversion flow of 1,000 cfs is 1.8 feet (ft). The Tarbert Landing discharge required to provide that head is 190,000 cfs. Expressing those discharges as a percentage gives a diversion coefficient of 0.5 %. When the Mississippi River discharge is 430,000 cfs, the head at Caernarvon is 3.7 ft. This will provide a diversion discharge of 6,000 cfs, and that is 1.4% of the Mississippi River flow. As the Mississippi River discharge increases above 430,000 cfs, the diverted percentage must decrease because the maximum discharge from Caernarvon is 6,000 cfs. The resulting diversion percentages are shown in Figure 14.

The Regional Model sediment diversion coefficients at Caernarvon were retained in the Flowline Model.

Figure 12. Caernarvon tailwater rating curve, 2001–2006.

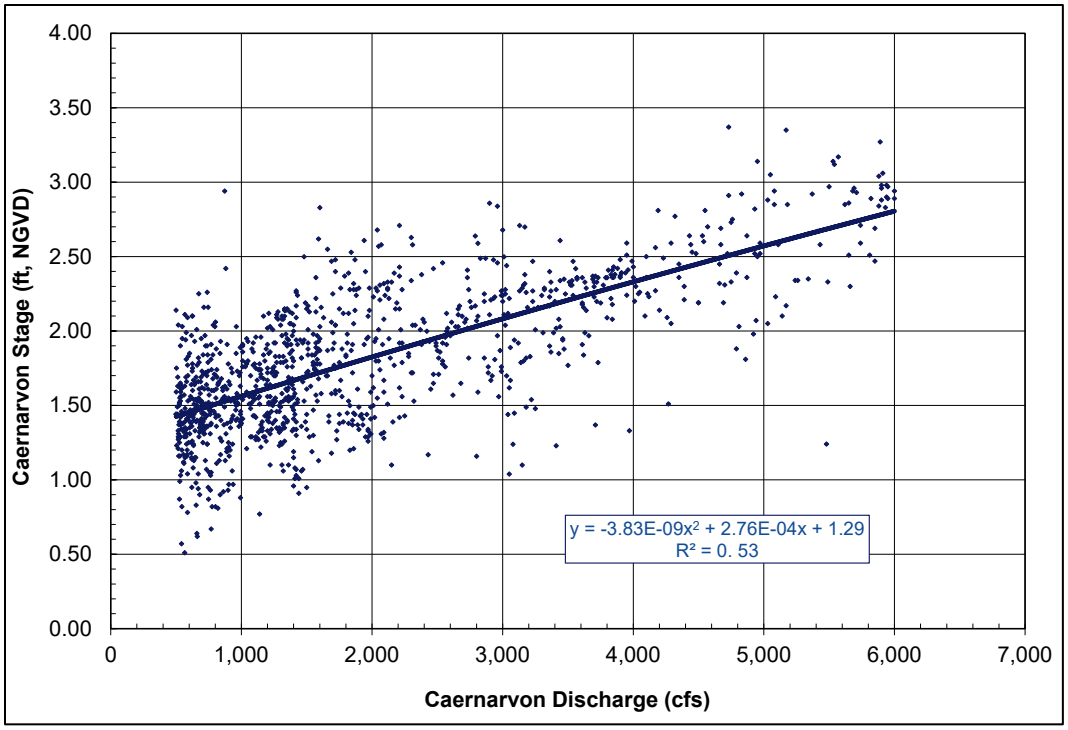

Figure 13. 2001 Stage-discharge rating curve Mississippi River at Caernarvon Inlet.

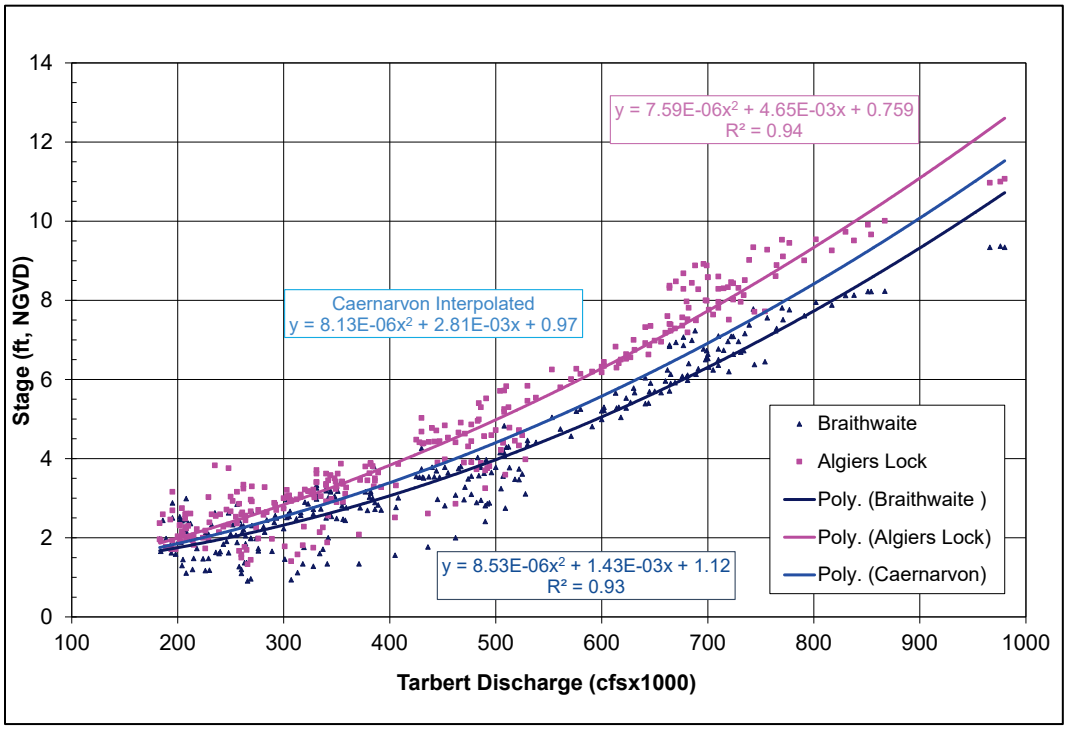

Table 14. Calculated Headwater upstream from Caernarvon Diversion Structure.

Discharge through Structure (cfs)	Tailwater (ft) NGVD	Head Differential (ft)	Headwater (ft) NGVD	Discharge Mississippi River (cfs)
6,000	2.8	0.9	3.7	430,000
5,000	2.55	0.7	3.25	385,000
4,000	2.3	0.55	2.85	340,000
3,000	2.05	0.4	2.45	290,000
2,000	1.8	0.3	2.1	240,000
1,000	1.6	0.2	1.8	190,000
500	1.5	0.1	1.6	<190,000

Figure 14. Percentage of upstream discharge diverted at Caernarvon.

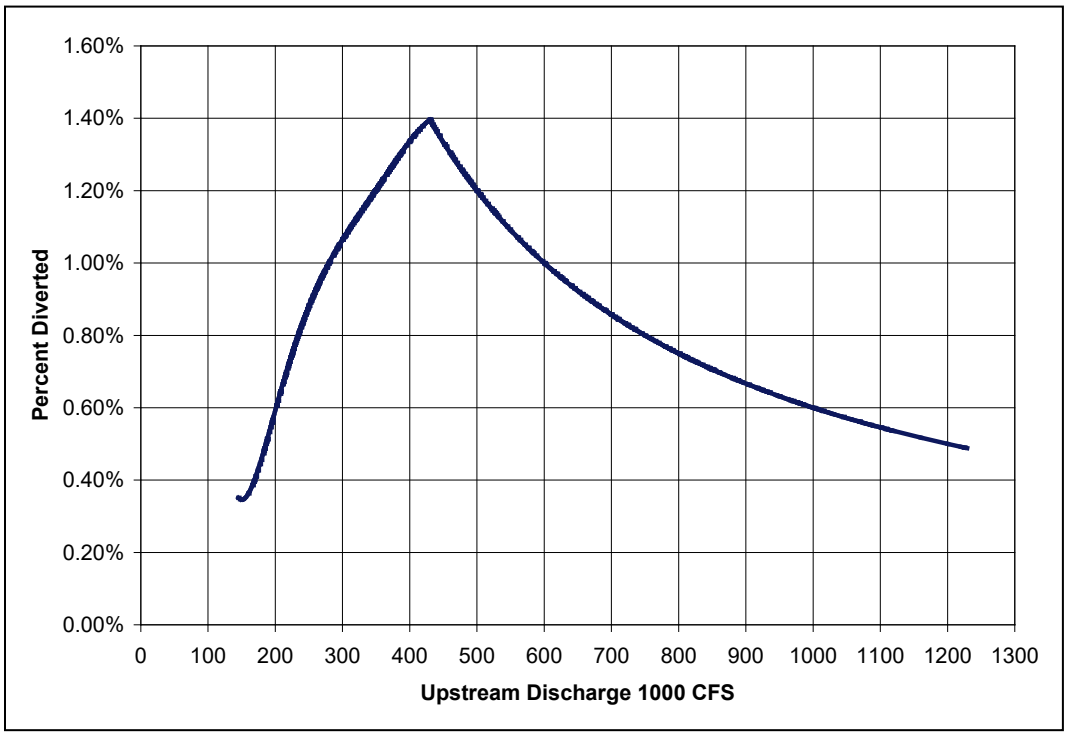

Davis Pond Diversion Structure

The David Pond Diversion Structure was included in the Flowline Model. The purpose of the Davis Pond diversion (RM 118.4) is to imitate historic spring floods and regulate estuary salinity by providing a controlled flow of fresh water and nutrients from the Mississippi River into a target area of the Barataria Basin. The project is expected to reduce marsh loss, enhance marsh vegetation, and increase fish and wildlife productivity. The maximum design flow diversion is 10,650 cfs. Davis Pond was opened 26 March 2002.

Flow through the diversion structure is controlled and is not a unique function of flow in the Mississippi River. This condition is not compatible with the HEC-6T option of assigning a percentage of the upstream discharge to determine the diversion discharge. However, for the systematic assessment purpose, assigning a diversion percentage based on average flows is adequate. For studies relating to the operation of the Davis Pond Diversion Structure itself and its effect on downstream and/or upstream conditions and/or sediment delivery to the Gulf of Mexico, more detailed definition of diversion flows in the numerical model hydrograph would be required.

Mean daily discharge data for Davis Pond Freshwater Diversion near Boutte, LA (295501090190400), are available from the USGS web site. The record includes numerous blank values for the daily discharge. These days were assumed to have zero flow in this analysis.

The daily diversion percentage is plotted against the Mississippi River discharge upstream from Davis Pond in Figure 15. The maximum discharge was set at 1,250,000 cfs to account for diversions at the Morganza and Bonnet Carré Structures. The figure demonstrates the absence of a relationship between Mississippi River discharge and flow diversion. The relationship used in HEC-6T reflects a simple mean value of the measured flows that generally follows a third-order polynomial regression curve. In the Flowline Model, the index station for Davis Pond was set at the upstream cross section.

Sediment diversion coefficients at Davis Pond were calculated using the Rouse equation. The invert elevation of the Davis Pond structure is -11 ft and was obtained from the Design Memorandum. Sediment concentration ratios were calculated for a range of Mississippi River discharges up to 1,250,000 cfs. Using the 2002–2014 mean daily flow data, an average diversion percentage of 0.35% was calculated. The average diversion percentage is calculated assuming that the structure is closed on days without reported mean daily discharge and therefore has zero discharge. Calculated sediment diversion coefficients for Davis Pond are shown in Table 16.

Figure 15. Diversion percentage at Davis Pond.

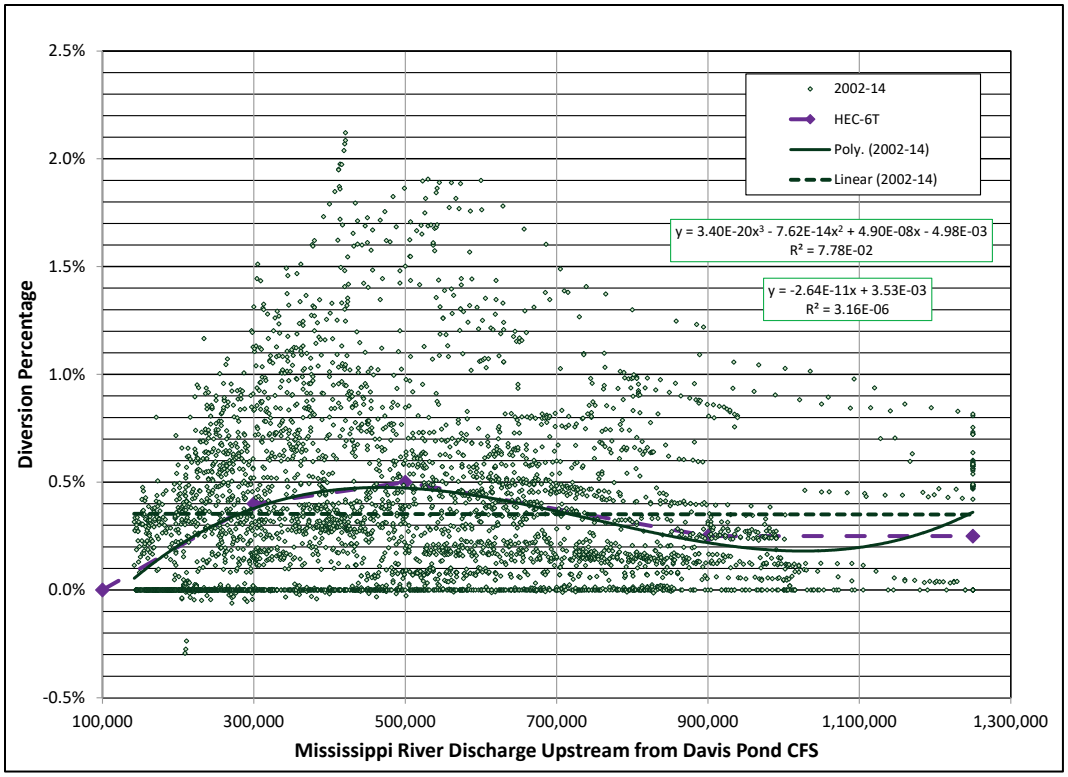

Table 15. Sediment diversion coefficients, Davis Pond.

Discharge CFS	12,000	4380	3230	2430	1350	810	540	1
Clay	1.0	1.0	1.0	1.0	1.0	1.0	1.0	1.0
Very fine silt	1.0	1.0	1.0	1.0	1.0	1.0	1.0	1.0
Fine silt	1.0	1.0	1.0	1.0	1.0	1.0	1.0	1.0
Medium silt	1.0	1.0	1.0	1.0	1.0	1.0	1.0	0.0
Coarse silt	1.0	1.0	1.0	1.0	0.93	0.82	0.68	0.0
Very fine sand	0.83	0.83	0.79	0.72	0.52	0.28	0.12	0.0
Fine sand	0.40	0.40	0.34	0.24	0.07	0.01	0.0	0.0
Medium sand	0.07	0.07	0.04	0.01	0.0	0.0	0.0	0.0

Bonnet Carré Spillway

The Bonnet Carré Spillway (RM 127–RM 129) was designed to operate such that the downstream discharge would not exceed 1,250,000 cfs. Diversion percentages at Bonnet Carré for the 1955 PDF and lessor floods were assigned in the Flowline Model to match the operation schedule. However, the maximum design flow through the Bonnet Carré Spillway is

250,000 cfs. Due to the higher discharges for the 2016 PDF estimate, both operation criteria cannot be achieved. Flowline Model diversion percentages for the 2016 PDF estimate were set to match the structure's maximum design capacity.

To be consistent with the Myrtle Grove Model and LMR1_FWOP_NRC1_Final_R19, flow diversion percentages were updated in the Flowline Model to account for leakage through the structure at discharges between 1,000,000 and 1,250,000 cfs. The index station was moved to the upstream cross section.

The sediment diversion coefficients from the Regional Model were retained.

Overbank flow at Manchac Point

Overbank flow across Manchac Point was included in the Flowline Model. The update is consistent with that used in the Myrtle Grove Model and LMR1_FWOP_NRC1_Final_R19. The approach used in these studies was deemed appropriate for the Flowline Assessment. A distributary outflow was added at RM 221, and a return flow was added at RM 210.8. Flow across Manchac Point begins when the discharge upstream exceeds 900,000 cfs. Ten percent of the upstream flow is diverted at 1,200,000 cfs and at 1,500,000 cfs. Diversion percentages were linearly interpolated between 900,000 cfs and 1,200,000 cfs. These percentages were determined for the Myrtle Grove Model using a stand-alone loop model. In the Flowline Model, the 10% diversion rate was held constant for all discharges exceeding 1,500,000 cfs. Flow depths for the PDF are approximately 20 ft in the right overbank across Manchac Point.

Sediment diversion coefficients for the outflow and inflow at Manchac Point were taken from the LMR1_FWOP_NRC1_Final_R19 model and were based on engineering judgement. Clay, silt, and very-fine sand diversion concentrations were set equal to the upstream sediment concentrations. Fine sand diversion concentration was set to 50% of the upstream sediment concentration. Sediment size classes greater than fine sand were not diverted. One hundred percent of the diverted clay was returned at RM 210.8. Ninety percent of the diverted very fine silt, 80% of the fine silt, 70% of the medium silt and 60% of the coarse silt was returned downstream from Manchac Point. None of the diverted

sand was returned. Sediment not returned is assumed to deposit on the overbank; however, the numerical model does not increase overbank elevations to account for this deposition.

Overbank flow at Devils Swamp

The Regional Model treated Devils Swamp (RM 244.2–RM 236) as an ineffective flow area. Using the version of HEC-6T available at the time, the left bank was not overtopped at any of the cross sections adjacent to Devils Swamp until the discharge exceeded 1,100,000 cfs. However, the May 2014 version of HEC-6T calculated higher water-surface elevations, and the left bank overtopped at lower discharges.

The Myrtle Grove Model and LMR1_FWOP_NRC1_Final_R19 treat overbank flow through Devils Swamp differently than the Flowline Model. The Myrtle Grove and LMR1_FWOP_NRC1_Final_R19 models extend the left overbank beyond the limits of available data and include a depression to accommodate overbank flow. Flow is also diverted upstream from RM 244.2 in LMR1_FWOP_NRC1_Final_R19. This approach, where both overbank flow and diversion flow are included, double counts the left overbank flow. The Myrtle Grove and LMR1_FWOP_NRC1_Final_R19 models have a flow diversion of 1% at flows less than 900,000 cfs. At 1,289,000cfs, 10% is diverted and at 1,500,000, 15% is diverted. These numbers were derived in the Myrtle Grove study using a stand-alone loop model.

The Devil's Swamp diversion was included in the Flowline Model, but the left overbank depression was excluded. The Flowline Model includes approximately 2000 ft of left overbank to account for flow adjacent to the channel around Thomas Point. The diversion percentage at 900,000 cfs was changed to 0% from 1%. The remaining flow diversion percentages from LMR1_FWOP_NRC1_Final_R19 were retained. In the Flowline Model, the 15% diversion rate was held constant for all discharges exceeding 1,500,000 cfs.

In LMR1_FWOP_NRC1_Final_R19 the sediment diversion coefficients for very fine sand and fine sand were set at 100%, and medium sand was set at 50%. These were changed to 0% for fine sand and medium sand in the Flowline Model. No sediment is returned from the Devils Swamp diversion.

Morganza Spillway

The Morganza Spillway (RM 280) was designed to operate such that the downstream discharge does not exceed 1,500,000 cfs. Diversion percentages at Morganza for the 1955 PDF were assigned in the Flowline Model to match the operation schedule. However, the maximum design flow through the Morganza Spillway is 600,000 cfs. Due to the higher discharges for the 2016 PDF estimate, both operation criteria cannot be achieved. Flowline Model diversion percentages for the 2016 PDF estimate were set to match the structure's maximum design capacity.

Old River Control Complex

The flow diversion percentages at the Old River Control Complex for existing conditions are based on historical data between 1991 and 2011. There is not a unique relationship between Mississippi River discharge and diversion percentage through any of the Old River structures. Therefore, average values and linear trend lines were used to estimate a long-term average diversion percentage for each structure. The maximum authorized flow diversion through the Old River Control Complex is 620,000 cfs. Due to the higher discharges for the 2016 PDF estimate, Flowline Model diversion percentages for discharges above 2,220,000 cfs were reduced to maintain a maximum diversion of 620,000 cfs.

Historical flow distribution fractions through the Auxiliary Structure, Low Sill Structure, Overbank Structure, and Hydropower Structure from the Regional Model were updated using 1991–2011 daily discharge data. There was no flow over the Overbank Structure between 1991 and 2011. Historical distribution fractions were determined for three distinct discharge ranges—less than 800,000 cfs; 800,000 to 1,600,000 cfs; and 1,600,000 to 2,220,000 cfs. For discharges less than 800,000 cfs, the Hydropower and the combined Auxiliary and Low Sill diversion fractions were taken to be the mean average determined for all the daily discharges less than 800,000 cfs for the 20-year period. A combined flow for the Auxiliary and Low Sill Structures was used because it is the combined flow that is used to maintain the designated flow split at Old River. The operational decision as to how much flow to discharge through each of the two structures is not based on Mississippi River discharge. For discharges between 800,000 and 1,600,000 cfs, average linear trend lines were determined for the Hydropower and the combined Auxiliary and Low Sill structures. Likewise, for discharges between 1,600,000 and

2,220,000 cfs, average linear trend lines were determined for the Hydropower and the combined Auxiliary and Low Sill structures. The individual fractions for the Auxiliary and Low Sill structures used in the HEC-6T model were determined using the combined distribution from the trend lines and the mean average flow fraction for each of the two structures for each of the three discharge ranges. The daily data points and the average trend lines are shown in Figure 16. Percentages used in the HEC-6T Model are tabulated in Table 17.

Figure 16. Daily diversion fractions at Old River, 1991– 2011, with the mean trend lines used in HEC-6T.

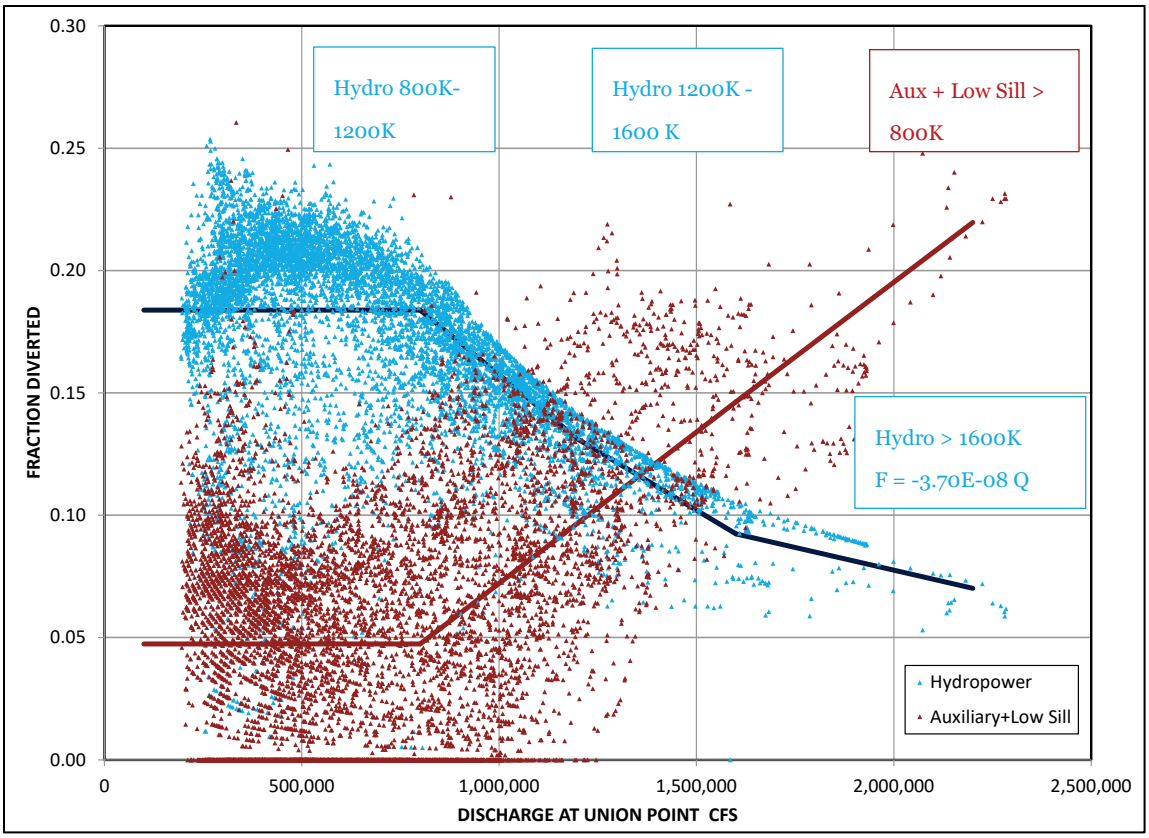

Table 16. Percent diverted at Old River distributaries from 1991–2011 data.

Distributary	1962 RM	Discharge at Union Point (cfs)				
		< 800,000	1,200,000	1,600,000	2,220,000	3,000,000
Auxiliary	312	4.2%	7.2%	7.6%	9.5%	6.60%
Low Sill	314.6	0.6%	2.5%	6.4%	12.4%	10.44%
Overbank	315.2	0	0	0	0	0
Hydropower	315.9	18.4%	13.5%	9.2%	7.0%	3.63%

At the Old River Complex, sediment diversion coefficients for each structure were the same as those used in the Regional Model, which in turn were extracted from a previous study (Catalyst-Old River Hydroelectric 1999). The sediment diversion coefficients from the 1999 study had been developed from available measured data (1991–1997) and numerical model calibration. Due to the wide scatter in the measured data, no attempt was made to vary the diversion coefficients with changes in discharge or with variations in operation schedules. A more detailed description of the historical measurements is contained in the Regional Model Study.

2011 Flood diversions

The New Madrid Floodway was open 2 May 2011 at 10:00 p.m. when the levee at RM 951 was breached. USGS published average daily measured flow at Birds Point (New Madrid Floodway Upper Inflow Breach at Birds Point – gage number 365659089073101) were used to determine outflow discharges in the Flowline Model for the 2011 flood. Diversion percentages are shown in Figure 17. Only flows diverted out of the Mississippi River at Birds Point were included in the model. The breach was located between cross sections 951.5 and 949 on Segment 23. In the HEC-6T hydrograph, the measured data were lagged 6 days so that the breach effectively occurs on 8 May 11 and the first daily discharge occurred on 9 May 11. Sediment diversion coefficients were arbitrarily set at 1.0 for clay and silt and 0.0 for sands and gravel.

A second controlled breach in the levee occurred on 5 May 2011 at RM 917.5B on the Bend of Island No. 8 (Big Oak/Crevasse #1). USGS-published average daily measured flow data were used to determine outflow discharges (New Madrid Floodway middle Breach No. 1 near Big Oak – gage number 363740089180601). Diversion percentages are shown in Figure 17. Only flows diverted out of the Mississippi River were included in the model. Diversion percentages were calculated based on the Mississippi River flow at RM 951.5, which is upstream from the Birds Point breach. The breach at Crevasse #1 was located between cross sections 914.6 and 913.8 on the west channel of the Island No. 8 loop (Segment 19). In the HEC-6T model hydrograph, the breach occurs on 12 May 11 to account for a 6-day lag to Vicksburg, MS. Sediment diversion coefficients were arbitrarily set at 1.0 for clay and silt and 0.0 for sands and gravel.

In the HEC-6T model hydrograph floodway flows returned to the Mississippi River at two locations. The first is a natural 1500 ft gap in the

levee at New Madrid, MO (RM 889.5), and the second was a controlled levee breach at Crevasse #2 (RM 891). USGS-published average daily measured flow data were used to determine inflow discharges (New Madrid Floodway Combined Outflow – gage numbers 363454089285900, 363524089302700 and 363618089251701). The return flows were treated as a single tributary in the HEC-6T model, returning between RMs 889.01 and 893.13. Sediment inflow concentrations were arbitrarily set at 0.0.

Figure 17. USGS-measured diversion percentages at Birds Point and Crevasse #1.

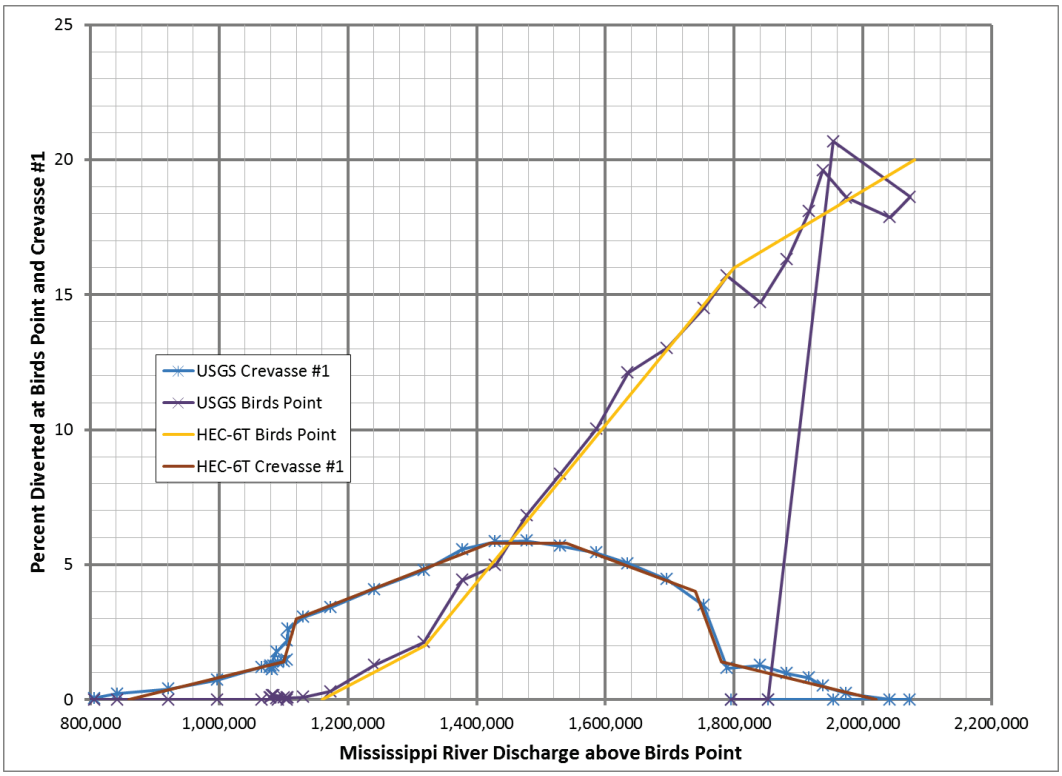

Project Design Flood (PDF) flow diversions

Computed results from the unsteady flow HEC-RAS model were used to determine flow diversions at Birds Point and Crevasse #1 for the 2016 PDF estimate. Diversion percentages are shown in Figure 18. Sediment diversion coefficients were arbitrarily set at 1.0 for clay and silt and 0.0 for sands and gravel.

Figure 18. PDF diversion percentages at Birds Point and Crevasse #1.

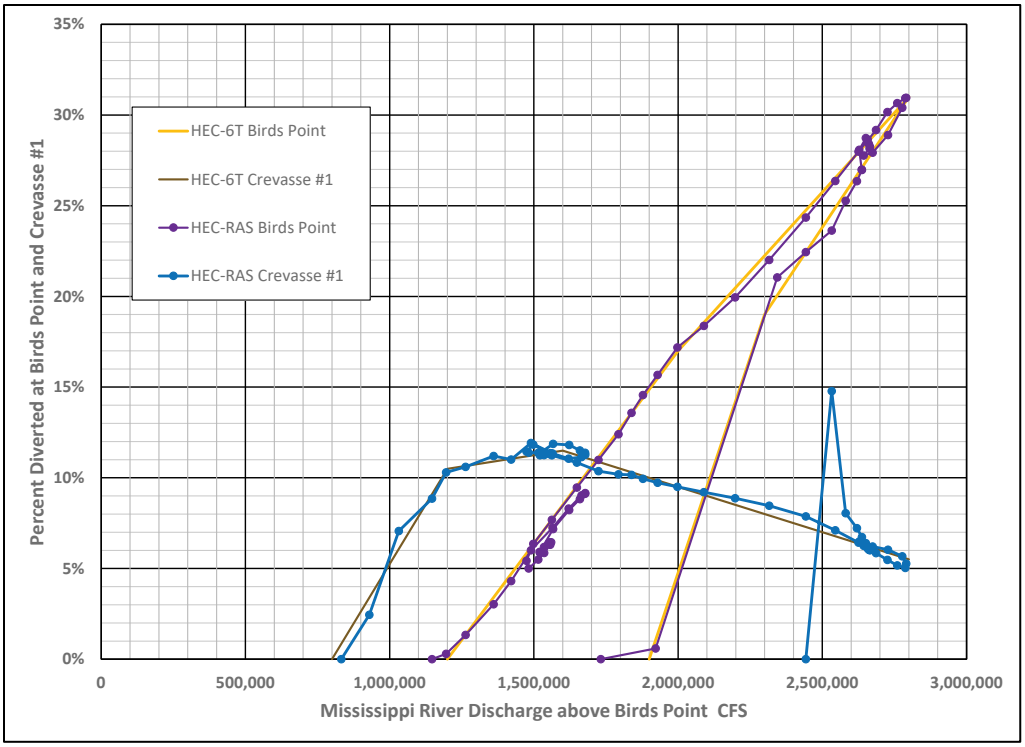

Temperature

Water temperature was based on 1965–2014 reported data from the USGS. Monthly averages were calculated from the observed data and assigned at the beginning of each month in the computational hydrograph. Mean monthly temperatures are shown in Table 18. In the HEC-6T hydrograph, daily values were assigned based on linear interpolation. The following gage data were used to determine the average monthly temperatures. This list includes the Excel files containing the data and analysis.

- Mississippi River at Thebes, IL (USGS 07022000) 1973–2013 (Tthebes.xlsx)
- Ohio River at Dam 53 near Grand Chain, IL (USGS 03612500) 1973–2013 (OhioSed.xlsx)
- Obion River at Highway 51 near Obion, TN (USGS 07026040) 1990–2005 (Obion.xls)
- Obion River at Obion, TN (USGS 07026000) 1975–1990 (Obion.xls)
- Hatchie River at Rialto, TN (USGS 07030050) 1977–2008 (Hatchie.xlsx)
- Hatchie River at Bolivar, TN (USGS 07029500) 1975–2006 (Hatchie.xlsx)

- St. Francis River at Madison, AR (USGS) 07047907) 1977–2009 (StFrancis.xlsx)
- White River at Clarendon, AR (USGS 07077800) 1965–1986 (White River-new.xlsx)
- White River at DeValls Bluff, AR (USGS 07077000) 1967–2014 (White River-new.xlsx)
- Arkansas River at Murray Dam near Little Rock, AR (USGS 07263450) 1975–1994 (ArkansasRiver.xlsx)
- Arkansas River at David D Terry Lock and Dam below Little Rock, AR (USGS 07263620) 1969–2014 (ArkansasRiver.xlsx)
- Arkansas River at Dam No. 2 near Gillett, AR (USGS 07265283) 1972–1994 (ArkansasRiver.xlsx)
- Yazoo River at Redwood, MS (USGS 07288800) 1972–1993 (YazooWQ-new.xlsx)
- Yazoo River below Steele Bayou near Long Lake, MS (USGS 07288955) 1994–2014 (YazooWQ-new.xlsx)

Table 17. Average monthly water temperature 1965–2014, °F.

	Jan	Feb	Mar	Apr	May	Jun	Jul	Aug	Sep	Oct	Nov	Dec
Upper Mississippi	36.2	37.6	45.2	55.5	66.8	76.5	82.4	82.3	76.9	62.9	48.6	39.8
Ohio	40.8	41.2	47.2	56.6	68.4	76.8	83.8	83.9	79.9	62.7	57.2	46.5
Obion	40.9	44.0	51.5	62.2	71.0	77.2	80.4	78.3	71.2	62.4	53.8	44.6
Hatchie	41.2	45.4	52.5	61.8	68.1	76.6	80.4	78.2	73.1	63.4	56.5	46.4
St. Francis	40.8	43.3	52.4	60.7	68.9	77.5	82.9	82.2	76.9	63.8	54.9	45.7
White	41.8	45.5	53.3	62.8	69.3	75.9	78.4	78.2	74.3	64.3	55.3	46.6
Arkansas	42.5	44.1	52.7	61.1	71.1	79.4	85.2	85.2	79.4	68.7	57.7	48.6
Yazoo	46.5	48.8	56.8	66.0	74.3	81.3	85.3	86.2	81.1	70.4	60.0	51.2

Downstream water-surface elevation

The NOAA tide gage at Grand Isle, LA (8761724) was used to set the downstream water-surface elevation for the model assessment. Consistent with previous studies, the downstream water-surface elevation was set to reflect seasonal variation in the mean tide elevation in the Gulf of Mexico. Mean monthly tide elevations were obtained from the NOAA web site (http://tidesandcurrents.noaa.gov) for the years 1978–2014. The data indicate a long-term increase in the mean tide elevation. To differentiate the seasonal variation from sea-level rise and/or subsidence effects, adjusted mean

monthly water-surface elevations were calculated. This was accomplished by increasing the magnitude of the older measurements so that a linear regression line through the adjusted data had a zero slope. The resultant adjusted mean monthly water-surface elevations represent 2014 conditions. The reported and adjusted tide elevations are shown in Figure 19. The adjusted water-surface elevations varied between 0.2 and 1.2 ft. and were approximately 0.3 ft. higher than those used in the Regional Model study. In the numerical model, mean daily values were determined by interpolation, assigning the mean monthly magnitude to the beginning of each month. Calculations are in GrandIsleNOAA.xlsx, and are tied to NGVD29 (NOAA Mean SeaLevel [MSL] + 0.8 ft). This conversion was also used in the IPET study (USACE 2006) for the City of New Orleans. The Grand Isle gage is in an area with significant changes in relative MSL (+9.24 mm/year), and tide elevations have a special epoch designation (2007–2011). There was no correlation to NOAA tide elevations and NGVD29 or NAVD88 found on its web site. Downstream water-surface elevations assigned in the Flowline Model are shown in Table 19.

Figure 19. Mean monthly tide elevations at Grand Island, LA, 1978–2014.

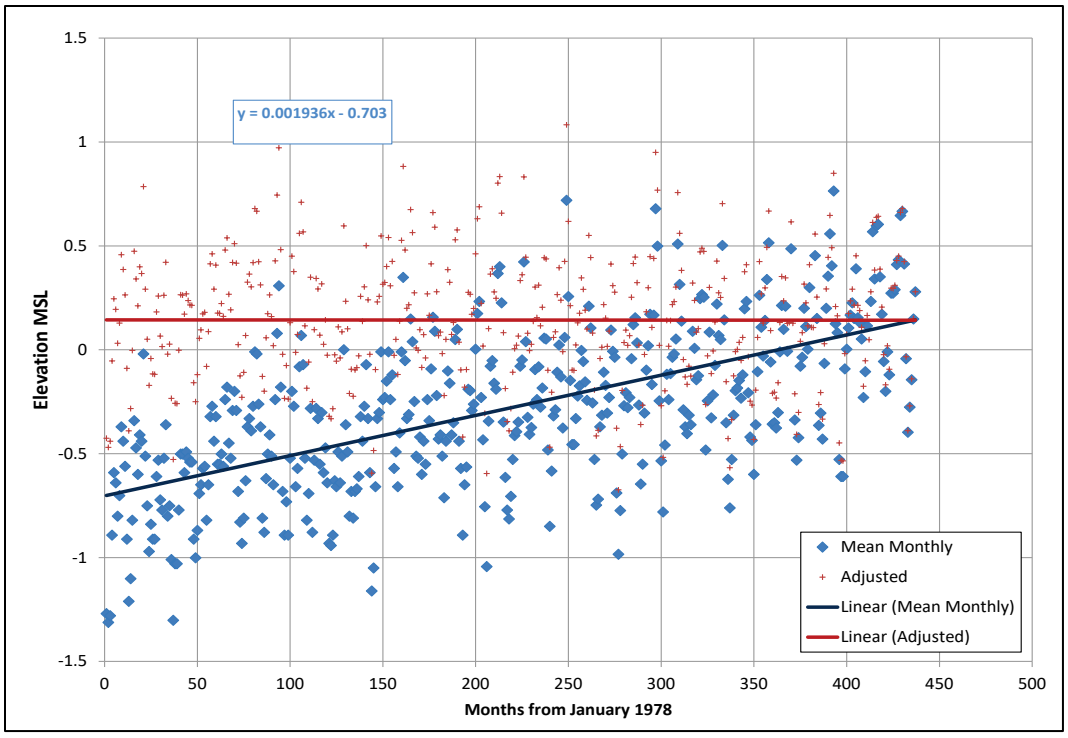

Table 18. Downstream water-surface elevations at Pilots Station.

Month	Feet NGVD	Month	Feet NGVD
January	0.55	July	0.97
February	0.61	August	1.09
March	0.75	September	1.35
April	0.91	October	1.26
May	1.06	November	1.02
June	1.07	December	0.70

Roughness coefficients

Flood discharges on the Mississippi River in 2011 produced stages significantly higher than those used to determine roughness coefficients for the Memphis District reach in the Regional Model. In the MVN, 2011 flood elevations were generally not higher than historical floods due to operation of the Morganza and Bonnet Carré Spillways. The Vicksburg District reach in the Regional Model had already been calibrated to 2011 flood data. In the Flowline Assessment, 2011 flood data were used to adjust high-flow roughness coefficients for the Memphis District reach.

Roughness coefficients were adjusted in the Flowline Model by running the 1991–2011 hydrograph and extracting daily calculated stages in 1991, 2002, and 2011. These are plotted with the reported mean daily discharges and stages in 1991, 2002, and 2011 at Helena, Memphis, and Hickman in Figure 20, Figure 21, and Figure 22, respectively. The reported daily discharges are calculated from measurements and are labeled as "measured" in the figures. The plots suggest a decline in the rating curve with time for discharges less than 1,000,000 cfs. This result is consistent with specific gage analyses presented later in this report.

Roughness coefficients used in the Flowline Model are listed in Table 20, Table 21, and Table 22.

Figure 20. Measured and calculated stages at Helena.

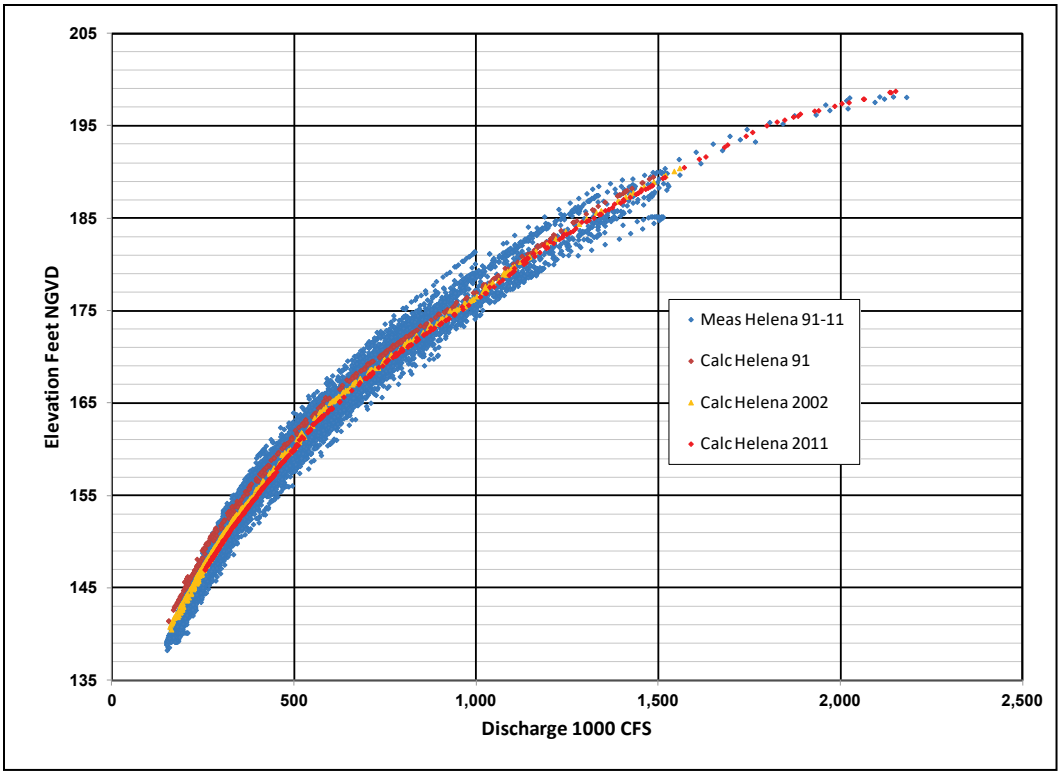

Figure 21. Measured and calculated stage at Memphis.

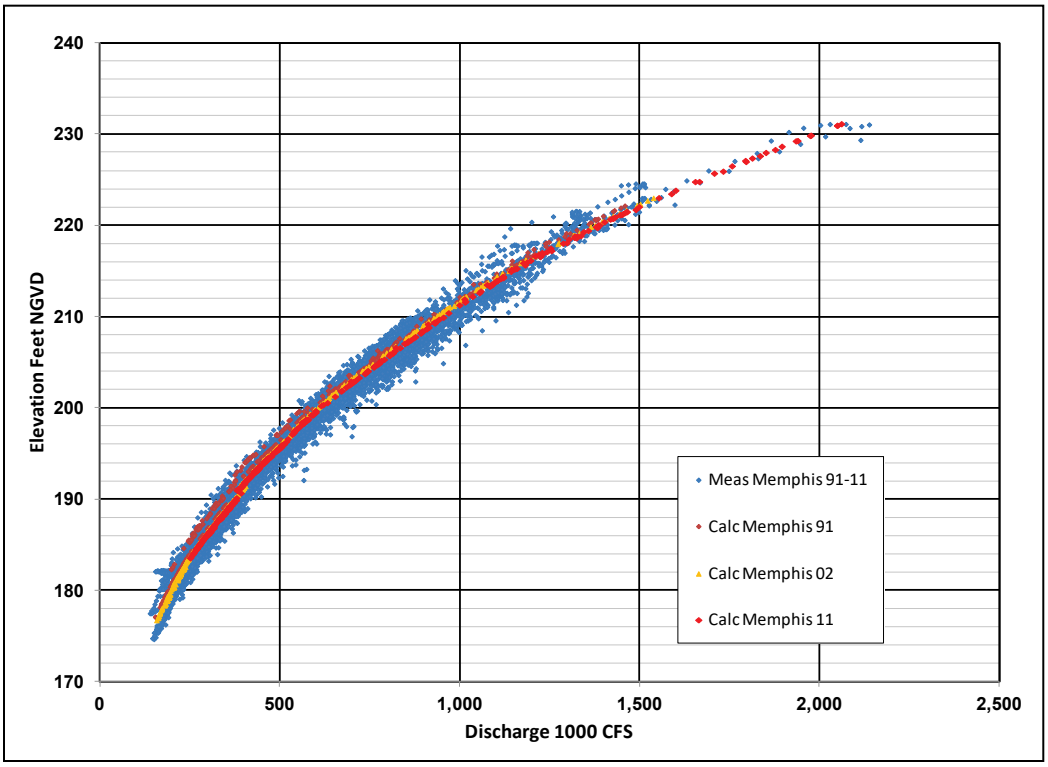

Figure 22. Measured and calculated stage at Hickman.

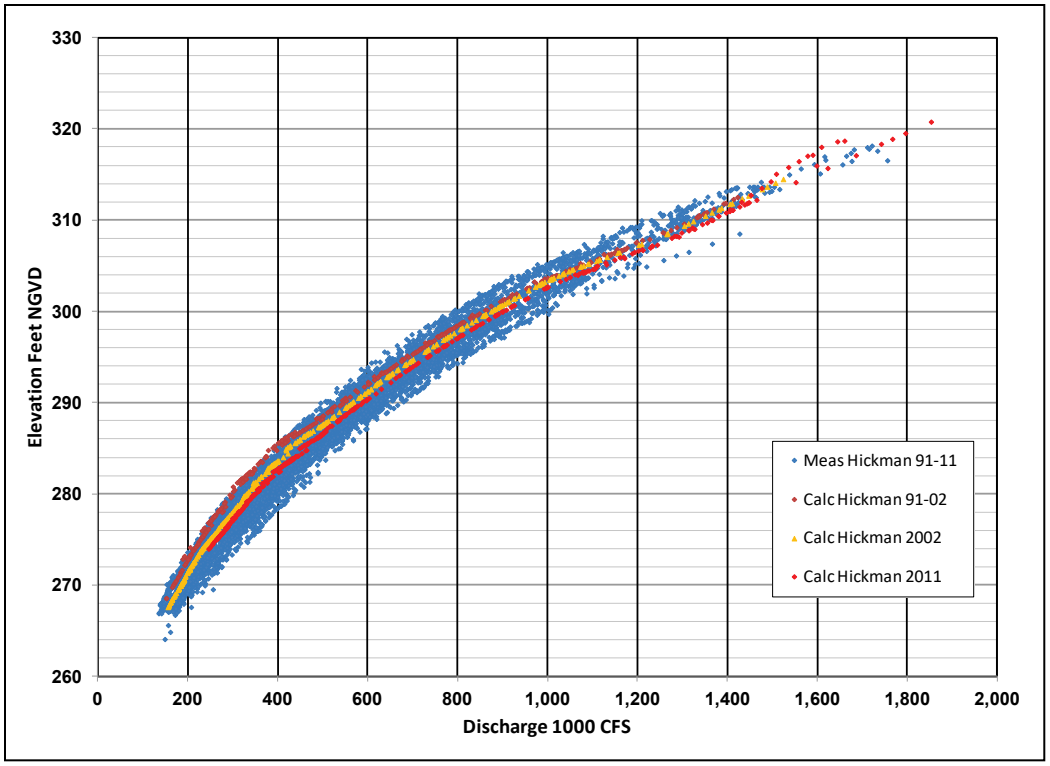

Table 19. HEC-6T roughness coefficients in MVN.

RM	Overbanks	Channel – 1,000 cfs				
		70	120	180	240	300
-18.0	0.05	0.038	0.026	0.022	0.022	0.0165
		190	320	450	580	710
0.0	0.15	0.038	0.026	0.022	0.022	0.0165
		250	600	800	900	1,200
11.05	0.20	0.024	0.019	0.019	0.015	0.014
		150	650	950	1,100	1,200
35.1	0.20	0.024	0.022	0.022	0.018	0.015
		275	650	850	950	1,300
53.0	0.20	0.027	0.026	0.024	0.023	0.0205
		275	650	950	1,200	1,500
105.0	0.20	0.029	0.026	0.025	0.0215	0.021
		275	550	950	1,200	1,500
141.6	0.20	0.028	0.026	0.024	0.021	0.022
		275	550	850	950	1,500
177.3	0.20	0.026	0.026	.025	0.022	0.021
195.3	0.20	0.026	0.026	.025	0.022	0.021
229.7	0.20	0.027	0.027	.026	0.025	0.024
		275	550	850	1,100	1,500
267.0	0.20	0.029	0.027	.024	0.023	0.020
		200	400	850	1,000	2,000
306.3	0.20	0.034	0.031	.031	0.030	0.026

Table 20. HEC-6T roughness coefficients in Vicksburg District.

RM		Overbanks	Channel – 1,000 cfs				
			200	400	900	1,400	1,800
328.6	Upstream Union Point	0.20	0.034	0.030	0.030	0.027	0.026
365.0	Upstream Natchez	0.20	0.027	0.027	0.0275	0.025	0.024
396.4	Upstream St Joseph	0.20	0.027	0.027	0.0275	0.025	0.024
			200	600	1,100	1,400	1,800
438.4	Upstream Vicksburg	0.20	0.027	0.025	0.025	0.024	0.023
			200	400	700	1,400	1,800
487.8	Upstream Lake Providence	0.20	0.033	0.029	0.027	0.027	0.027
			200	400	600	1,400	1,800
531.7	Upstream Greenville	0.20	0.032	0.027	0.026	0.027	0.027
			200	400	800	1,400	1,800
557.2	Upstream Arkansas City	0.20	0.033	0.030	0.030	0.027	0.023

Table 21. HEC-6T roughness coefficients in Memphis District.

RM		Overbanks	Channel – 1,000 cfs				
			200	400	800	1,400	1,800
580.8	Upstream Arkansas River	0.20	0.033	0.030	0.030	0.027	0.023
			900	1,100	1,600	1,800	2,200
600.1	Upstream White River	0.15 -0.25	0.029	0.030	0.031	0.030	0.029
			200	500	1,000	1,400	2,200
666.01	Upstream Helena	0.15 -0.25	0.029	0.028	0.027	0.027	0.027
			200	500	1,000	1,400	2,000
744.98	Upstream Memphis	0.15 -0.25	0.036	0.034	0.033	0.033	0.034
			100	500	1,000	1,250	2,000
910.54	Island 8 Main	0.15 -0.25	0.036	0.036	0.036	0.036	0.036
910.54	Island 8 Secondary	0.15 -0.25	0.036	0.024	0.024	0.024	0.024
			200	500	1,000	1,400	2,000
915.59	Upstream Island 8	0.20	0.036	0.034	0.033	0.033	0.034
			50	100	250	625	1,000
931.53	Wolf Island Secondary	0.20	0.036	0.035	0.031	0.027	0.034
931.53	Wolf Island Main	0.20	0.024	0.023	0.024	0.025	0.032
			200	500	1,000	1,400	2,000
936	Upstream Wolf Island	0.15 -0.25	0.036	0.034	0.033	0.033	0.034

Stages at Cairo are influenced by the combined discharge from the Ohio River and the Mississippi River. This makes roughness coefficient adjustment to a general rating curve of Ohio River discharges difficult. Calibrating roughness coefficients for flood discharges are further complicated by the diversion into the New Madrid Floodway. The diversion significantly reduces backwater downstream. Roughness coefficients for the 2011 flood were therefore determined based on plotting the stage at Cairo versus the combined discharge and accounting for diverted flows in both the HEC-6T calculations and the measured data. Roughness coefficients for discharges greater than 1,250,000 cfs, from the original model, were increased between Hickman and Cairo to achieve the results shown in Figure 23.

Figure 23. Calculated and measured elevation at Cairo, April 1 to June 30, 2011.

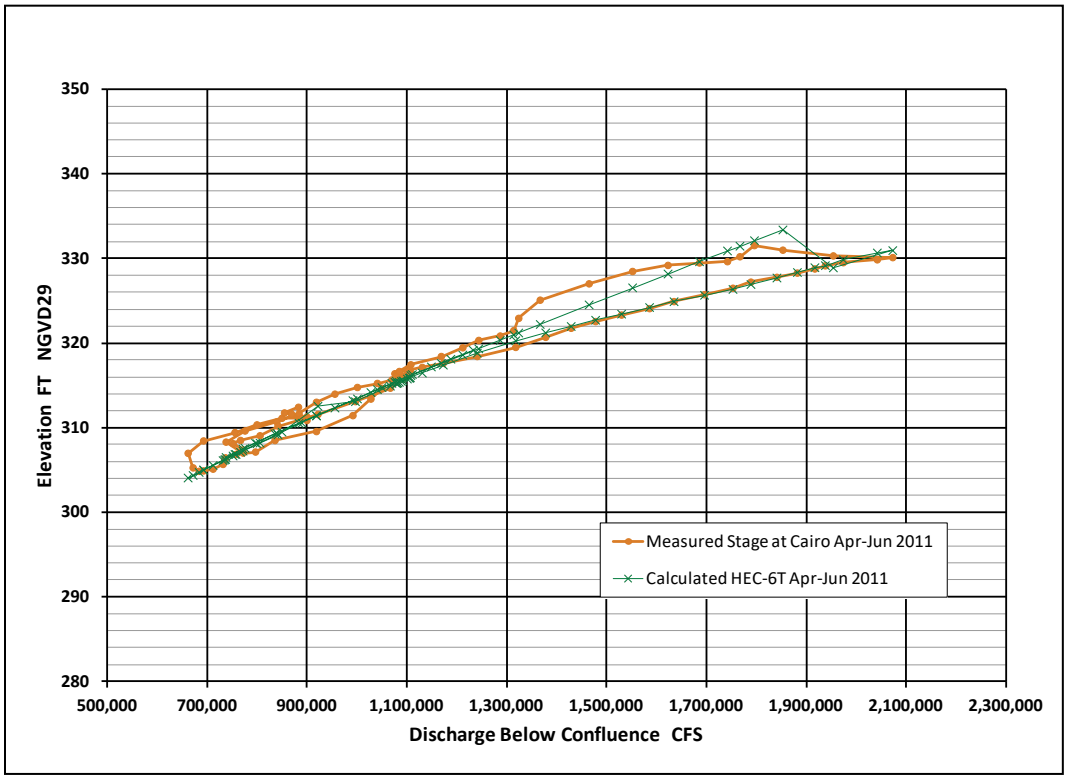

No adjustment to roughness coefficients at high discharges was required to replicate measured water-surface elevations at Metropolis. The channel roughness coefficient was 0.026 for all discharges. Metropolis is located at Ohio RM 943, which is approximately 38 miles upstream from the Mississippi River confluence. Measured water-surface elevations between 1991 and 2011 are compared to calculated stages in Figure 24. A comparison of polynomial regression curves

through the two data sets demonstrates that average water-surface elevations are similar confirming that roughness coefficients are reasonable. A wide scatter in the stage-discharge relationship is expected at this station because stage is significantly affected by inflow from the Mississippi River above Cairo. This effect is apparent in both the measured and calculated data.

Figure 24. 1991–2011 measured and calculated water-surface elevations, Ohio River at Metropolis.

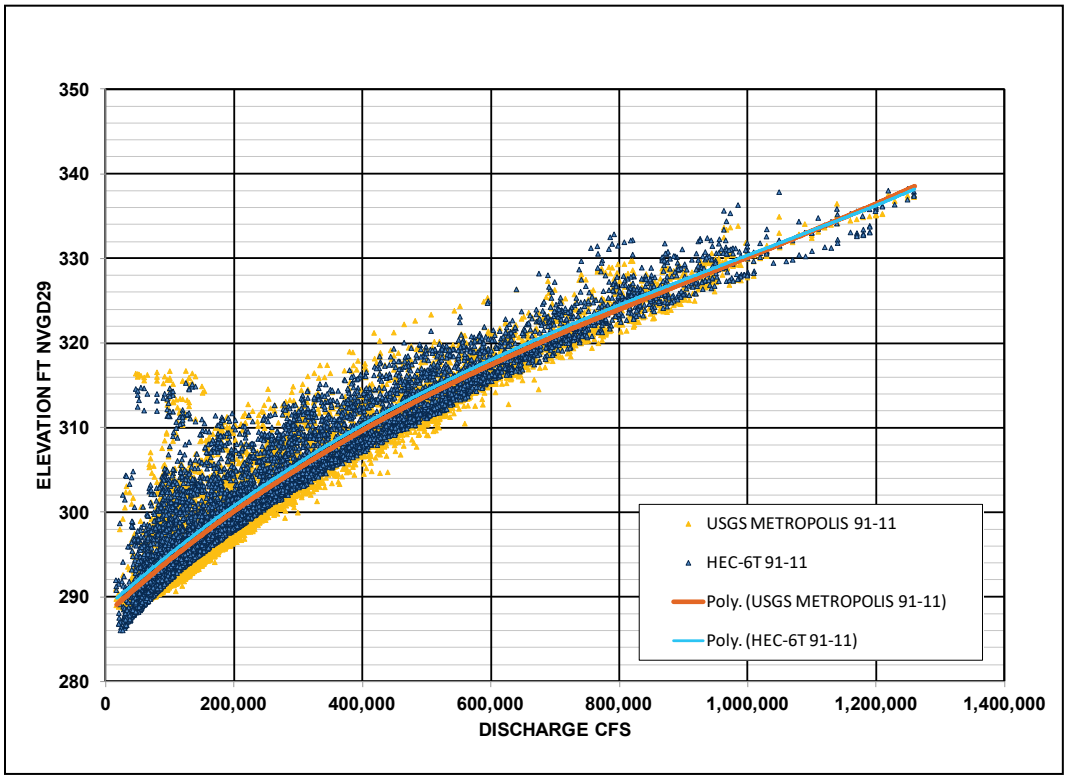

Sand transport function

The sand sediment transport function in the HEC-6T numerical model calculates transport of the total sand and gravel sediment loads. This includes both the sand and gravel bed-material load and the sand wash load. The bed-material load includes size classes found in substantial quantities in the bed and moves as bed load and suspended load. The armoring and sorting algorithm in the numerical model also allows for transport of sand sizes, not found in the bed, as suspended wash load.

The sediment transport function for sand and gravel chosen for this assessment was the Toffaleti-Meyer-Peter Muller function. With this function, bed load is calculated using the Toffaleti (1968) and the Meyer-

Peter Muller (1948) methods and the larger of the two is used. Suspended bed-material load is then calculated using the Toffaleti method. The Toffaleti-Meyer-Peter Muller function is capable of calculating both sand and gravel transport rates for the size classes. The Toffaleti equation was developed for large rivers like the Mississippi River. The Meyer-Peter Muller equation was important to facilitate the transport of gravel size classes known to be in the river bed in the Memphis District reach.

Silt and clay transport functions

The equation for silt and clay deposition used in HEC-6T is the Krone (1962) equation. The required calibration coefficient is the critical bed shear stress below which deposition occurs. In HEC-6T this coefficient has a variable name *DTCL* for clay and *DTSL* for silt. The Krone equation is

$$\frac{C}{C_o} = e^{-k't}$$

$$k' = \frac{\omega\left(1 - \tau_b / \tau_d\right)}{2.3\,D}$$

where:

C = concentration at end of time-step
C_o = concentration at beginning of time-step
t = time = reach length / flow velocity
ω = settling velocity of sediment particle
τ_b = bed shear stress
τ_d = critical bed shear stress for deposition (*DTCL* and *DTSL*)
D = water depth.

Erosion in HEC-6T is calculated based on work by Parthenaides (1965) as adapted by Ariathurai and Krone (1976). The Ariathurai and Krone equation for particle erosion is

$$C = \frac{M_1\, S_a}{Q\,\gamma}\left[\frac{\tau_b}{\tau_s} - 1\right] + C_o$$

where:

M_1 = erosion rate for particle scour
$[\tau_b * ERME/(STME-STCD)]$ $(STCD < \tau_b < STME)$
S_a = surface area exposed to scour
Q = water discharge
τ_s = critical bed shear stress for particle scour *(STCD)*
γ = specific weight of water.

As the bed shear stress increases, particle erosion gives way to mass erosion, and the erosion rate increases. Because the mass erosion can theoretically be infinite, a characteristic time, T_c, is used. With a computation time interval of Δt, the Ariathurai and Krone equation for mass erosion is

$$C = \frac{M_2 S_a}{Q\gamma} \frac{T_c}{\Delta t} + C_o$$

where:

M_2 = erosion rate for mass erosion $(ERME + ER2\ \{\tau_b - STME\})$ $\Delta t / T_c$
T_c = characteristic time of erosion (1 hour)
Δt = duration of time-step.

The critical shear stresses and erosion rates for fine material used in this assessment relate to recently deposited alluvial material and not to the underlying Pleistocene prodelta clay into which the Mississippi River has eroded below New Orleans. It is the cohesive properties of the clay that determine the erosion rate of the recently deposited alluvial material. For this reason, the same coefficients are used for silt and clay in HEC-6T. Further, in HEC-6T the erosion of non-cohesive material is limited by the erosion rate of the clay if there is more than 10% clay in the active layer.

The Flowline Model used the same fine sediment deposition and erosion coefficients as the Regional Model. In turn, the Regional model used the same coefficients as two previous numerical sedimentation studies of the Lower Mississippi River (Copeland 1991; Copeland and Thomas 1992). The coefficients from the 1992 studies were initially based on the work of Thomas et al. (1988) but were adjusted during model calibration to match reported dredging records in Southwest Pass. The use of the same fine

sediment coefficients in the Flowline Model retains the validity of the 1992 model calibration.

Silt and clay deposition coefficients were varied in the models. One set of coefficients was used in Southwest Pass, another in the reach between Head of Passes and RM 11.0, and another upstream from RM 11.0. Varying these coefficients was deemed reasonable to account for the effects of salinity on sediment deposition. Silt and clay coefficients used in all the models are shown in Table 23.

Different coefficients were used in the Myrtle Grove Model and LMR1_FWOP_NRC1_Final_R19.t5. This is attributed to the calibration methodology employed by the researchers who conducted those studies.

Table 22. Silt and clay coefficients for Parthenaides and Krone equations.

Coefficient	Variable Name in HEC–6T	Southwest Pass	RM 0.0 to 11.05	Fresh Water	Units
Shear threshold for clay deposition	DTCL	.005	.003	.001	lb/ft^2
Shear threshold for silt deposition	DTSL	.014	.014	.002	lb/ft^2
Shear threshold for erosion of silt and clay particles	STCD	.025	.020	.020	lb/ft^2
Shear threshold for mass erosion	STME	.04	.04	.04	lb/ft^2
Erosion rate at STME	ERME	.001	.001	.001	lb/ft^2/hr
Slope of the erosion rate curve for mass erosion	ER2	.03	.03	.03	1/hr

Sediment inflow

A combination of measured and calculated data was used to establish sediment inflow boundary conditions. To model sedimentation trends in the Mississippi River, it is necessary to account for movement and storage of each sediment size class. HEC-6T allows for this accounting; however, the required input data are generally lacking. Long-term size class sediment data are available in the study reach, at the upstream boundary on the Middle Mississippi River at Thebes, located 43.7 miles upstream from the Ohio River confluence, and Chester, located

109.9 miles upstream from the Ohio River confluence. Long-term size class data are also available at Union Point (RM 326.6) and Coochie (RM 317.3), which are located upstream from the Old River Control Complex and at Tarbert Landing (RM 306.3), which is located downstream from the Old River Control Complex. A shorter record is available at Belle Chasse, located 76 miles above Head of Passes. Data for the major tributaries, including the Ohio River, are generally limited to the sediment concentrations greater and less than 0.062 mm. The lack of boundary condition data required that size class percentages be estimated by calculation and/or judgment. A continuing sediment data collection program is essential to verify and enhance future sediment inflow predictions.

Sediment concentration is typically measured by mechanical samplers so that only a very small fraction of the actual load is physically measured. However, convention defines the measured suspended load as the sediment load that can be approximated from measured samples. The accuracy of the sediment measurement depends on the sampling collection method, the laboratory analysis of the samples, and the protocol used to calculate average sediment concentration from the sample concentrations. The unmeasured load typically refers to the bed load plus the suspended load between the bed surface and the lowest sampled depth of the sampler's intake nozzle.

In this assessment, sediment transport rating curves at model boundaries and at gages within the study reach were based on the measured (reported) sediment data. Near the upstream boundary of the numerical model, at Thebes, sediment samples are collected using a depth-integrated sampler at five verticals using the equal-discharge increment (EQI) method. The unsampled zone is approximately 4 inches (in.). At this boundary, the unmeasured load includes the bed load and the suspended load in the first 4 in. above the bed. At Tarbert Landing and at Coochie and Union Point, sediment samples are collected using a point sampler. Over the years, the number of verticals and the number of sampling points along each vertical has varied. Theoretically, the entire suspended load is considered to be measured. Practically, this is doubtful for the coarser sediment particles because the concentration profile for coarser particles increases exponentially near the bed and the lowest point samples were taken between 70% and 95% of the depth. Nevertheless, only the bed load is considered

unmeasured at the three gages near the Old River Control Complex. At Belle Chasse, samples are collected approximately 16 times a year with depth-integrated samplers and approximately 18 times a year with a point sampler. The depth integrated samplers have an unmeasured zone of approximately 4 in., and samples are collected at three fixed verticals. The point samples have been collected at four fixed verticals (changed to four EQI in April 2017) with points at 0.1, 0.3, 0.5, 0.7, and 0.9 of total depth at each vertical.

The unmeasured load has been historically estimated to be 15% of the total measured load. This approximation was first suggested by Dr. Hans Einstein in a personal communication in the 1960s (Copeland and Thomas 1992). Based on subsequent studies and investigations, the MVN concluded that the 15% estimate was appropriate (USACE MVN 1980). Numerical sediment studies conducted on the Lower Mississippi River increased the measured bed material load by 10% to 15% to account for unmeasured load at upstream model boundary (Copeland 1990; Copeland and Thomas 1992; Catalyst-Old River Hydroelectric 1999; Thomas 2012 [p. 124]; Sharp et al. 2013). Uncertainty related to the unmeasured load decreases as the distance between the area of interest and the upstream boundary increases. This occurs because the numerical model calculates the total bed-material load. As the sediment calculations move in a downstream direction, the sediment continuity equation is solved, extracting material from the streambed as required to meet the total bed-material load transport capacity. However, the uncertainty increases as the simulation time increases.

Recent development of the ISSDOTv2 methodology (Abraham et al. 2011) has made it possible to physically measure the bed-form component of bed load by mapping the movement of dunes using sonar equipment. Measurements taken in the Mississippi River in the vicinity of the Old River Control Complex (Heath et al. 2015) demonstrated that the bed load percentage of the bed-material load varied with discharge. The bed load percentage of the bed-material load varied from highs near 45% to low values of approximately 10%.

The relative importance of boundary condition precision at each model boundary is related to the contribution of water and sediment from that tributary. The percentage of the annual Mississippi River discharge at Vicksburg for the years 1991–2002 is listed in Table 24. Over 80% of

the annual discharge at Vicksburg comes from the Ohio and Middle Mississippi Rivers. Boundary conditions for these two rivers are by far the most important in the model assessment.

Table 23. Percentage of the annual Mississippi River discharge at Vicksburg 1991–2002.

Ohio River	45.1
Middle Mississippi River	37.4
Arkansas River	8.2
White River	4.4
Yazoo River	3.0
St. Francis River	0.8
Hatchie River	0.6
Obion River	0.5

After completion of the Regional Model study, additional data became available for the Middle Mississippi, Ohio, White, and Yazoo Rivers. New sediment-inflow rating curves were developed for the Flowline Model for these four rivers. The following list contains the Excel file names and USGS gages used to develop both the original and new sediment inflow rating curves. Available data points are shown in parenthesis.

- Upper Mississippi River Tthebes.xlsx; UpperMiss.xlsx
- USGS 07020500 Mississippi River at Chester, IL, 1980–1991 (36)
- USGS 07022000 Mississippi River at Thebes, IL, 1973–2013 (570)
- Ohio River OhioSed.xlsx
- USGS 03612500 Ohio River at Dam 53 near Grand Chain, IL, 1973–2013 (381)
- USGS 03294500 Ohio River at Louisville, KY, 1979–1982 (11)
- Obion River Obion.xlsx
- USGS 07026000 Obion River at Obion, TN, 1975–1990 (145)
- USGS 07026040 Obion River at Highway 51 near Obion, TN, 1990–2005 (56)
- Hatchie River Hatchie.xlsx
- USGS 07030050 Hatchie River at Rialto, TN, 1977–2008 (47)
- USGS 07029500 Hatchie River at Bolivar, TN, 1975–2006 (225)
- St. Francis River StFrancis.xlsx
- USGS 07047907 St. Francis River at Madison, AR, 1977–2009 (450)
- White River White River-new.xlsx

- USGS 07074500 White River at Newport, AR, 1978–1994
- USGS 07077000 White River at DeValls Bluff, AR, 1967–2014 (348)
- USGS 07077800 White River at Clarendon, AR, 1965–1986 (154)
- Arkansas River ArkansasRiver.xlsx
- USGS 07263450 Arkansas River at Murray Dam near Little Rock, AR, 1975–1994 (225)
- USGS 07263620 Arkansas River at David D. Terry L&D below Little Rock, AR, 1969–2014 (444)
- USGS 07265283 Arkansas River at Dam No. 2 near Gillett, AR, 1972–1994 (231)
- Yazoo River YazooWQ-new.xlsx
- USGS 07288800 Yazoo River at Redwood, MS, 1972–1993 (242)
- USGS 07288955 Yazoo River below Steele Bayou near Long Lake, MS, 1994–2014 (378)

A statistical correction factor was applied to the power regression equations to account for bias created by using a least-squares regression for the logarithm of concentration. This bias occurs because the power regression produces a geometric mean instead of an arithmetic mean. The geometric mean is necessarily lower than the arithmetic mean, so concentrations are underestimated using the biased equation. The bias increases with the degree of scatter about the regression. A correction factor proposed by Ferguson (1986) was used to produce an unbiased estimator for both the total measured load and the sand load. The correction factor is given in the following equation:

$$\overline{C_i} = \hat{C}_i \exp\left(2.651\, s^2\right)$$

$$s^2 = \frac{\sum_{i=1}^{n} \left(\log C_i - \log \hat{C}_i\right)^2}{n - 2}$$

where:

$\overline{C_i}$ = unbiased concentration at discharge event i
$\hat{C}_i$ = concentration from biased regression curve
C_i = measured concentration
n = number of measurements.

Middle Mississippi River

Sediment data are available for the Mississippi River at Thebes, IL (07022000), located 43.7 miles upstream from the Ohio River, and at Chester, IL *(*07020500), which is located 109.9 miles upstream from the Ohio River. The number of measurements at Chester is much smaller than at Thebes. Total measured suspended sediment and measured suspended sand data were collected at Thebes between 1973 and 2013 and at Chester between 1982 and 1985. Size class data were collected at Thebes between 1980 and 1991 and at Chester between 1980 and 1991.

The Flowline Model incorporated additional USGS measurements collected through February 2014. The 2003–2012 regression curves at Thebes were revised to account for the additional year of data. There are 165 total suspended load measurements and 129 sand load measure-ments between 2003 and 2013 in the USGS data base (as of 22 May 14). The revised regression equations indicate a significant decrease in sand concentration. The HEC-6T model was updated to use the new regression curves starting on 1 Oct 03. New plots were developed to show total sediment (Figure 25) and total sand (Figure 26) inflow concentrations by decade. These plots show a steady decline in sediment inflow since 1973. A new plot showing the sediment inflow regression curves and equations developed from 2003–2014 is shown in Figure 27. This is the curve that was used to predict future sedimentation trends in the Flowline Model. Table 25 shows the sediment inflow concentrations used in the HEC-6T model.

The Flowline Model unbiased estimators for the measured total and sand concentrations are given by the following equations:

$$C_{total} = 0.001996\,Q^{0.9488}$$

$$C_{sand} = 0.0007843\,Q^{0.8930}$$

Sediment inflow data trends need to be continually monitored to see if the decreased concentration is due to washout from the 2011 flood and if sand concentrations increase again with time.

Size class percentages for each size class were determined using the measured suspended data at Thebes and Chester. Linear regression equations were calculated in EXCEL (UpperMiss.xlsx*)* using 35 samples from Thebes, collected between 1973 and 1991, and 36 samples from

Chester, collected between 1980 and 1991. Multiple samples collected at the two stations on the same day in June 1984 were not included in the analysis to avoid bias. There were no size class data available after 1991. Plots of the regression curves are shown in Figure 28. Although there was considerable scatter for individual measurements, the regression analysis showed little variation in the size class percentage with discharge.

Sediment inflow for the sand size classes determined from regression curves was increased by 15% to account for unmeasured load.

Figure 25. Measured total suspended sediment Mississippi River at Thebes, IL, 1973–2013.

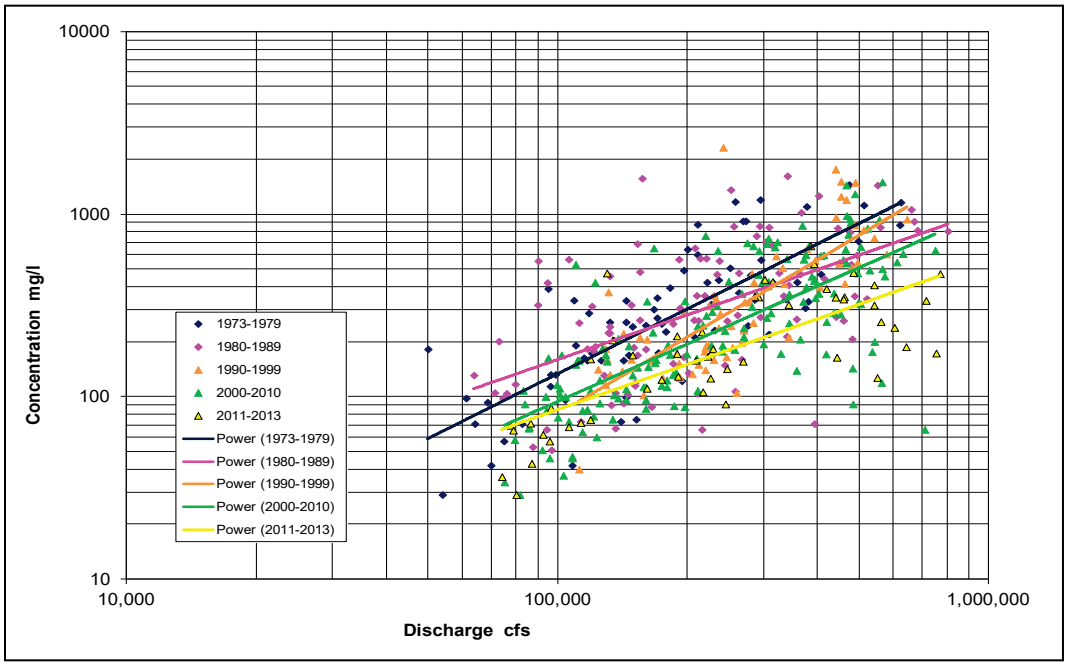

Figure 26. Measured sand Mississippi River at Thebes, IL, 1973–2013.

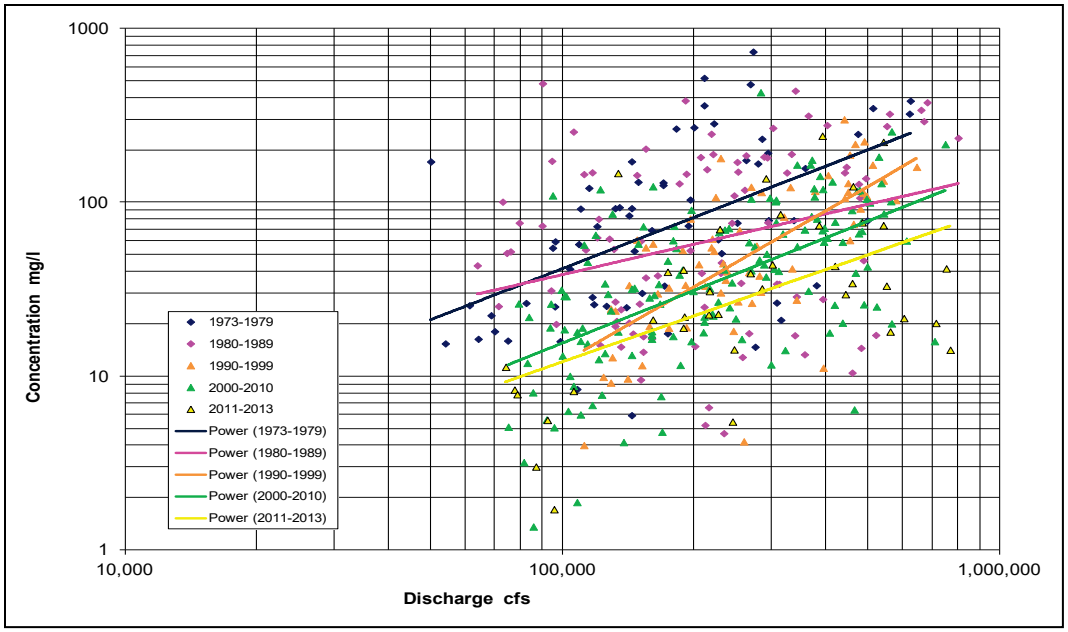

Figure 27. Measured Suspended Sediment Mississippi River at Thebes, IL, 2003–2013.

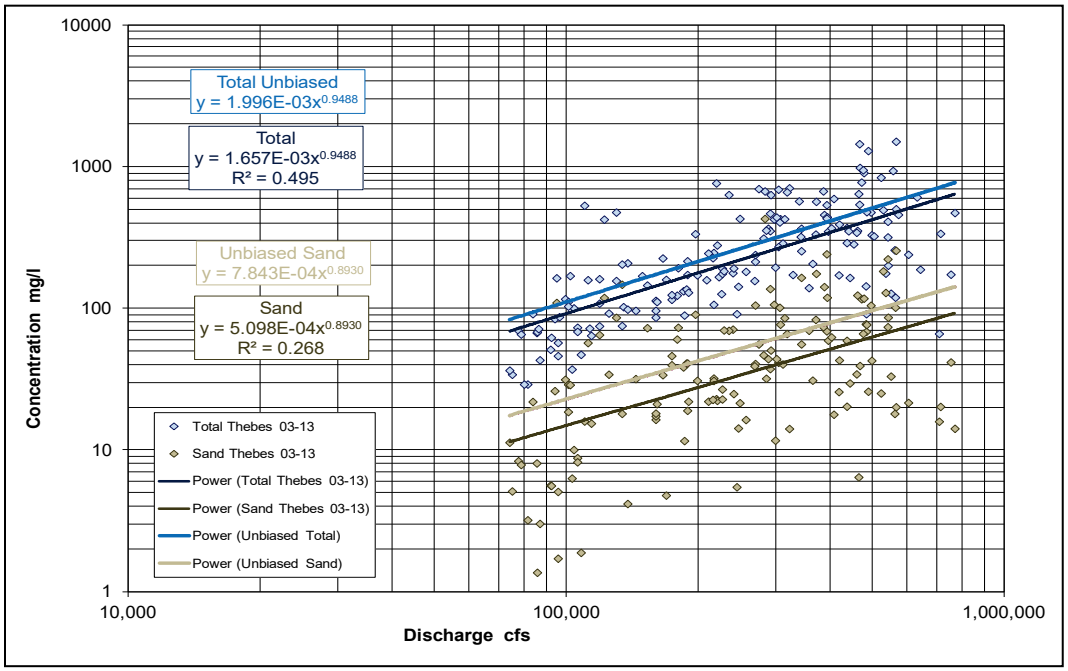

Figure 28. Size class percentages at Thebes, 1973–1991, and Chester, 1980–1991.

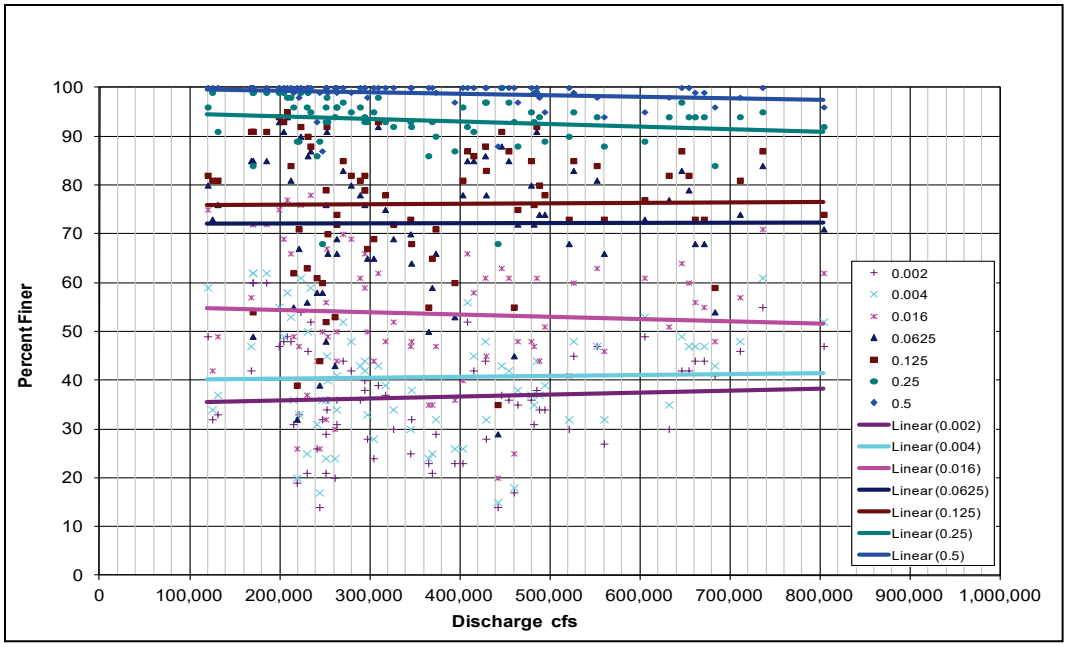

Table 24. 2003–2013 sediment inflow for Middle Mississippi River - Segment 25.

Discharge (cfs)	10,000	60,000	100,000	300,000	500,000	800,000	1,200,000
Concentration mg/L	76.79	76.79	122.30	260.62	423.16	660.96	660.96
Fractions							
Clay	0.4011	0.4011	0.4011	0.0451	0.4090	0.4150	0.4150
Very fine silt	0.0733	0.0733	0.0733	0.0669	0.0605	0.0510	0.0510
Fine silt	0.0733	0.0733	0.0733	0.0669	0.0605	0.0510	0.0510
Medium silt	0.0861	0.0861	0.0861	0.0911	0.0961	0.1035	0.1035
Coarse silt	0.0861	0.0861	0.0861	0.0911	0.0961	0.1035	0.1035
Very fine sand	0.0397	0.0397	0.0397	0.0403	0.0410	0.0419	0.0419
Fine sand	.02155	0.2155	0.2155	0.2011	0.1868	0.1653	0.1653
Medium sand	0.0578	0.0578	0.0578	0.0626	0.0674	0.0746	0.0746
Coarse sand	0.0031	0.0031	0.0031	0.0106	0.0180	0.0292	0.0292
Very coarse sand	0.0000	0.0000	0.0008	0.0016	0.0025	0.0039	0.0039
Very fine gravel	0.0000	0.0000	0.0003	0.0006	0.0010	0.0015	0.0015
Fine gravel	0.0000	0.0000	0.0001	0.0002	0.0003	0.0005	0.0005
Medium gravel	0.0000	0.0000	0.0000	0.0001	0.0001	0.0002	0.0002
Coarse gravel	0.0000	0.0000	0.0000	0.0000	0.0000	0.0000	0.0000
Very coarse gravel	0.0000	0.0000	0.0000	0.0000	0.0000	0.0000	0.0000

Ohio River

The Ohio River sediment rating curves in the Regional Model were based on total suspended sediment and suspended sand data collected at Dam 53 between 1973 and 2010. The Flowline Model incorporated additional USGS measurements collected through January 2014. The original text from the Regional Model report has been modified to reflect the updates and is presented in the following paragraphs.

Sediment inflow from the Ohio River was determined from measured suspended sediment data collected at two USGS gages. The gage closest to the upstream model boundary is at Dam 53 near Grand Chain, IL (03612500), which is 17 miles upstream from Cairo (Ohio River RM 962.6). The second gage is considerably upstream from the model boundary at Louisville, KY (03294500), which is approximately 372 miles upstream from Cairo (Ohio River RM 607.3). Total measured suspended sediment concentration and sand percentages were collected at Dam 53, between 1974 and 2014. Size class percentage data for clay through medium sand were collected at Louisville between 1979 and 1982. The Louisville gage is located a considerable distance upstream from the Mississippi River confluence at Cairo, and the available data were collected 10 years prior to the calibration simulation period. However, the Louisville data are the only suspended size class data available. The Ohio River, in the study reach, essentially has a rigid boundary where most of boundary materials do not actively exchange with the suspended load. Although, sand frequently moves as bed load throughput over a primarily gravel bed, calculation of suspended bed material load from available bed material gradations is not reliable.

During the 40 years between 1974 and 2014 (January), 403 measurements of the total suspended sediment load and 287 measurements of the suspended sand load were available from the Dam 53 gage. Data are compiled in EXCEL file OhioSed.xls/Dam53. Power regression curves were determined from the Dam 53 data for 5 decades covering the span of the measured data. When the sediment concentrations are plotted against discharge in Figure 29, it is apparent that there is considerable scatter, indicating that concentration is a function of more variables than just the discharge. The data plotted in Figure 29 also suggest no long-term trend in the total concentration over the 40-year period. However, the data indicate that the 1990s had a slightly lower average sediment inflow than

the preceding and following decades. Considering the data scatter, this conclusion is accompanied with considerable uncertainty.

Measured total suspended sediment load and measured suspended sand load data collected at Dam 53 between 1991 and 2002 were used to calculate power regression curves for the HEC-6T sediment inflow rating table in the Regional Model. There were 158 measurements for the total suspended concentration and 108 measurements for the sand concentration. The data are plotted in Figure 30. A simple power regression fit of the data produced the following equations, with an R^2 value of 0.59 for the total suspended concentration and 0.50 for the sand concentration:

$$C_{total} = 1.008E-04\, Q^{1.0505}$$

$$C_{sand} = 3.744E-08\, Q^{1.4368}$$

The unbiased power regression curves are

$$C_{total} = 1.244E-04\, Q^{1.0505}$$

$$C_{sand} = 6.4752E-08\, Q^{1.4368}$$

The 1991–2002 unbiased power regression curves used to develop sediment inflow for the HEC-6T model are compared to 1978–2014 measured data and 1978-2014 power regression curves in Figure 31. Considering the extent of the data scatter and the similarity in the unbiased regression equations, the 1991–2002 inflow curves were not changed for the predictive simulations.

There were no suspended sediment size class data available for the 1991–2002 calibration period. In the HEC-6T model, size class percentages for each size class were estimated using the measured suspended data at Louisville collected between 1979 and 1982. Samples were collected on 11 days during these 4 years, with a discharge range between 200,000 and 450,000 cfs. Multiple samples collected on the same day, were averaged to avoid bias. Linear regression equations were calculated in EXCEL (OhioRiver.xls/2011SizeClass%*)* to obtain percentages at specific discharges in the sediment input table. Plots of the regression curves are shown in Figure 32.

The sediment inflow rating curves used in the HEC-6T model, for the Ohio River, are shown in Table 26. Sand loads for very fine, fine, and medium sand were determined from the sand regression curve, and fine load was determined from the difference between the total and sand load regression curves. The range of discharges used to develop the sediment inflow regression curves was between 50,000 and 1,200,000 cfs. In Table 26, the calculated concentration at 1,200,000 cfs was used for discharges greater than 1,200,000 cfs. Assuming a flat concentration curve at higher discharges is typically closer to prototype behavior than an extrapolation of the regression curve.

Size class percentages were calculated from the size class regression curves between 200,000 and 450,000 cfs. Percentages were held constant for discharges beyond the data limits. Sediment inflow for the sand size classes determined from regression curves were increased by 15% to account for unmeasured load. The coarse sand to medium gravel size classes were transported in the unmeasured zone, so inflow fractions for these sediment sizes were determined using the recirculation option in HEC-6T. With this option, a series of steady state discharges are run for a period of time (in this case 25 days) where the sediment load calculated at the downstream end of the segment is re-introduced at the upstream end of the segment for the next time-step until the calculated inflow and outflow of sediment is approximately equal during a time-step. This is equivalent to assuming that the reach is in equilibrium with respect to sediment continuity.

Uncertainty exists with this approach because these calculations are directly dependent upon the designated bed gradation. In this case, the bed gradation came from an average of multiple samples collected at Olmstead Lock and Dam located at RM 970.5 (mileage calculated by adding to Mississippi River mileage at Cairo). Medium sand load was determined using the larger of the fractions calculated from the regression equations or the recirculation option. HEC-6T input calculations are contained in EXCEL file OhioSed.xsl/2011-HEC-6Tin.

Figure 29. Total measured suspended sediment concentration at Dam 53.

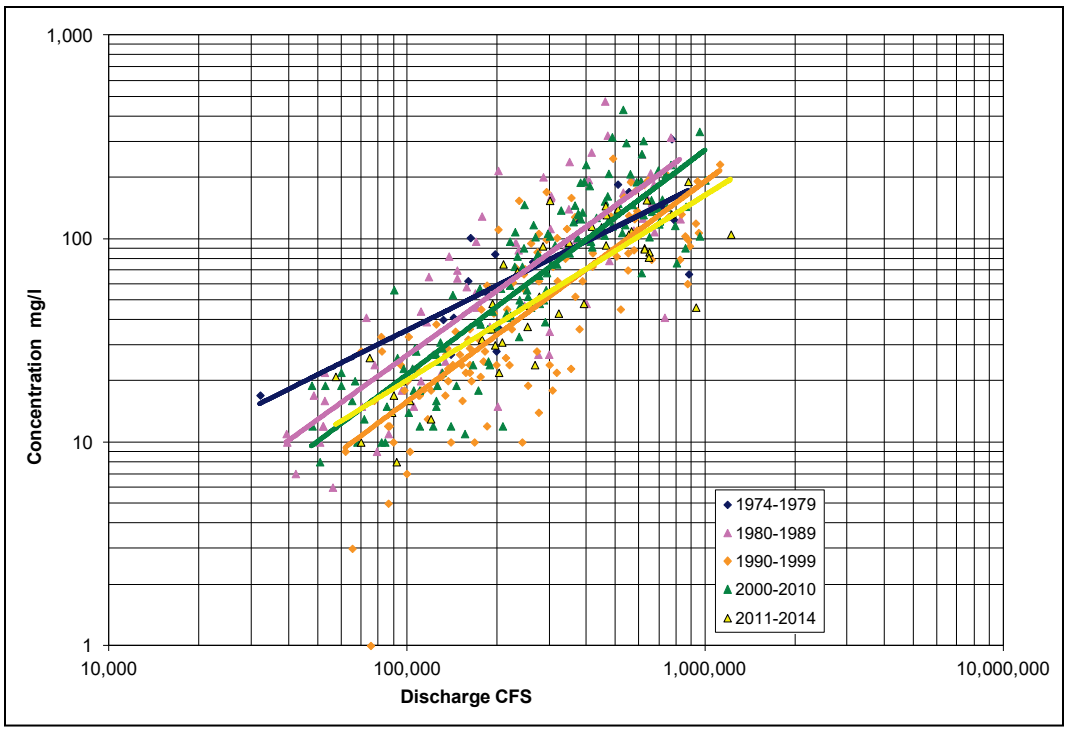

Figure 30. Measured suspended total and sand concentrations at Dam 53.

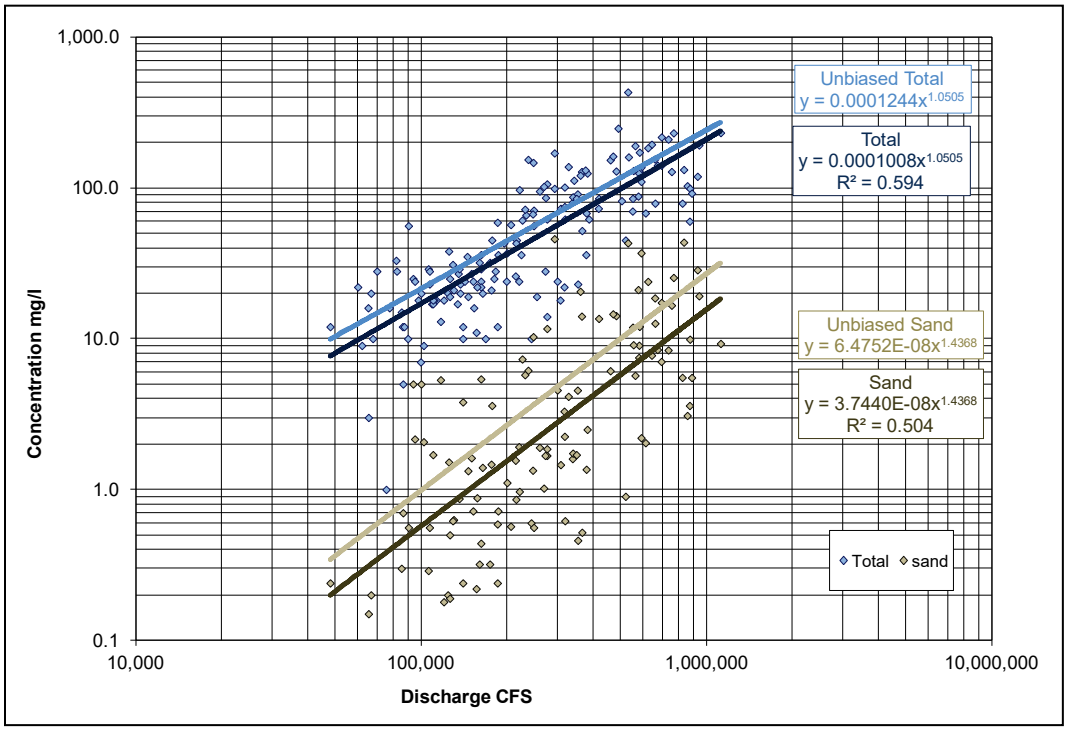

Figure 31. Comparison of sediment regression equations between 1978 and 2014 at Dam 53.

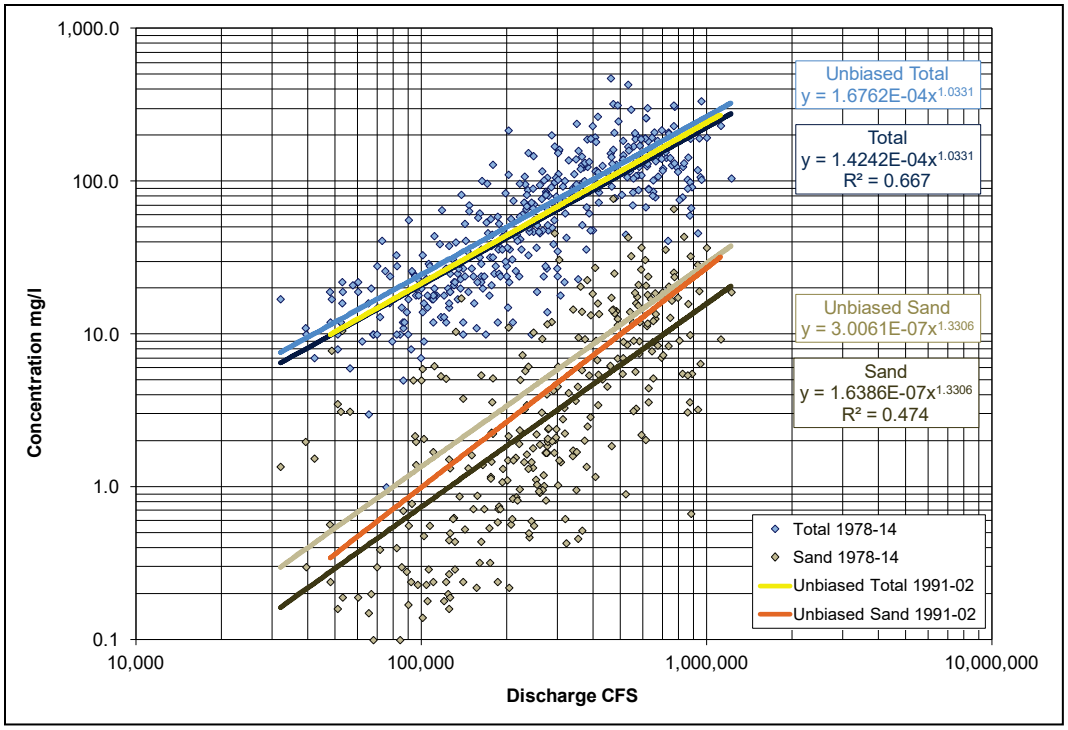

Figure 32. Measured size class percentages at Louisville.

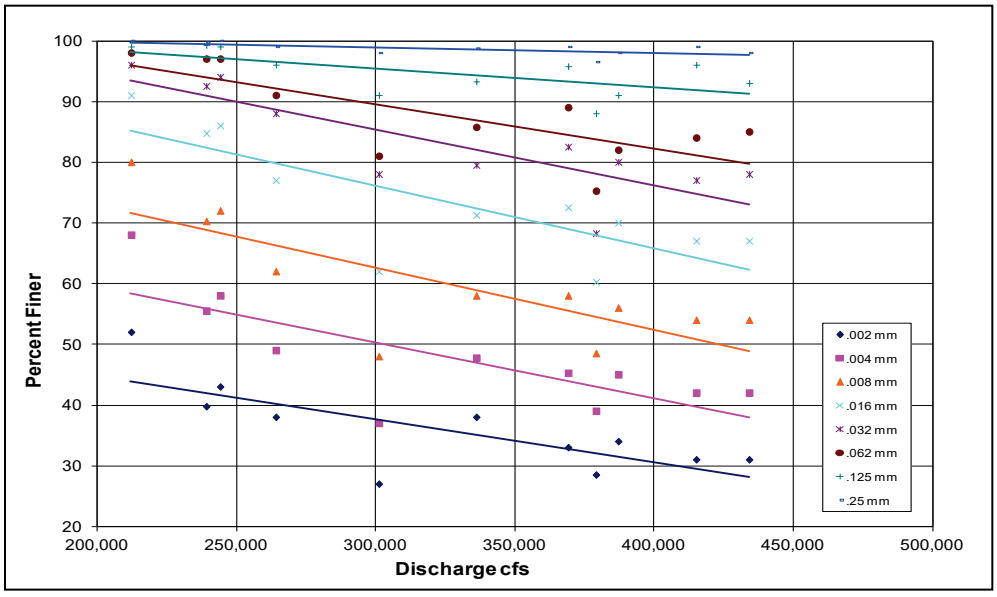

Table 25. Sediment Inflow for Ohio River - Segment 24.

Discharge 1,000 cfs	10	50	100	200	450	800	1000	1200	2000
Concentration mg/L	1.98	10.74	22.24	46.07	108.0	197.7	249.9	302.6	302.6
Fractions									
Clay	0.6035	0.5938	0.5873	0.5788	0.4280	0.4187	0.4145	0.4108	0.4108
VF silt	0.1349	0.1327	0.1313	0.1294	0.1256	0.1229	0.1216	0.1205	0.1205
F silt	0.1377	0.1355	0.1340	0.1321	0.1557	0.1523	0.1508	0.1494	0.1494
M silt	0.0818	0.0805	0.0796	0.0785	0.1287	0.1259	0.1247	0.1235	0.1235
C silt	0.0235	0.0231	0.0229	0.0225	0.0817	0.0799	0.0791	0.0784	0.0784
VF sand	0.0112	0.0208	0.0272	0.0355	0.0527	0.0658	0.0718	0.0770	0.0770
F sand	0.0092	0.0171	0.0223	0.0292	0.0293	0.0366	0.0399	0.0428	0.0428
M sand	0.00090	0.00168	0.00347	0.0137	0.0174	0.0361	0.0326	0.0279	0.0279
C sand	0.0	0.0	0.00118	0.00621	0.0113	0.0137	0.0137	0.0120	0.0120
VC sand	0.0	0.0	0.0	0.00307	0.00667	0.00898	0.00867	0.00806	0.0806
VF gravel	0.0	0.0	0.0	0.0	0.00068	0.00230	0.00226	0.00209	0.00209
F gravel	0.0	0.0	0.0	0.0	0.0	0.00050	0.00101	0.00118	0.00118
M gravel	0.0	0.0	0.0	0.0	0.0	0.0	0.0	0.00015	0.00015
C gravel	0.0	0.0	0.0	0.0	0.0	0.0	0.0	0.0	0.0
VC gravel	0.0	0.0	0.0	0.0	0.0	0.0	0.0	0.0	0.0

Obion and Hatchie Rivers

There were no additional data available for the Obion and Hatchie Rivers. Sediment inflow rating curves from the Regional Model were used in the Flowline Model. The Obion River rating curve was based on data from 1975 to 1995. The Hatchie River rating curve was based on data from 1977 to 1995 and 2004 to 2008.

St. Francis River

There were no additional data available for the St. Francis River. Sediment inflow rating curves from the Regional Model were used in the Flowline Model. The St. Francis River rating curve was based on data from 1977 to 2009.

White River

The White River sediment rating curves in the Regional Model were based on total suspended sediment and suspended sand data collected at three gages between 1974 and 2011. Eleven new measurements (2011–2013) at Devalls were available since completion of the Regional Model study. The Flowline Model incorporated these data into new sediment inflow rating curves. New equations and plots are contained in White River-new.xlsx. The original text in the Regional Model report has been modified to reflect the updates and is presented in the following paragraphs.

The purpose of the White River Segment in the HEC-6T model is to provide sediment inflow to the Mississippi River. Sediment data for the White River were limited and are insufficient for calibration of the White River Segment. Total suspended and sand inflow concentrations were available for a wide range of discharges. However, bed material gradation data and individual size class percentages of the suspended load were lacking. In the HEC-6T model, the White River bed was not allowed to scour below the initial cross-section elevations. Therefore, the river bed was not allowed to contribute any sediment to the Mississippi River. However, deposition was allowed in the model so that sediment inflow at the model boundary could be computationally reduced if hydraulic conditions were favorable. Calculated morphologic changes in the White River are not reliable.

Measured suspended sediment concentrations from three gages on the White River were used to determine sediment inflow concentrations for the HEC-6T model. The USGS reported sediment data at gage number 07077800, White River at Clarendon, AR, between 1974 and 1986. This gage is at the upstream boundary of the model at RM 99.1. A more recent record was reported by the USGS at gage number 07077000, White River at DeValls Bluff, AR, which is located at RM 121.8. Data at this gage extend between 2001 and 2013. At RM 255.0 is USGS gage number 07074500, White River at Newport, AR. Data were collected at this gage between 1978 and 1994. Measured total sediment concentrations and measured sand concentrations from the three gages are compared in Figure 33 and Figure 34, respectively. The figures show considerable scatter for both the total and the sand concentrations. Power regression equations were included on the two figures to help identify data differences at the gages. There were only 12 measurements at DeValls Bluff and 23 measurements at Newport collected during the 1991–2002 calibration period. Considering the data

scatter, it was deemed appropriate to use the measurements from the entire 1974–2013 time period and from all three gages to develop sediment inflow rating curves.

Measured total suspended sediment concentrations and measured suspended sand concentrations collected at Clarendon, DeValls Bluff, and Newport between 1974 and 2013 were used to calculate power regression curves for the HEC-6Tsediment inflow rating table. There were 285 measurements of the total suspended concentration and 281 measurements of the sand concentration. The data are plotted in Figure 35. A simple power regression fit of the data produced the following equations, with an R^2 value of 0.048 for the total suspended concentration and 0.041 for the sand concentration:

$$C_{total} = 7.3323Q^{0.2081}$$

$$C_{sand} = 0.2909\,Q^{0.3323}$$

The unbiased power regression curves are

$$C_{total} = 9.1520\,Q^{0.2081}$$

$$C_{sand} = 0.5694\,Q^{0.3323}$$

The measured White River data included a sand-silt break, and these data were used to determine the inflow concentrations for fines and sand. However, there were no additional size class percentage data available. The sand size class percentages were taken to be the same as the average sand size class percentages at Thebes and Chester. Likewise, the clay and silt size class percentages were taken to be the same as the average clay and silt size class percentages at Thebes and Chester. These were determined by summing the percent finer data from 71 Chester and Thebes samples collected between 1973 and 1991. These percentages are independent of discharge.

The sediment inflow rating curves used in the HEC-6T model, for the White River, are shown in Table 27. The discharge range used to develop the sediment inflow regression curves was between 3,000 and 300,000 cfs. In Table 27, the calculated concentration at 300,000 cfs was used for higher discharges. A flat concentration curve at higher discharges is typically closer to prototype behavior than an extrapolation of the regression curve. In the

HEC-6T sediment inflow table, fine sand through coarse sand size class percentages were increased by% to account for unmeasured load. Calculations for the sediment inflow table are in EXCEL file WhiteRiver-new.xls/HEC-6T.

Figure 33. Measured suspended sediment concentrations at three gages, White River.

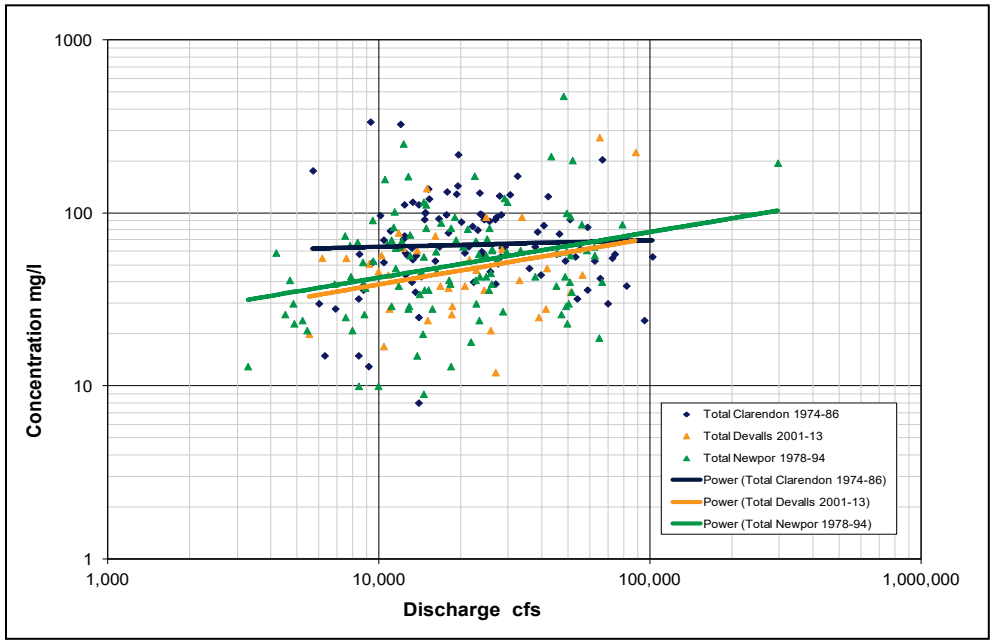

Figure 34. Measured suspended sand concentrations, White River.

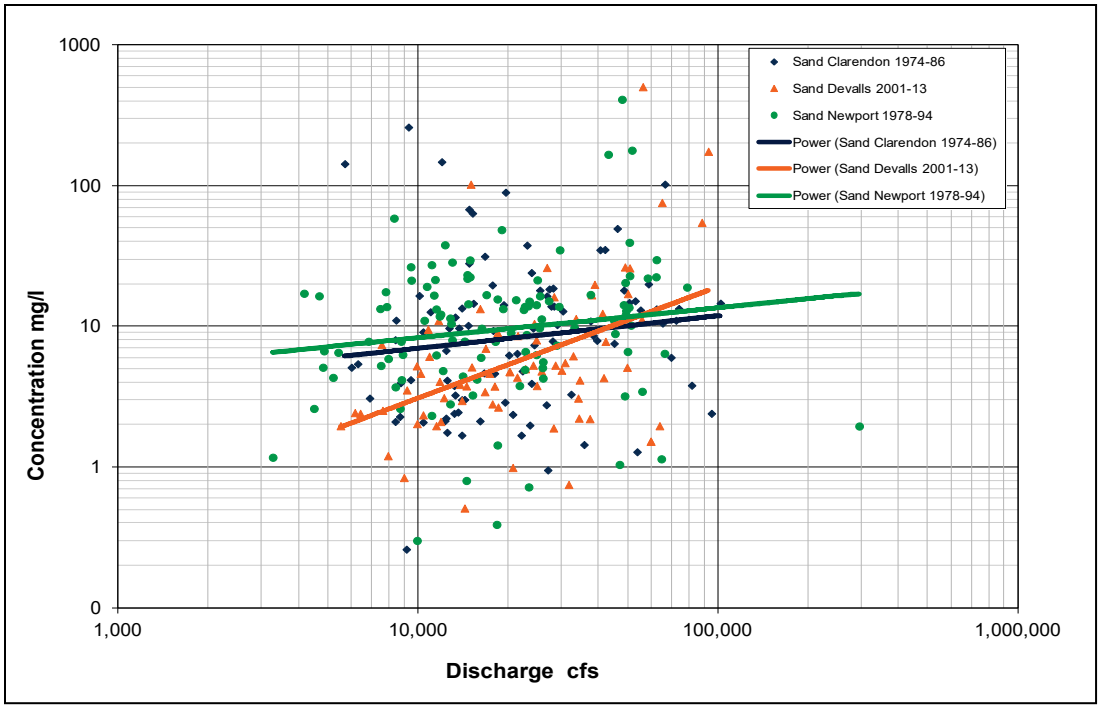

Figure 35. Measured suspended sediment concentrations White River, 1974–2013.

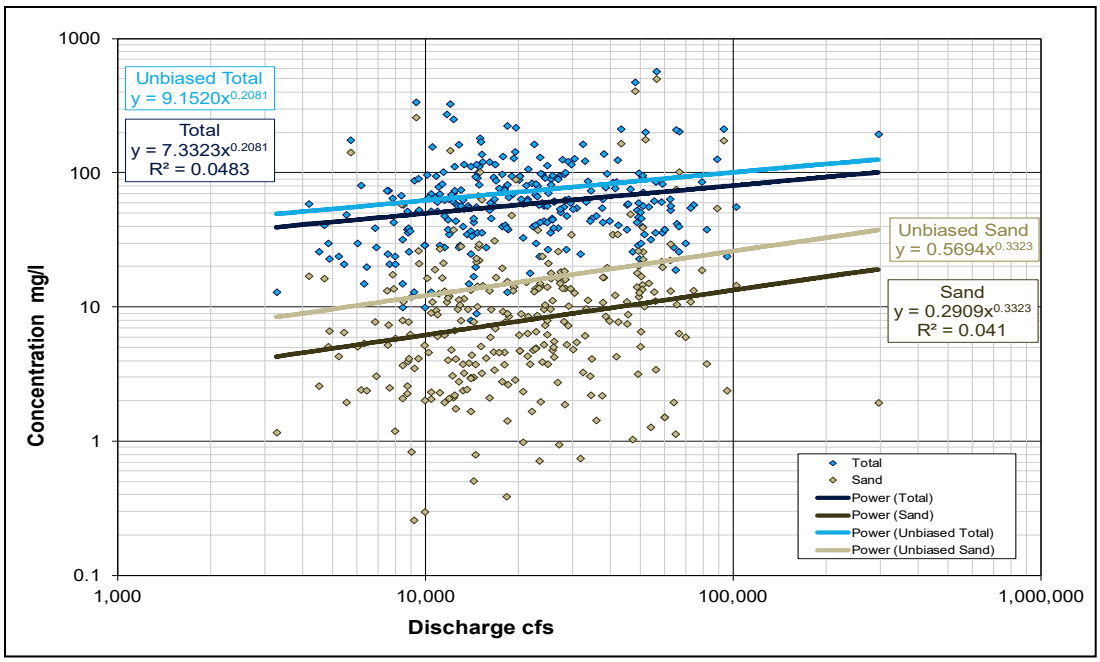

Table 26. Sediment inflow for White River - Segment 10.

Discharge	1000	3000	10,000	50,000	100,000	300,000	800,000
Concentration mg/L	48.4	48.4	62.2	87.0	100.5	126.3	126.3
Fractions							
Clay	0.4707	0.4707	0.4554	0.4309	0.4188	0.3973	0.3973
VF silt	0.0729	0.0729	0.0705	0.0667	0.0648	0.0615	0.0615
F silt	0.0747	0.0747	0.0723	0.0684	0.0664	0.0630	0.0630
M silt	0.1068	0.1068	0.1033	0.0977	0.0950	0.0901	0.0901
C silt	0.1068	0.1068	0.1033	0.0977	0.0950	0.0901	0.0901
VF sand	0.0280	0.0280	0.0326	0.0398	0.0434	0.0497	0.0497
F sand	0.1185	0.1185	0.1376	0.1681	0.1832	0.2100	0.2100
M sand	0.0390	0.0390	0.0453	0.0553	0.0603	0.0691	0.0691
C sand	0.0074	0.0074	0.0086	0.0104	0.0114	0.0131	0.0131
VC sand	0.0000	0.0000	0.0000	0.0000	0.0000	0.0000	0.0000
VF gravel	0.0000	0.0000	0.0000	0.0000	0.0000	0.0000	0.0000
F gravel	0.0000	0.0000	0.0000	0.0000	0.0000	0.0000	0.0000
M gravel	0.0000	0.0000	0.0000	0.0000	0.0000	0.0000	0.0000
C gravel	0.0000	0.0000	0.0000	0.0000	0.0000	0.0000	0.0000
VC gravel	0.0000	0.0000	0.0000	0.0000	0.0000	0.0000	0.0000

Arkansas River

There were no additional data available for the Arkansas River. Sediment inflow rating curves from the Regional Model were unchanged. The Arkansas River rating curve was based on data from 1974 to 2010.

Yazoo River

The Yazoo River sediment rating curves in the Regional Model were based on total suspended sediment and suspended sand data collected at two gages between 1978 and 2013. Two new measurements (Oct 2010) at Redwood and 211 new measurements at Steel Bayou (2004–2013) were available since completion of the Regional Model study. The Flowline Model incorporated these data into new sediment inflow rating curves. New equations and plots are contained in YazooWQ-new.xlsx. The original text in the Regional Model report has been modified to reflect the updates and is presented in the following paragraphs.

The purpose of the Yazoo River Segment in the HEC-6T model is to provide sediment inflow to the Mississippi River. Data are insufficient for calibration of the Yazoo River Segment, and calculated morphologic changes should be treated with caution. There are significant suspended sediment measurements of the total and sand load available for a wide range of discharges. However, only two bed samples were available, and there were no data defining the individual size class percentages in the suspended load.

The USGS has measured suspended sediment at Redwood (RM 16.7) and downstream from Steel Bayou (RM 9.5). Suspended sediment samples were collected at the Yazoo River at Redwood, MS, gage (USGS 07288800) between 1978 and 1993 and in 2010. Suspended sediment samples were collected at the Yazoo River below Steele Bayou near Long Lake, MS, gage (USGS 07288955) between 1995 and 2013. The data from both gages were plotted together to determine power regression equations for the total load and the sand load. Unbiased regression equations were calculated for both. The measured data and regression curves are shown in Figure 36.

The total measured load data were used to evaluate the possibility of a declining or increasing trend in the sediment delivery to the Mississippi River. Power regression curves were calculated for the 1991–2002 and

2003–2013 time periods. These curves were found to be very close to the regression curve for the entire 1978–2013 period as shown in Figure 37.

The inflowing sediment load size class percentages for fines and sands were assumed to be the same as the measured size class percentages from 1991–2002 data at Coochie and Union Point. These sediment gages are located at Mississippi RMs 317 and 326, respectively, and are the closest gages with size class data. The total fine sediment concentration was determined from the measured Yazoo River data, and then the fine sediment size class distribution was taken from the Coochie and Union Point fine sediment size class distribution data. Similarly, the total sand concentration was determined from the measured Yazoo River data, and then the sand size class distribution was taken from the Coochie and Union Point data. This methodology results in a significant discontinuity between coarse silt and very fine sand concentrations in the inflowing sediment load rating curves.

The sand concentrations were arbitrarily increased by 15% to account for the unmeasured load. The sediment inflow rating curves for the Yazoo River are shown in Figure 38.

Only two bed material samples were available for the Yazoo River. The USGS collected these samples at the Steele Bayou Gage. Both samples were collected in August, one in 1995 that contained only 8% sand and one in 1997 that contained 5% sand. These data suggest that the bed of the Yazoo River is primarily cohesive. Therefore, the bed sediment reservoir in the HEC-6T model was set to zero. The initial bed gradation in the Yazoo River was determined based on the two measurements, normalizing them to 100% sand. Since the bed sediment reservoir has been given a zero depth, this bed gradation only serves as a starting point in the numerical solution of the sediment continuity equation.

Figure 36. Sediment concentration Yazoo River at Redwood and Steel Bayou, 1978–2013.

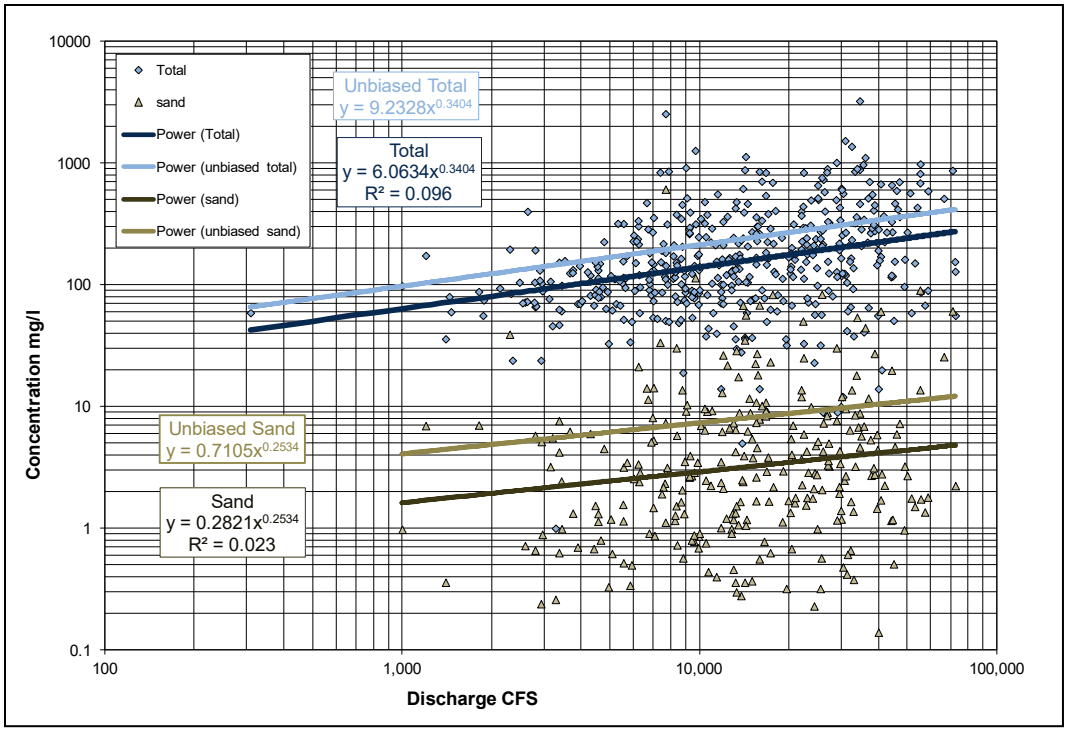

Figure 37. Total sediment concentration trends Yazoo River, 1978–2013.

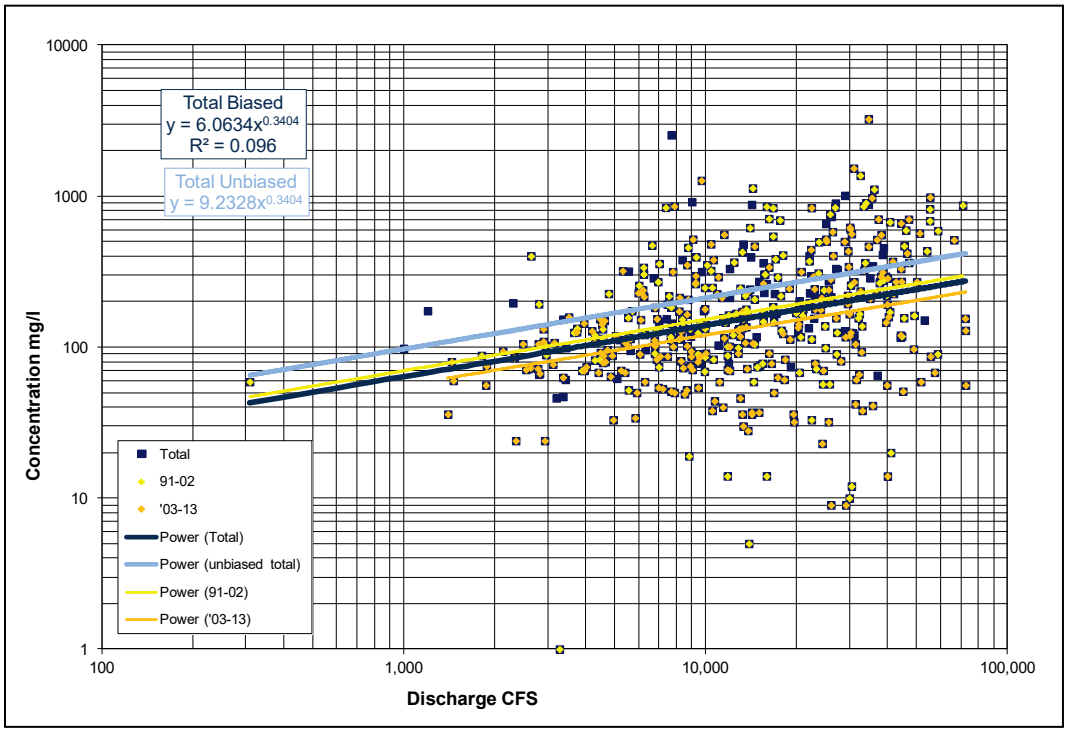

Figure 38. Sediment inflow rating curves for Yazoo River.

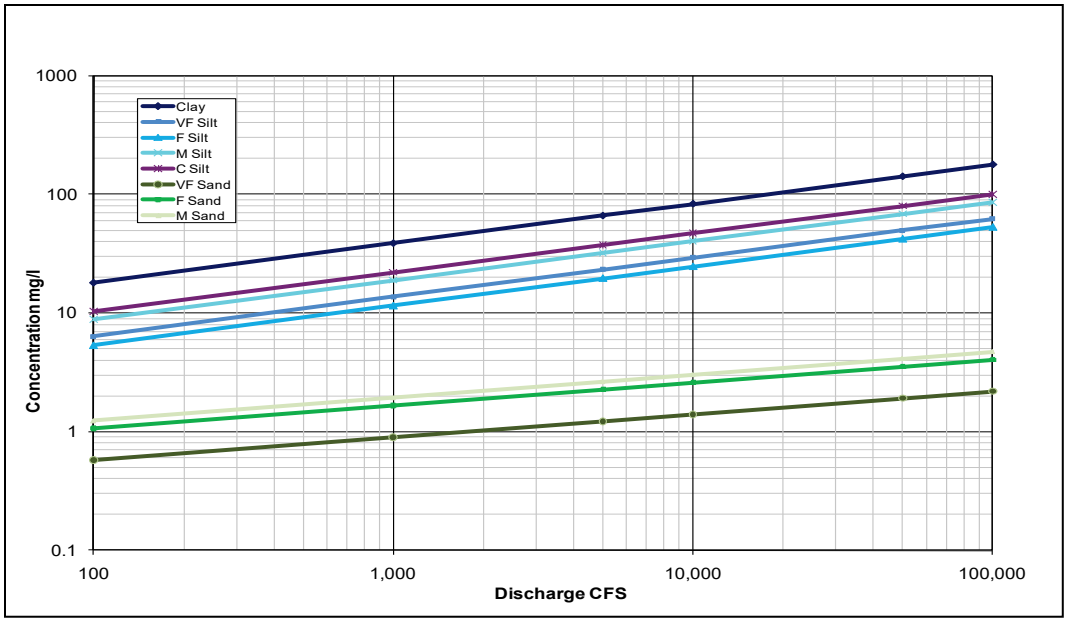

3 Calibration and Verification

Calibration and verification of the regional model

The Regional Model was calibrated and verified according to the methodologies described in USACE, HEC (1992) and Thomas and Chang (2008). Terminology for the assessment process of preparing a numerical model for predictive use is not consistent. Calibration, circumstantiation, validation, and verification are common terms used in practice. Terminology from the above sources was adopted for use in this assessment. Calibration is defined herein to be the process of arriving at roughness coefficients, a sediment transport function, model parameters, and representative data that will allow the model to calculate values that agree with values measured in the prototype. Verification is defined herein as the process that demonstrates that the calibrated model will match the prototype when specified boundary conditions, such as time period or cross section geometry, are changed.

Calibration of the Regional Model is described in detail in the Regional Model Report. The calibration process included selection of model parameters, sediment transport function, steady-state fixed-bed tests, steady-state movable-bed tests, and quasi-unsteady movable-bed tests.

Model parameters of computational time-step and sediment exchange increment were chosen based on convenience and experience. The model time-step was 1 day. Previous studies on the Lower Mississippi River had shown that a longer computational time-step could be used, but since discharge data are typically provided as a mean daily value, it is more convenient to use a constant 1-day time-step. The exchange increment used in the sorting and armoring algorithm was 1/20 day. This value was found to reproduce the same results as a much shorter exchange increment calculated by the program.

The sediment transport function chosen for this assessment was a combination of the Toffaleti (1968) and Meyer-Peter Muller (1948) equations. This function reproduced measured sand size class yields at downstream sediment gages between 1991 and 2002.

Steady-state, fixed-bed tests were conducted to calibrate roughness coefficients and to ensure that the model reproduced acceptable hydraulic

results. Roughness coefficients were adjusted so that the calculated water-surface profiles matched 1991–2002 average stages at gages in the study reach. Channel velocity and channel discharge profiles were plotted to ascertain if the model were reproducing acceptable hydraulic results. Adjustments to channel geometry were made in cases where the adjacent cross sections had unreasonable differences.

Steady-state, movable-bed tests were conducted with a constant channel-forming discharge run for approximately 5 years. This test was used to adjust the initial bed-material gradation to reflect reach averaged conditions. The test also demonstrated that cross-section changes over time tended to converge on an equilibrium condition in response to a constant-discharge simulated hydrograph. This test also validated the choice of computational time-step.

The quasi-unsteady flow movable-bed test was conducted simulating the 1991–2002 hydrograph. In a sense, this test was a verification of the numerical model because no further adjustments were made to achieve the reported results. The model reasonably duplicated 1991–2002 specific gage trends that had been developed from measured data. Measured and calculated bed-material gradations from 1991 and 2005 were compared and found to be within a reasonable range. Measured and calculated sediment concentrations and size class distributions at Tarbert Landing and Belle Chasse were found to be reasonable. Measured and calculated sediment concentrations and total sand yields at Union Point/Coochie, Vicksburg, and Memphis were also compared and found to be consistent.

The quasi-unsteady movable bed test was also used to adjust the model to measured dredging quantities in Southwest Pass. This was strictly a calibration test as cohesive sediment parameters were adjusted to match reported dredging between 1991 and 2002.

The Regional Model was verified/validated by simulating a deposition trend in the Mississippi River downstream from the Old River Control Complex. Measured deposition between RMs 310.1 and 315.4, as determined from the 1992 and 2002 hydrographic surveys, was compared to calculated deposition from the HEC-6T model. The calculated deposition was 90% of the measured deposition. These results provide an indication of the accuracy associated with quantifying deposition. Of course, systematic and random errors are attached to both the measured

data and the calculated data, and neither can be assumed to be *truth*. All things considered, the comparison suggests that the numerical model is very successful in predicting deposition on a reach scale.

The Regional Model was further verified by simulating erosion that occurred at Smithland Crossing (RM 297.45–300.3) in response to construction of a dike field between 1990 and 1996. The HEC-6T model did not reproduce the changes in channel shape due to the 1D limitations of the model. However, calculated degradation in the dike field was within 10% of the measured change determined from the 1992–2002 hydrographic survey.

As a result of the calibration/verification analysis, the Regional Model was established as a tool to evaluate the effects of various boundary condition changes upon long-term sedimentation processes in the Lower Mississippi River. The Regional Model's comprehensive calibration/verification analysis applies equally to the Flowline Model. Additional calibration of roughness coefficients was conducted for the Flowline Model to account for the record flood discharges in 2011. Additional verification was achieved using specific gage trends for the additional simulation time between 2002 and 2013 as discussed in the following section of this report.

Calculated specific gage trends

Stage is typically a better indicator of geomorphic change than bed elevation. Specific gage plots, which are based on historical stage and discharge data, have been used extensively to document trends in water-surface elevations at gages. Specific gage analyses provide important perspectives relative to past river behavior at a specific location.

There are a number of limitations associated with specific gage analysis. Specific gage depicts conditions at a gaging station, which may or may not be representative of conditions further upstream or downstream. Specific gage records chart the historical record and cannot be extrapolated to predict future conditions. Specific gage incorporates all the morphological factors influencing stage and cannot be used to identify the effect of an individual variable.

The advantage of a numerical model is that it can be used to predict future trends in water-surface elevations and it can be used to predict both past and future trends between gages. The reliability of the model's prediction

is predicated upon the model's ability to simulate the significant geomorphic processes that influence long-term change in stage. The HEC-6T numerical model accounts for future aggradation and degradation of the river bed but does not account for possible future changes in bed roughness, floodplain roughness, or change in channel shape due to meandering. There is also uncertainty associated with future changes in the boundary conditions, such as sediment inflow. Confidence in numerical model prediction is enhanced when historical changes in specific gage are correctly reproduced by the model. This success implies that the most significant geomorphic processes have been accounted for in the numerical simulations.

River bed elevations can change significantly with discharge. An example is shown in Figure 39 where calculated bed-elevation changes with time at two adjacent cross sections are plotted. At RM 415, average bed elevations tend to increase at high flow and decrease at low flow. The opposite trend occurs at RM 411.2. In addition, the change in bed elevation occurs more slowly than the change in discharge. There is not a direct correlation between discharge and bed elevation because the bed elevation is heavily dependent on antecedent conditions.

Figure 39. Calculated bed elevation change with time at a bend and at a crossing.

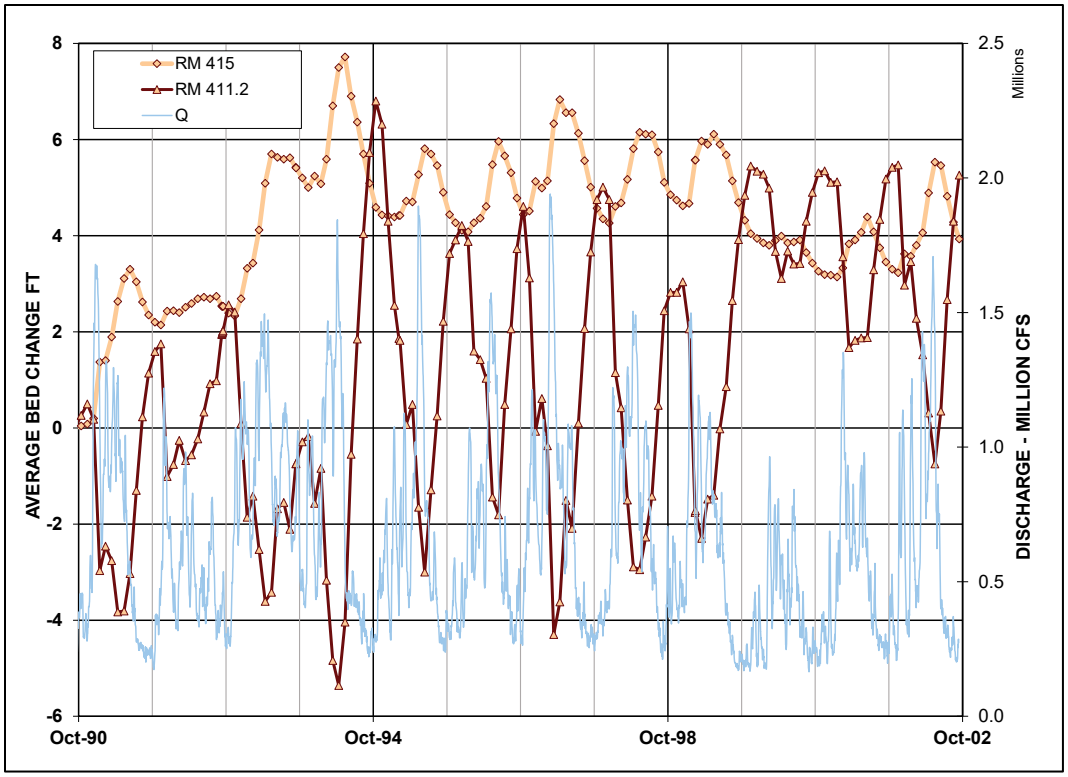

Specific gage plots at major gages along the Mississippi River using both traditional specific gage techniques and HEC-6T numerical model calculations are presented in Figure 40 through Figure 46. Historical specific gage data were provided by Biedenharn et al. (2017). They presented specific gage plots for 22 gages along the Lower Mississippi River between Cairo and Donaldsonville. Only the gages with both discharge and stage measurements are compared herein. Both the historic and HEC-6T calculated curves were developed using the direct step method (defined by Biedenharn et al. [2017]) with a bin range of ± 2.5%. The bin includes all the discharges within a specified percentage of the nominal discharge. The historic data are subject to random errors and natural variability about the stage discharge relationship. The HEC-6T results are subject to systematic errors and represent average conditions, neglecting natural variability about the stage-discharge relationship. The historical data come from actual field measurements. The HEC-6T results come from daily calculations and are thus more numerous.

Results from both methods can be compared for the period between 1991 and 2013. No adjustments were made to the numerical model to match the specific gage data. The favorable correlation of measured and calculated stages between 2002 and 2013 provides verification of the Regional Model.

Figure 40. Specific gage at Red River Landing – RM 302.4.

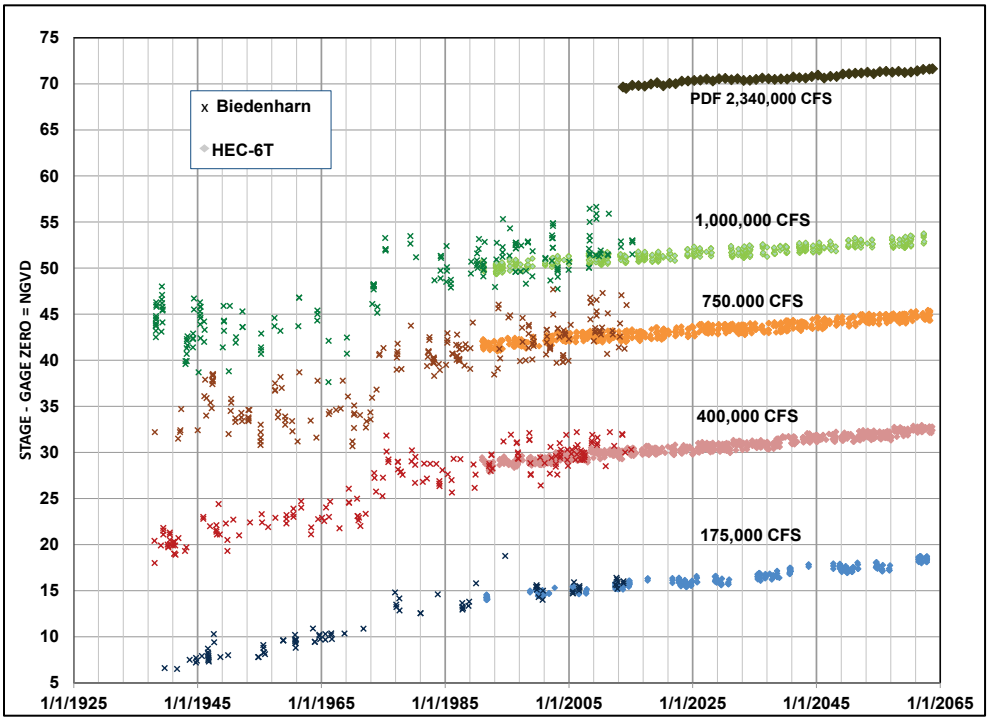

Figure 41. Specific gage at Natchez – RM 363.3.

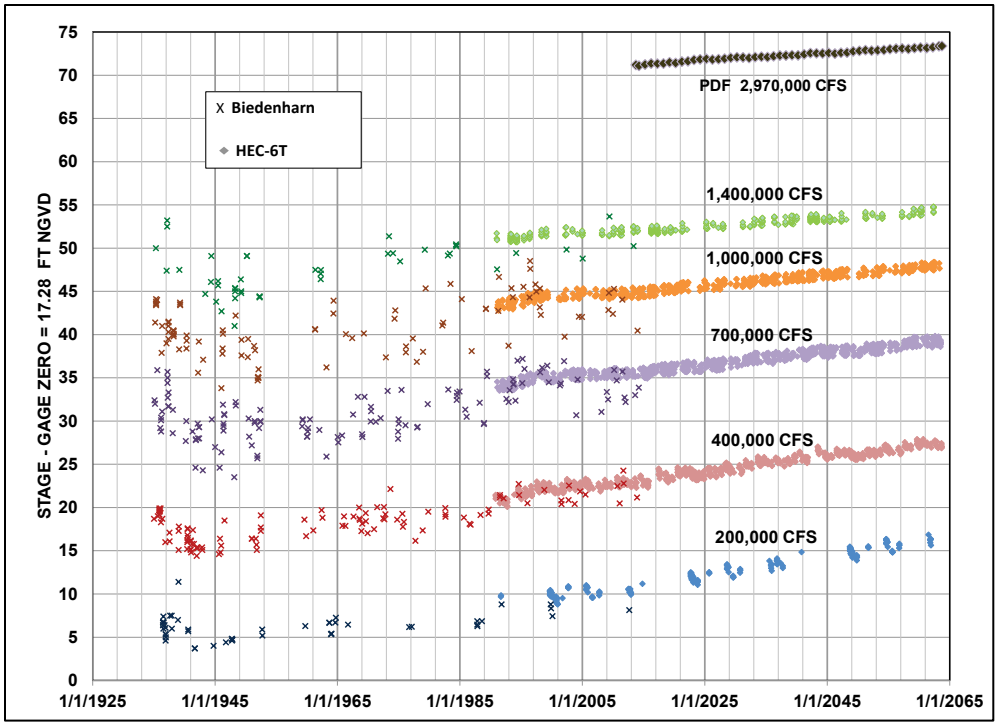

Figure 42. Specific gage at Vicksburg – RM 435.7.

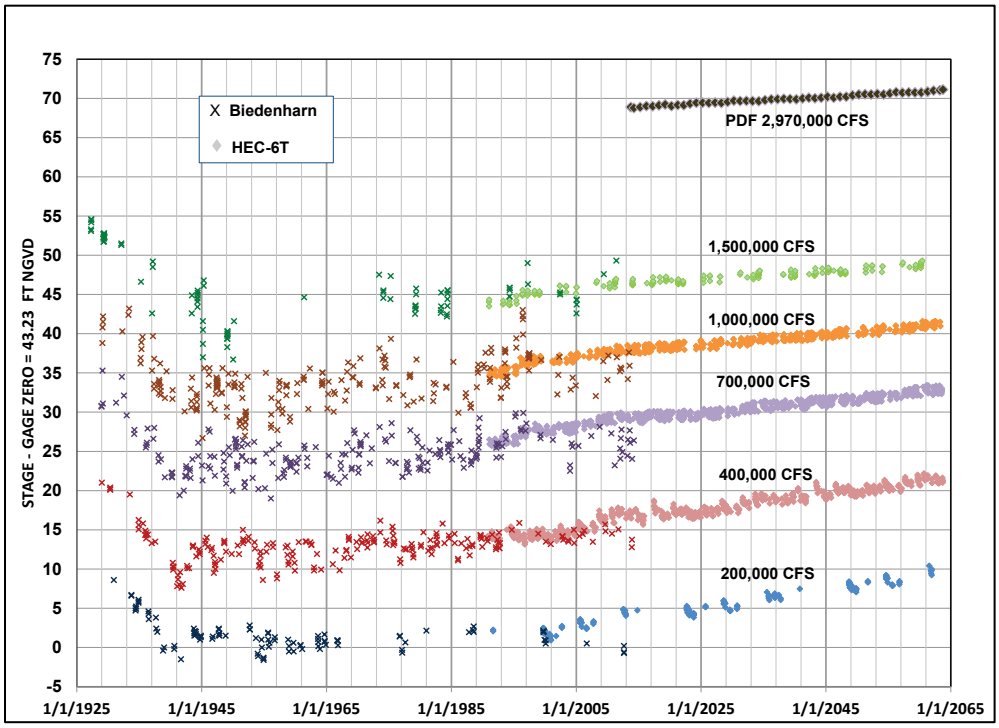

Figure 43. Specific gage at Arkansas City – RM 554.1.

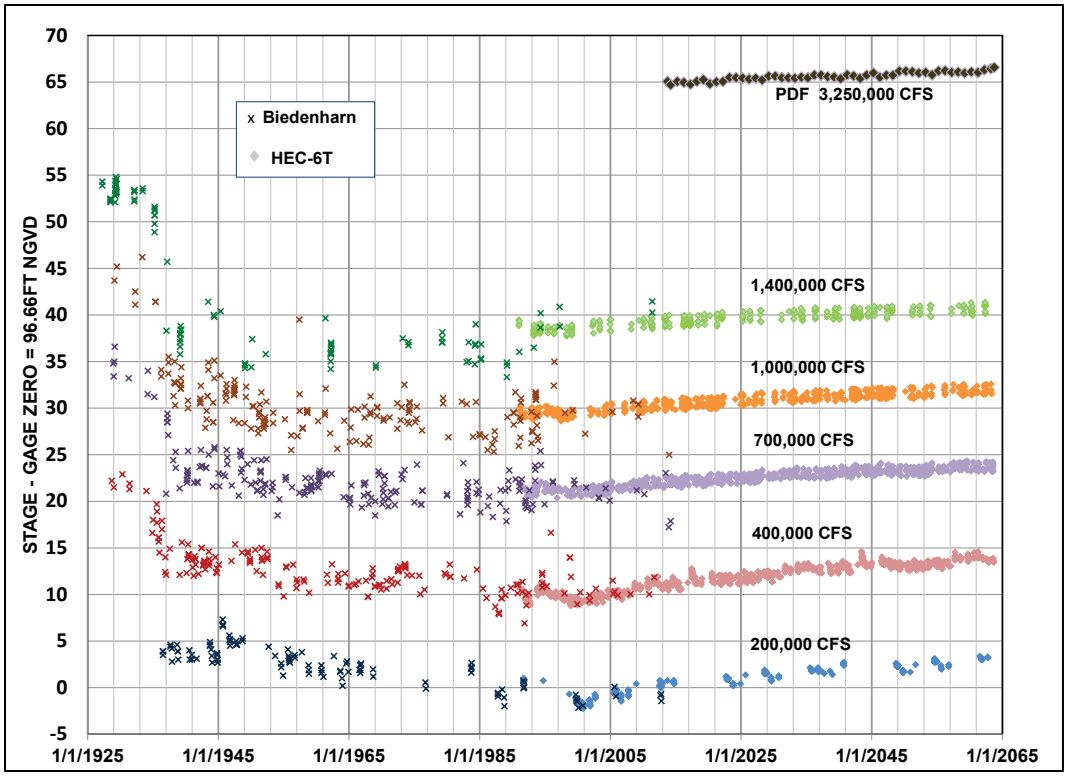

Figure 44. Specific gage at Helena – RM 663.

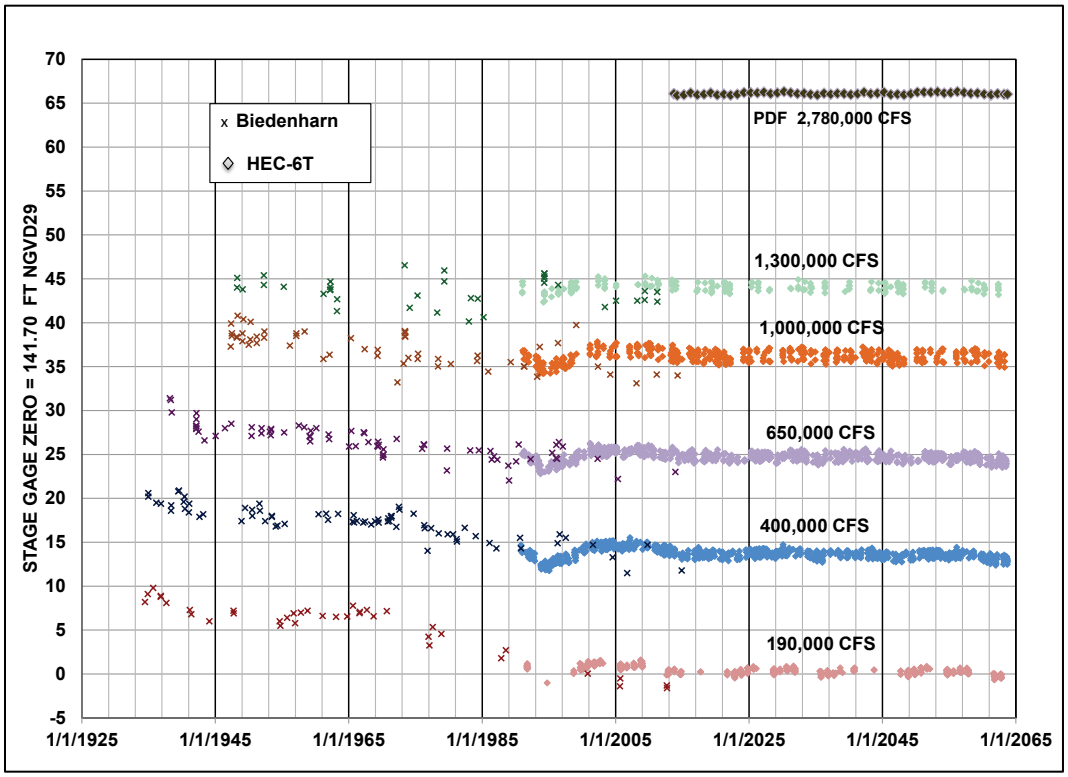

Figure 45. Specific gage at Memphis - RM 734.4.

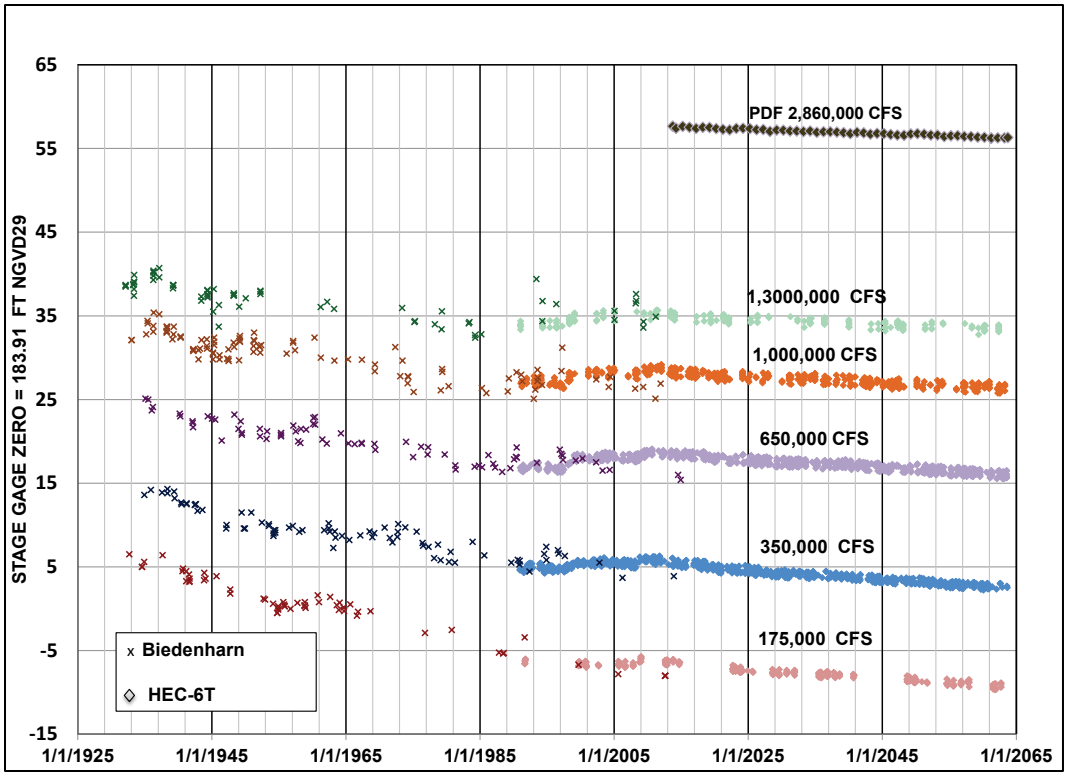

Figure 46. Specific gage at Hickman – RM 922.

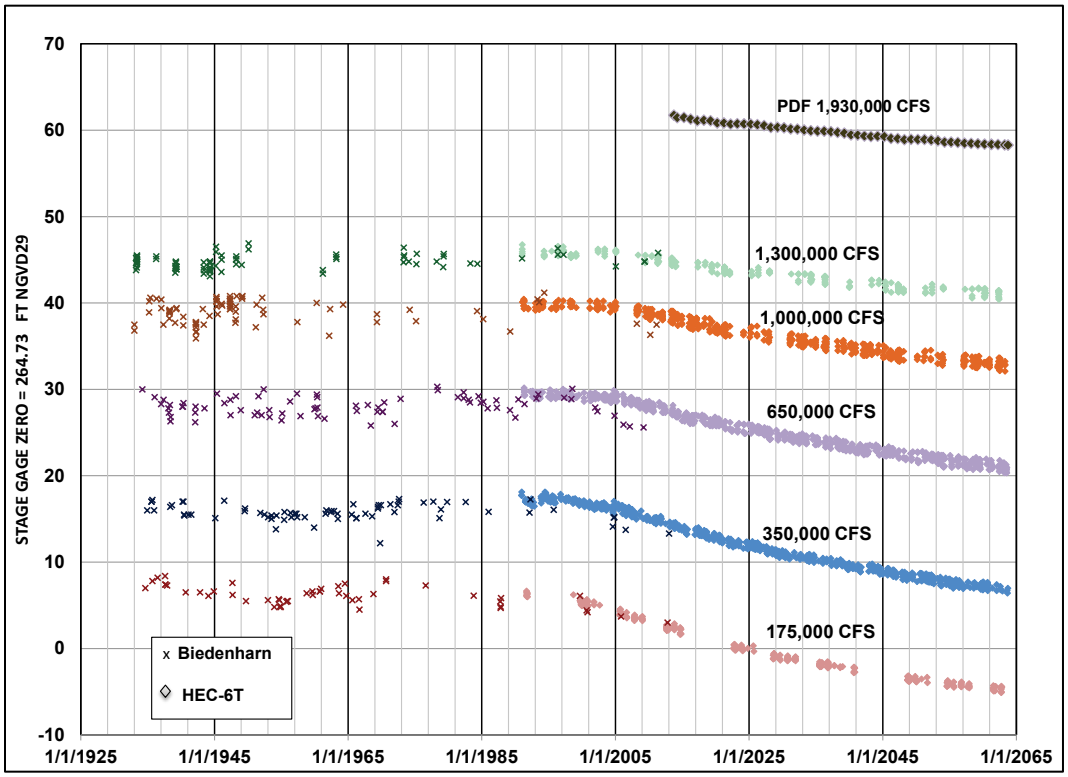

Specific gage analyses typically refer to a long-term decline in water-surface elevation as degradation and a long-term increase in water-surface elevation as aggradation. This terminology conflicts with sediment studies that typically refer to degradation as a long-term decline in bed elevation and aggradation as a long-term increase in bed elevation. Bed elevation change does not necessarily correlate with water-surface elevation change. The calculated bed elevation and PDF water-surface elevation change after 50 years is shown in Figure 47. The figure shows significant fluctuation in bed elevation from station to station. Water-surface fluctuations are less pronounced. However, the overall trends are consistent. Of particular interest is the hard point in the vicinity of Hickman (RM 922) where the bed change is zero but the water-surface elevation is declining. The hard point is submerged by the river and does not act as an effective control on water-surface elevation.

Figure 47. Calculated water-surface elevation and bed changes for the 1955 PDF after 50 years.

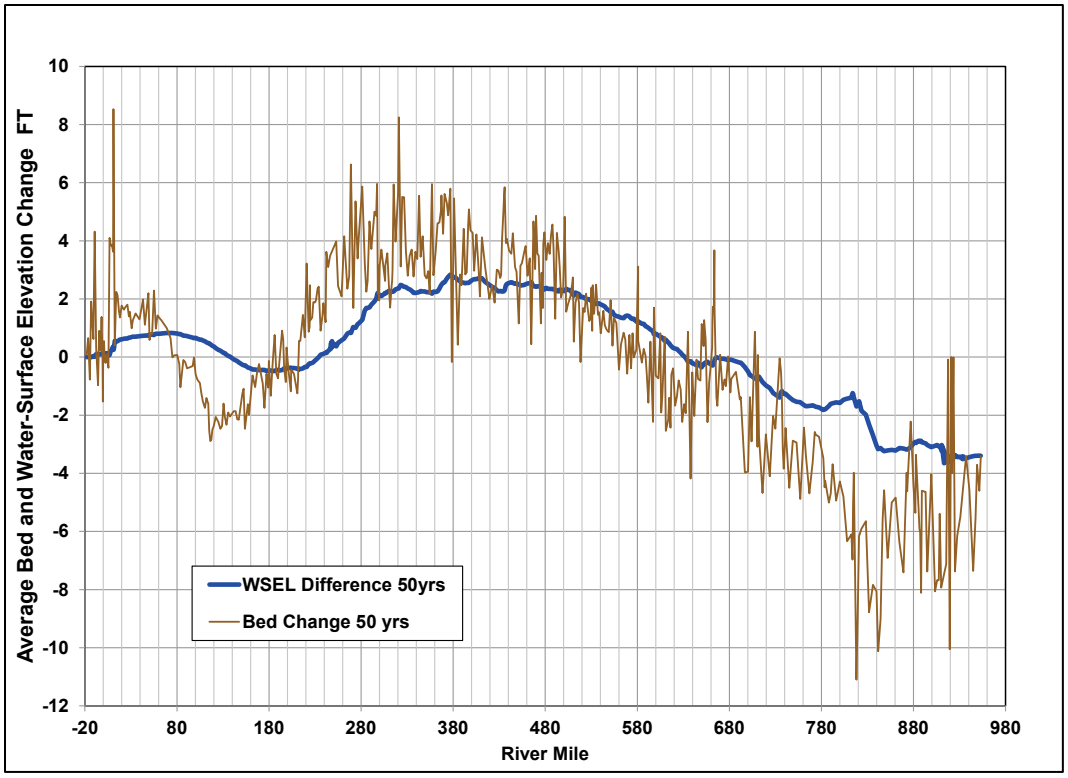

4 Predicted Increase in Project Design Water-Surface Elevation Due to Sedimentation

Project Design Flood (PDF)

The sediment assessment was initiated and essentially completed before completion of the hydrologic assessment that estimated a PDF. Most of the sedimentation assessment objectives were achieved during the course of this investigation using the 1955 PDF. The 1955 PDF was used to determine long-term sedimentation effects on the design flowline and to evaluate the effects of various geomorphic influences on the river regime. The 2016 PDF estimate was used to confirm results calculated using the 1955 PDF hydrograph. The 2016 PDF estimate was also used specifically to determine the effect of the rising flood hydrograph on channel change and maximum stage.

The 2016 PDF estimated discharges were significantly higher than those determined in 1955. Consequently, floodway structures in the MVN were operated according to modified protocols. The initial assumption by the Flowline Assessment Team is that the structures will be operated at design capacity rather than by authorized diversion percentages and limits. The result of this assumption is a higher percentage of the flood discharge passing by Red River Landing and New Orleans.

Sedimentation assessment results, using the 1955 PDF, are reported first in this report. Numerical simulation results are typically presented as differences in PDF-calculated water-surface elevation between a base test and a test with a specific variable change. Conclusions are based on differences in calculated water-surface elevation rather than on magnitudes. Therefore, the magnitude of the PDF should have an insignificant effect on results. This assumption was validated toward the end of this assessment by comparing results from the 1955 PDF and 2016 PDF estimate. The 1955 and estimated 2016 PDFs are compared to the 2011 flood at Arkansas City in Figure 48. In the figure, the hydrographs have been positioned so that the flood peaks coincide.

Figure 48. 2011 flood and 1955 and estimated 2016 PDFs at Arkansas City.

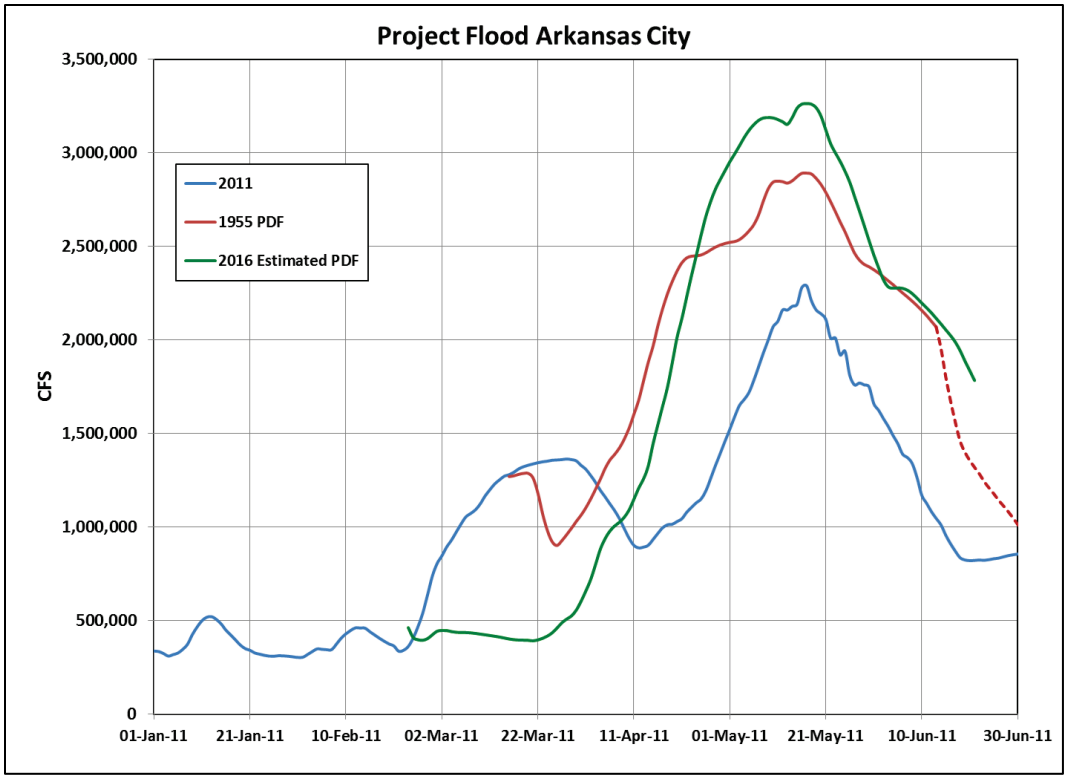

1955 Project design hydrograph

Numerical model results can be used to determine the specific gage trends between gages. For purposes of this assessment, it is more useful to display those results as a profile of the differences in PDF peak water-surface elevation for two points in time. Figure 49 shows the change in calculated peak water-surface elevation between 2013 and 50 years into the future due to sedimentation. This profile can be used to estimate the increased levee height required to contain the PDF, 50 years into the future, to account for sedimentation in the Lower Mississippi River.

The HEC-6T results predict that after 50 years of aggradation and degradation in the Lower Mississippi River, Project Design peak water-surface elevations will generally be higher downstream from Helena and lower upstream from Helena. At New Orleans, peak water-surface elevations are predicted to be approximately 1 ft higher after 50 years. Peak water-surface elevations between Red River Landing and Arkansas City are predicted to be between 2 and 3 ft higher after 50 years. At Hickman, peak water-surface elevations are predicted to be approximately 3 to 3.5 ft lower in 50 years.

Figure 49. Difference in 1955 PDF peak water-surface elevations after 50 years of sedimentation.

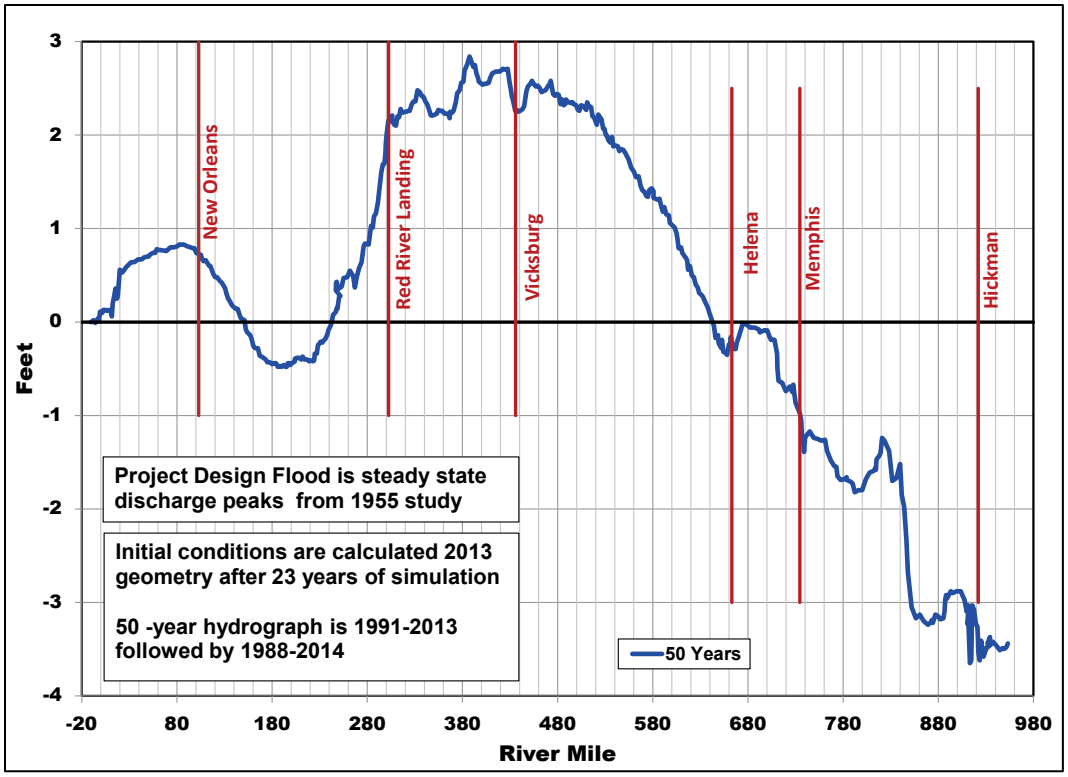

Channel geometry may change significantly with the rise and fall of a flood hydrograph. The channel change is not so much affected by the increase in bed sediment transport due to the increased discharge but by the difference in transport capacity between adjacent reaches. Thus, at any given time, the bed elevation of some cross sections may rise while others may decline. The numerical model was used to predict the difference in PDF water-surface elevations due to channel changes during the rise of the 1955 hydrograph.

The approach was to first calculate a steady-state water-surface profile using only the peak discharges with the 2013 geometry. This profile was compared to the peak water-surface profile calculated by simulating the PDF hydrograph starting with the 2013 initial geometry. This methodology was also applied after 50 years of sedimentation was calculated.

As shown in Figure 50, channel changes that occur during the flood rise result in water-surface elevation differences of less than 1 ft. As the flood rises, the river upstream from RM 250 scours, and the sediment supply increases. Downstream from RM 250, the river deposits sediment and water-surface elevations are higher. Trends after 50 years of sedi-mentation are very similar to those calculated at the beginning of the simulation.

Figure 50. Difference in PDF peak water-surface elevation due to rising hydrograph.

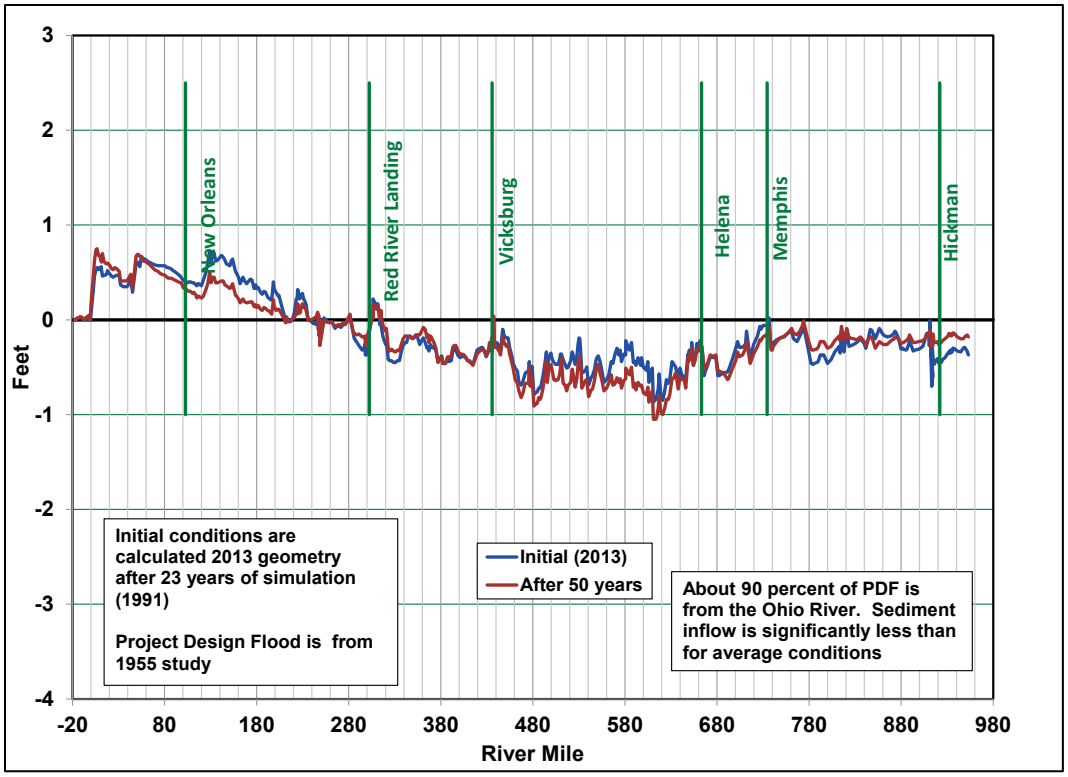

Effect of HEC-6T sorting and armoring algorithm

The Exner 7 sorting and armoring algorithm was used in HEC-6T to adjust the surface bed gradation with time. This is the same algorithm that was used in the Regional Model. However, other HEC-6T studies of the Mississippi River between Tarbert Landing and the Gulf have used the Exner 5 algorithm. In general, the Exner 5 algorithm tends to have a more stable surface layer than Exner 7 and thus predicts less degradation. The difference in PDF peak water-surface elevations after 50 years of sedimentation was calculated using both Exner 7 and Exner 5. Results are compared in Figure 51. There are significantly more deposition and increased water-surface elevations downstream from Vicksburg when Exner 5 is used in the calculations.

Figure 51. Difference in PDF peak water-surface elevations after 50 years of sedimentation calculated using Exner 5 and Exner 7.

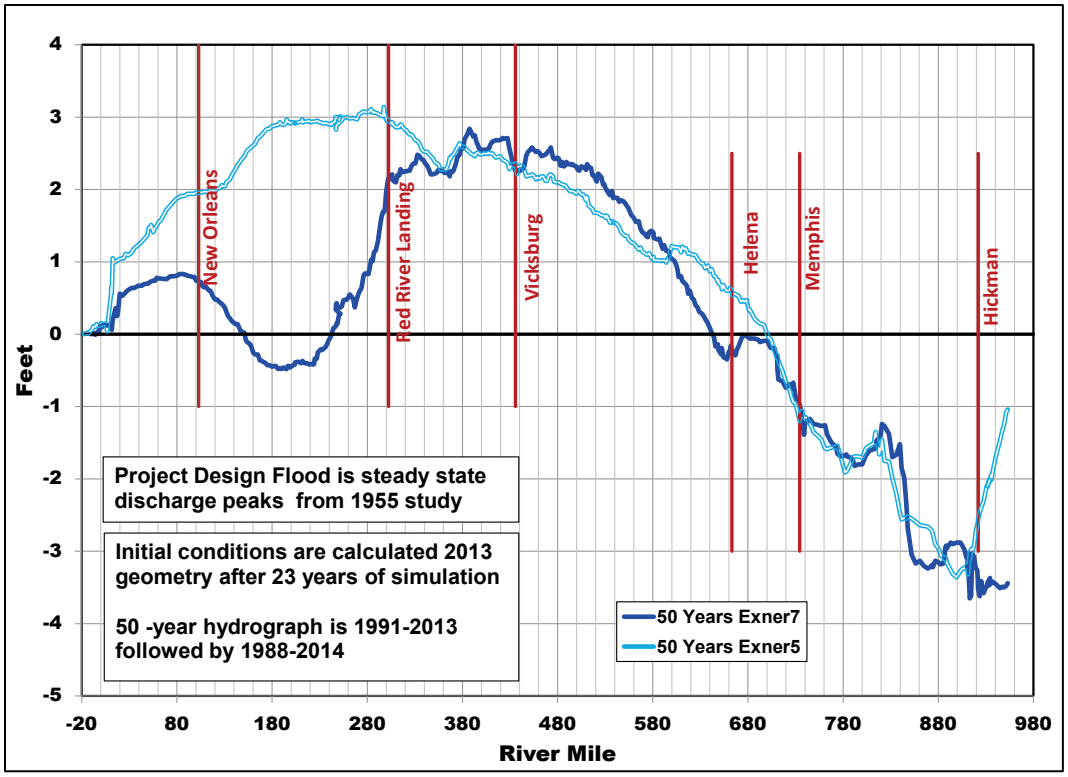

Model calibration of the Regional Model and the Flowline Model was achieved by matching calculated and measured sediment concentration rating curves, bed material gradations, and dredging quantities. Volumetric bed changes in two disequilibrium reaches were used to verify the model. The Exner algorithm was not considered as a calibration parameter. Exner 7 was chosen for the Flowline Assessment Model based on experience gained from previous numerical model studies using HEC-6T on the Mississippi River (Catalyst-Old River Hydroelectric 1999), the Atchafalaya River[1], the Missouri River (Copeland 1993; Copeland 2013), the Sacramento River (Hall et al. 2010), the Red River (Copeland 2002), and the San Lorenzo River (Copeland 1993; USACE SPN 2014). Earlier studies on the Mississippi River (Copeland and Thomas 1992; Copeland 1990) had demonstrated that Exner 5 did not produce results as well as the original Exner 1 algorithm. Detailed comparisons of the Exner 5 and Exner 7 algorithms with flume and river examples are contained in Copeland 1993. These examples demonstrated that Exner 7 was more appropriate than Exner 5 in sand-bed rivers.

[1] Copeland, R. R., and L. Lombard. In preparation. *Numerical Sedimentation Investigation, Mississippi River Vicksburg to Pilots Station*. U.S. Army Corps of Engineers.

In the MBH and ERDC models (Thomas 2012; Sharp et al. 2013), comparison of the measured and calculated accumulated bed-volume change between 1992 and 2004 between Head of Passes and Profit Island was used to conclude that a better reproduction of the accumulated sediment could be simulated using Exner 5. The assessment reports acknowledge that comparing hydrographic surveys, collected over a period of 1 year and at different locations on the annual hydrographs, could result in "very unreliable" results (Thomas 2012). It was concluded that the unreliability would be "reconciled" by averaging. This conclusion assumes that the errors associated with lack of survey synchrony are random errors and not systematic errors. Systematic errors are further magnified when sediment deposition quantities are accumulated over long distances. Additional errors are associated with datum differences, subsidence, equipment, and measuring methodology. Sharp et al. (2013) conclude that "the vertically adjusted data are thought to be within ± 1 foot." Using the MBH calculated channel surface area at elevation zero between RM 18 and RM 246.3 of 79,825 acres, ± 1 ft corresponds to ± 129 million cubic yards. Calculated deposition from the hydrographic survey estimated between 1990 and 2003 in the 250-mile reach was 75 million cubic yards. Uncertainty from survey data is almost twice the calculated difference from simulated deposition. This result confirms the conclusion from Copeland and Thomas (1992) that "the calculated longitudinal distributions of aggradation and degradation from the numerical model and the hydrographic surveys were dissimilar. This difference was attributed to annual variations in prototype bed elevation, which appear to be more significant than any long-term aggradation or degradation trend."

There is considerable uncertainty associated with estimating sediment deposition from survey data. The same hydrographic survey data from 1992 and 2004 were used by ERDC (Little and Biedenharn 2014) and MBH (Thomas 2012) to estimate the sediment deposition over that 12-year period. Different methodologies were used in the two studies. Reported accumulated sediment deposition between Venice and Tarbert Landing from the two studies is compared in Figure 52. Two lines are shown from the MBH study. One line represents the 12-year difference determined using the actual hydrographic survey elevations. The second line represents a line adjusted to account for datum differences. The figure demonstrates that the *measured* data are in fact subject to significant uncertainty related to assumptions required in the analysis.

Figure 52. Accumulated sediment deposition upstream from Venice, 1992–2004. Calculated from hydrographic surveys.

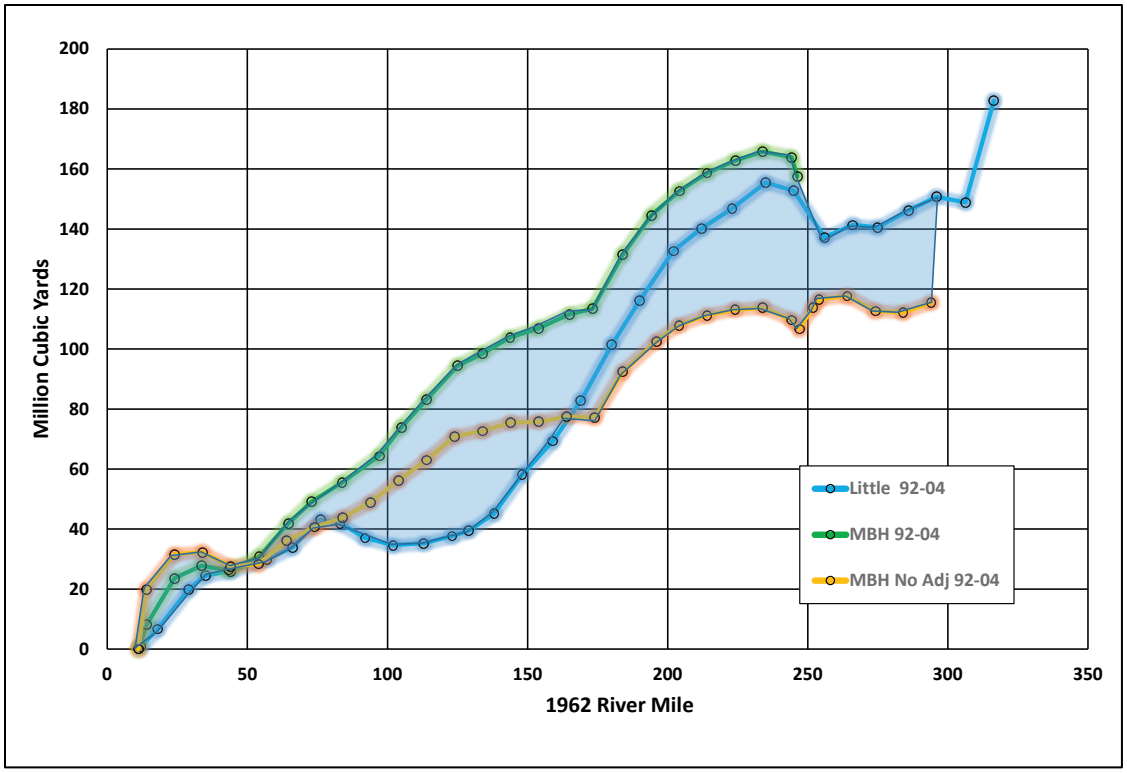

Calculated accumulated sediment deposition between Venice and Tarbert Landing between 1992 and 2004 was calculated using the Flowline Model using both the Exner 7 and Exner 5 algorithms. The results are shown in Figure 53. Both computed lines are higher than the range of measured estimates. The HEC-6T calculations were for the period between 23 Oct 1992 and 24 Aug 2003.

Figure 53. Accumulated sediment deposition between Venice and Tarbert Landing between 1992 and 2004 estimated from hydrographic survey data and computed by HEC-6T.

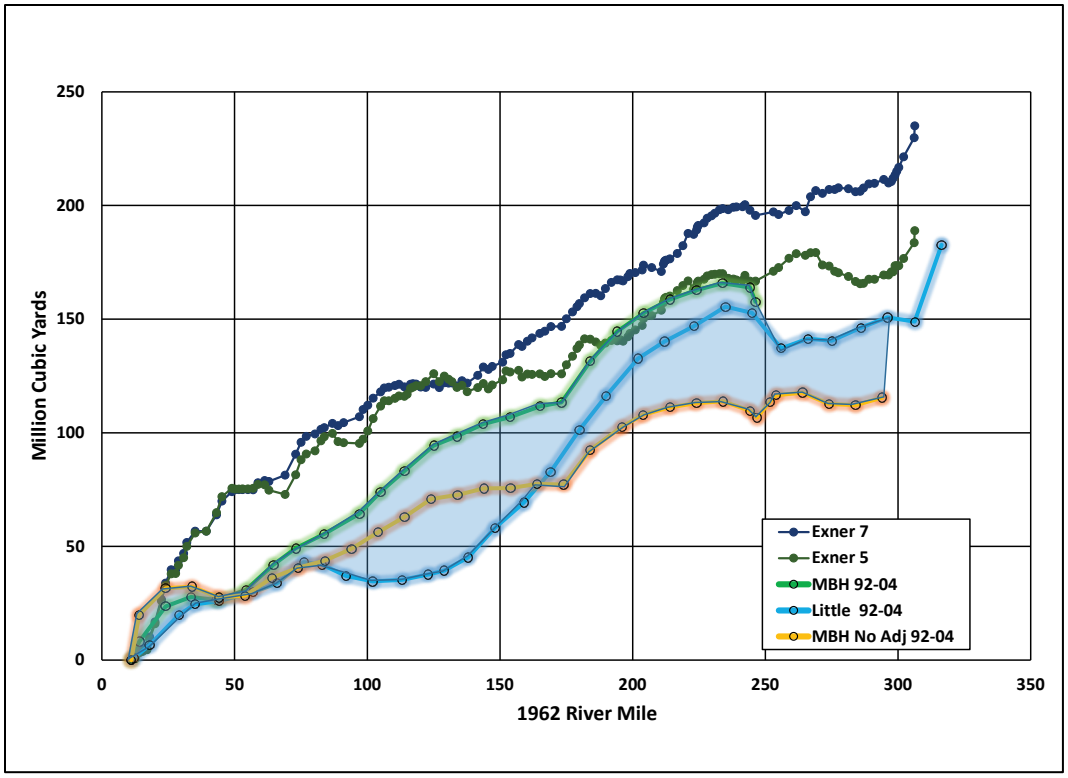

One issue with using accumulated sediment deposition is that calculations at the beginning of the accumulation carry through to the end of the analysis. Considering the issues of unsynchronized survey data, comparisons of deposition determined by hydrographic survey calculations and numerical simulations can be misleading. For example, Figure 54 shows a comparison of accumulated sediment deposition between RM 50 and Tarbert Landing between 1992 and 2004 developed from the same data as the previous figure. Different conclusions would be reached relative to the reliability of the numerical simulation based on replicating hydrographic survey data.

Figure 54. Accumulated sediment deposition between RM 50 and Tarbert Landing between 1992 and 2004 estimated from hydrographic survey data and computed by HEC-6T.

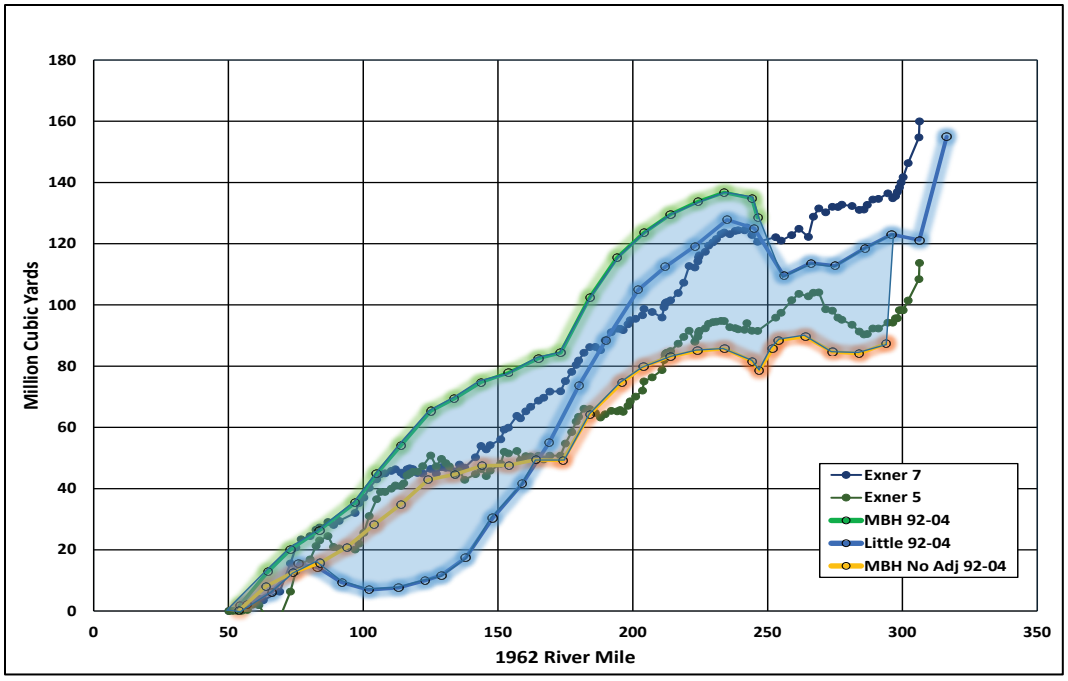

Based on the preceding arguments, it was concluded that using hydrographic surveys over long reaches of the Mississippi River is an unreliable method for model calibration. However, matching channel volume changes over short reaches where some significant channel modification has caused a change in channel morphology is a reasonable approach. Matching dredging volumes, measured sediment concentrations, and sediment yields are reliable means for calibrating numerical sediment models. Exner 7 was deemed the appropriate algorithm to use in the numerical model.

5 Factors Affecting Morphological Change

The HEC-6T numerical model allows one to evaluate specific driving variables to determine which agents of change are the most significant in determining the future character of the Mississippi River. With the numerical model, a single variable may be changed to determine its effect. Historical data mask the effect of individual variables because the driving variables act together at the same time.

The historic record of discharge and stage on the Mississippi River has been affected by a variety of factors. There has been a significant change in the hydrologic regime due to the construction of reservoirs in the watershed. Flood peaks have been dramatically reduced on both the Middle Mississippi and Ohio Rivers. There has been a significant reduction in sediment supply due to sediment storage in reservoirs and behind navigation structures, watershed soil conservation measures, bank stabilization, and channel stabilization in tributaries. Engineering structures and channel modifications have also affected the sediment delivery through the river.

Effect of floods

The numerical model was used to analyze the effects of large flood events on the long-term sedimentation process. The question may be asked: Are sedimentation effects the result of a steady trend or a series of abrupt reactions to flood discharges? To answer this question, the difference in PDF peak water-surfaces was calculated after 12, 24, 46, and 47 years. The 46- and 47-year time frames were chosen because the 2011 flood hydrograph occurred between the 46th and 47th year in the HEC-6T hydrograph. In terms of wetness, the mean daily flow for the first 12 years was 99.5% of the 50-year mean daily flow; between years 12 and 24, the mean daily flow was 99.1% of the 50-year mean daily flow; between years 24 and 46, the mean daily flow was 100.5% of the 50-year mean daily flow; between years 46 and 47, which is the 2011 flood year, the mean daily flow was 122.1% of the 50-year mean daily flow; and for the last 3 years, the mean daily flow was 94.9% of the 50-year mean daily flow. As shown in Figure 55, the progression of water-surface aggradation and degradation is relatively constant over time. There is no abrupt change between year 46 and 47 as a result of 2011 flood. This figure also highlights the point that the maximum difference in Project Design peak water-surface elevations may

not occur after 50 years. Upstream from New Orleans, the maximum increase in water-surface elevation occurs between the 12th and 24th years.

Figure 55. Difference in Project Flood peak water-surface elevation due to sediment aggradation/degradation over time.

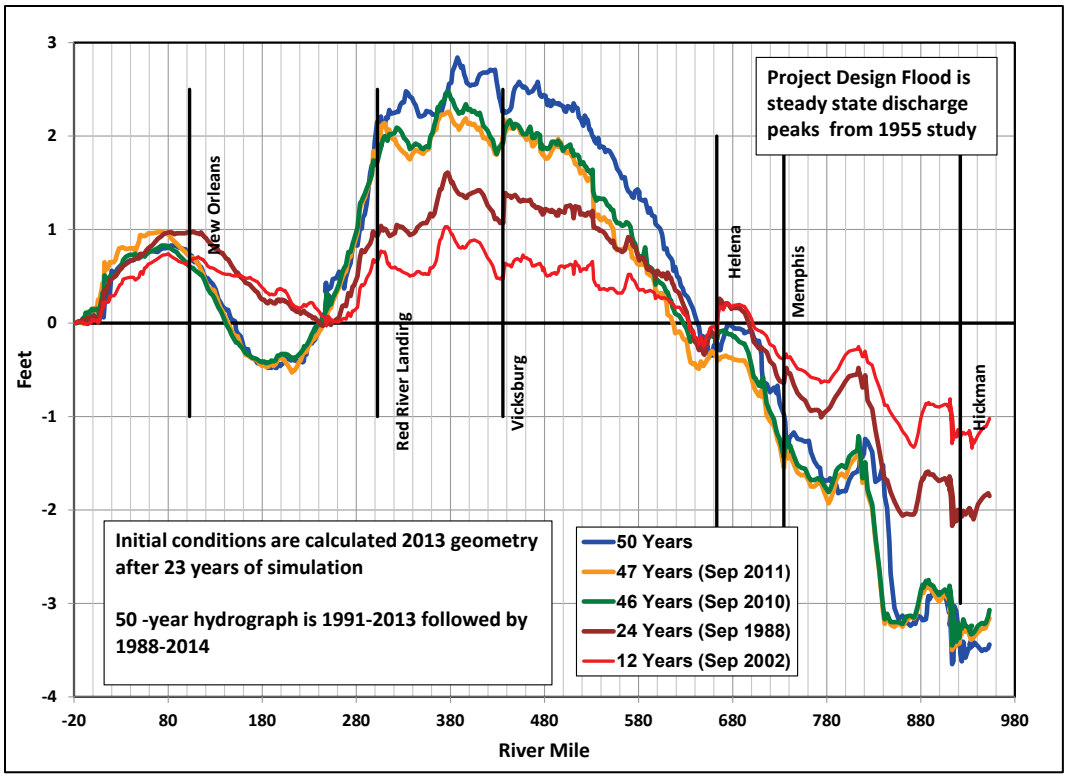

Another way to analyze the effect of large floods on aggradation/ degradation trends is to look at calculated average bed elevation changes at specific cross sections. In Figure 56, two cross sections near Memphis are compared. Major floods that occurred in April 1997, April 2008, and March 2011 are shown on the figure. Over the course of the 50-year simulation, there was significant variability in average bed elevation change at both cross sections 737 and 729.98. Degradation during floods appears to be more significant at cross section 737 than at cross section 729.98. Despite these short-term bed changes, the beds oscillate about a relatively stable long-term trend. Floods do not seem to have a significant effect on the long-term degradation trend.

Figure 56. Calculated 50-year bed change at Memphis.

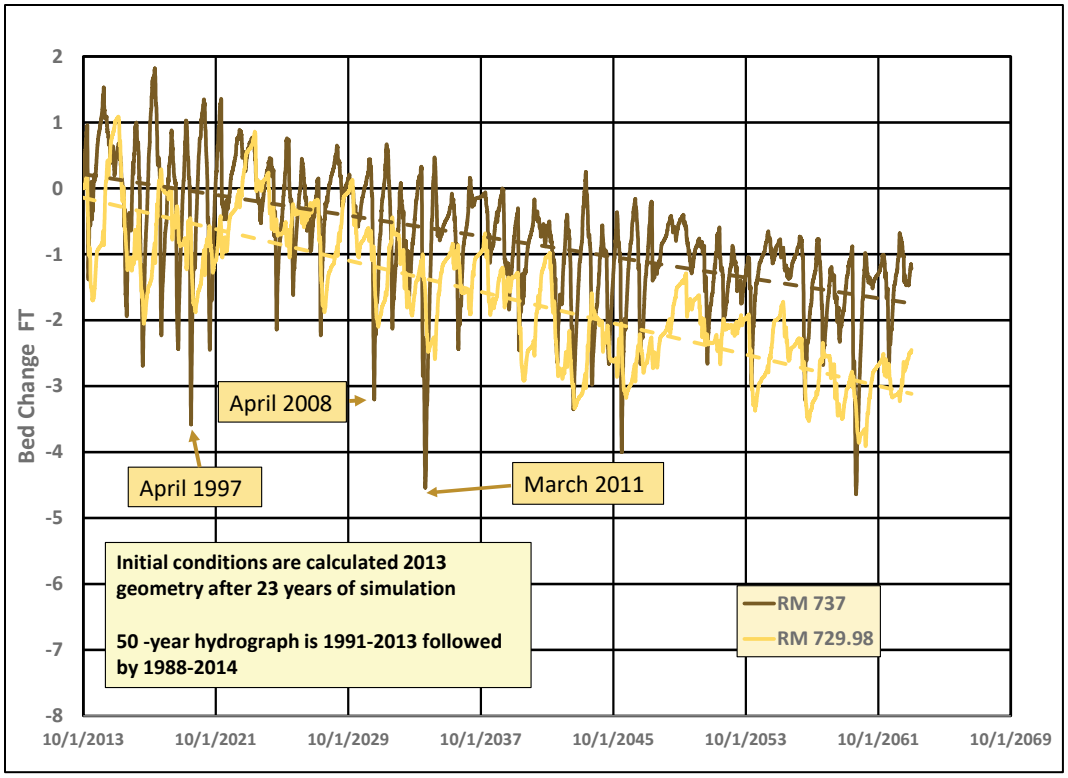

A similar analysis was conducted at two cross sections near Vicksburg. Major floods that occurred in May 1996 and March 2011 are shown in Figure 57. As was the case at Memphis, over the course of the 50-year simulation, there was significant variability in average bed elevation change at both cross sections 435.37 and 433. Aggradation during floods appears to be more significant at cross section 435.37 than at cross section 433. Despite these short-term bed changes, the beds oscillate about a relatively stable long-term trend, and floods do not seem to have a significant effect on the long-term aggradation trend.

Figure 57. Calculated 50-year bed change at Vicksburg.

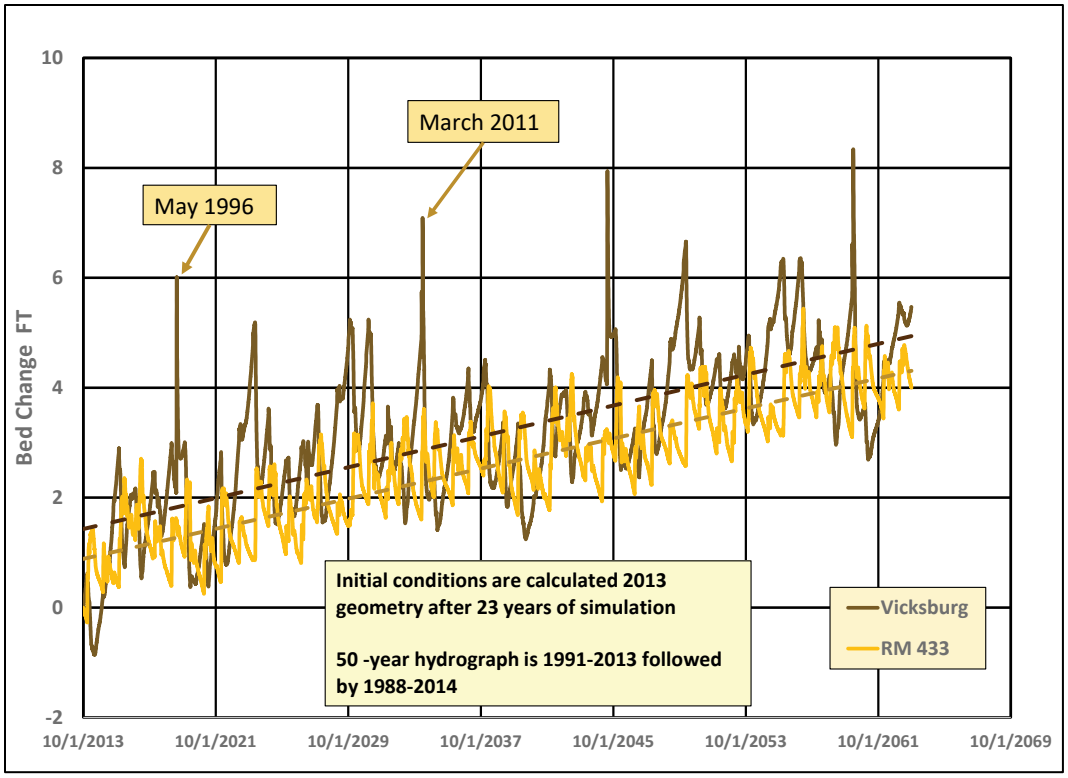

Extended projection of trends

Although project life is typically focused around 50 years, it is important to look past the 50-year time frame to predict project requirements into the future. Obviously, any prediction extending out 100 years contains significant uncertainty. This simulation assumes that the 2003–2013 sediment inflow at Thebes remains constant over the entire 100-year period. Nevertheless, it is important to analyze whether or not the Mississippi River is moving toward a stable equilibrium. The 100-year hydrograph simulated in the HEC-6T model represented the historical record from 1991 to 2013 followed by the 1988–2014 historical record and then 1991–2013 and 1988–2014 again. Results are shown in Figure 58. The HEC-6T numerical prediction is for a continuation of the aggradation and degradation trends with no evidence of an equilibrium condition being achieved in the next 100 years.

Figure 58. Difference in PDF peak water-surface elevation due to sediment aggradation/degradation after 100 years.

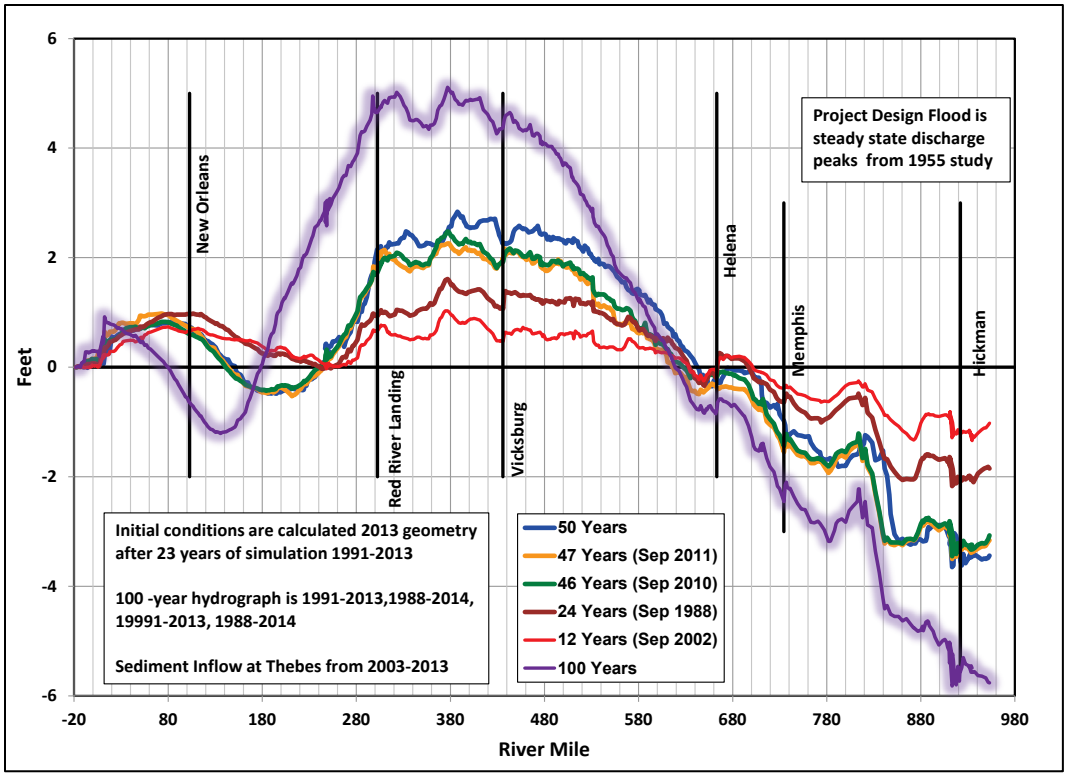

Effect of the bed source

Results of the HEC-6T simulation suggest that the Mississippi River bed above Helena might be the source of the material that is depositing between Red River Landing and Helena. To test this hypothesis, the bed source upstream from the Arkansas River (RM 580) was eliminated from the model. Results of this test are shown in Figure 59. Sediment transport capacity downstream from the Arkansas River is much greater than the sediment inflow so significant degradation occurs downstream. As a result, the water-surface elevations are lower for 100 miles upstream to Memphis due to the reduction in base level elevation. Degradation initially calculated downstream from Cairo has been transferred downstream to RM 580. Downstream from the Arkansas River, degradation is induced, increasing sediment transport. The degradation trend occurs between RMs 580 and 450. Thereafter, downstream effects are similar to the base test. This test confirms that the material depositing in the Mississippi River in Vicksburg District is coming primarily from the bed of the river upstream.

Figure 59. Difference in Project Flood peak water-surface elevations after 50 years of sediment aggradation/degradation with bed source in Memphis District eliminated.

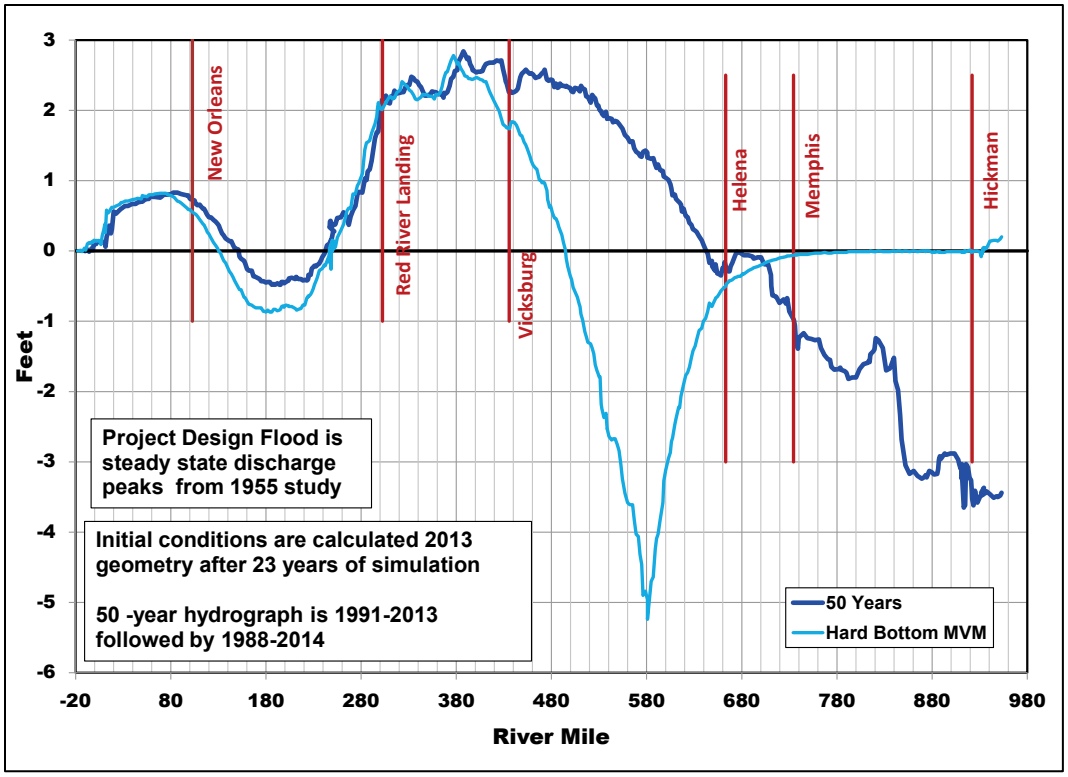

Effect of sediment inflow

The decline in sediment supply to the Lower Mississippi River downstream from Cairo is one factor that could be responsible for the predicted future degradation trend in the Memphis District and the subsequent aggradation trend in the Vicksburg District. It has been estimated from USGS measurements (Heimann et al. 2011) that there has been a 62% reduction in sand load from the Missouri River to the Middle Mississippi due to construction of Missouri River reservoirs. The numerical model was used to determine if increasing the sediment load during the 50-year simulation would eliminate the degradation trend in the Memphis District.

Most of the current sediment inflow to the Lower Mississippi River is coming from the Middle Mississippi River and is measured at Thebes. Figure 26 shows measured sand concentration at Thebes between 1973 and 2013. The data scatter is attributed to measurement errors associated with both the discharge and the sediment concentration and to the fact that sand concentration is a function of more variables than just the discharge. Sand concentration is heavily dependent on antecedent

conditions as well as the primary source of the flow. The Missouri River typically has a much higher sand concentration than the Upper Mississippi River above St Louis. The measured data by itself have so much scatter that trends are difficult to determine. The power regression curves shown on Figure 26 help define long-term trends. Average sand concentrations were much higher in the 1970s than after 2000. Sediment inflow for the base test was developed from the 2003–2013 data. To evaluate the effect of sediment inflow concentration, sediment inflow was increased in three different test cases. The first test used the 1991–2002 sediment inflow rating curve from the Regional Model. Second, the 1973–79 rating curve was used to evaluate the highest decade of record. Finally, the entire 1973–2013 record was used to develop a rating curve that was then doubled to represent a pre-impoundment condition. (The third test required allowance for overbank deposition in the Middle Mississippi River reach above Cairo to prevent clogging of the channel). As shown in Figure 60, increasing sediment inflow resulted in more aggradation and less degradation in the study reach. However, even with the pre-impoundment sediment inflow condition, the calculated Project Flood water-surface elevations after 50 years have a similar pattern to those calculated using current sediment inflow conditions. Degradation continues to be significant in the Memphis District reach. It can be concluded that the sediment inflow definitely affects the magnitude of aggradation and degradation, but it is not the dominant variable driving the current and future trends.

Figure 60. Difference in Project Flood peak water-surface elevations after 50 years of sediment aggradation/degradation for various Middle Mississippi River sediment inflow conditions.

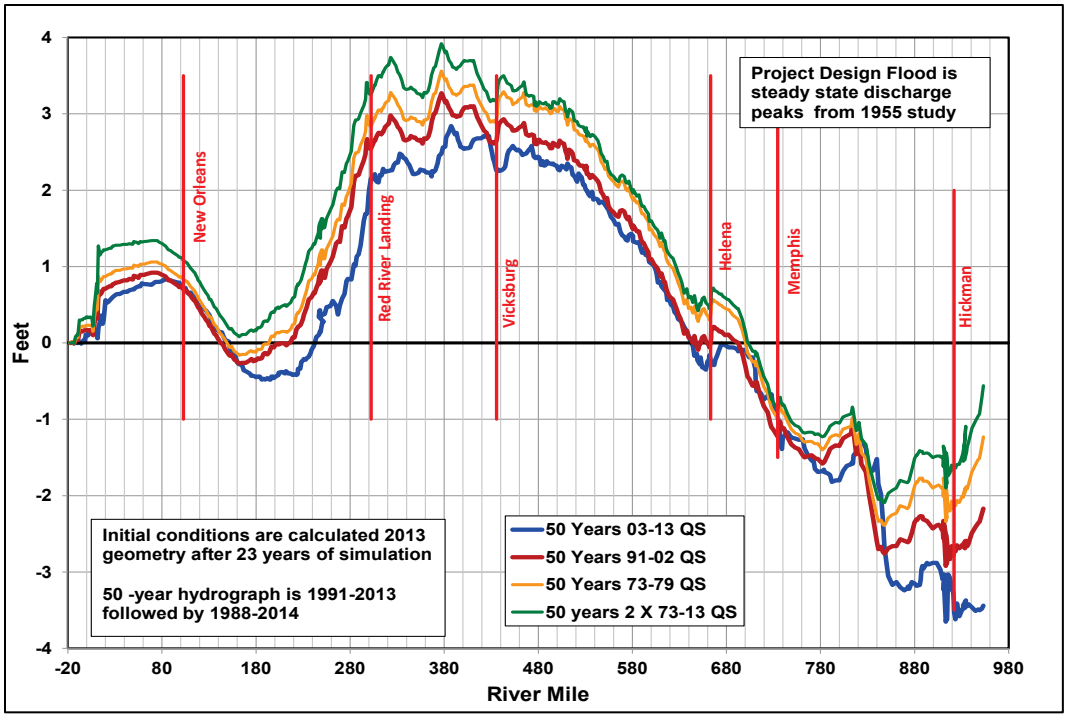

The Ohio River basin also has reservoirs, locks and dams, and bank stabilization that have reduced historical sediment loads. USGS data collected between 1991 and 2002 at Lock and Dam 53, which is 17 miles upstream from Cairo, were used to determine the sediment inflow rating curve for the base condition in the HEC-6T assessment. No definite long-term trend after 1990 could be determined from additional data collected through 2014. Sediment measurements are inadequate for predicting a pre-impoundment sediment load. However, sediment concentrations measured between 1978 and 1982 at Louisville are higher than the more recent data at Lock and Dam 53. Louisville is 372 miles upstream from Cairo and passes approximately 43% of the Ohio River discharge at Cairo. The sediment measurements at Louisville and Lock and Dam 53 are compared in Figure 61.

The Louisville sediment concentration inflow rating curve was inserted into the model at Metropolis to determine the effect of increasing Ohio River sediment loads on aggradation and degradation in the Mississippi River downstream from Cairo. The difference in Project Flood peak water-surface elevations after 50 years with the increased sediment loads from both the Ohio and Middle Mississippi Rivers is shown in Figure 62. Note that the Ohio River segment was depositional throughout the simulation with the

Louisville sediment inflow. Even with extreme sediment inflow conditions, the overall degradation trend in the Memphis District and the aggradational trend in the Vicksburg District are predicted. Increasing Ohio River sediment inflow confirms the previous conclusion that the sediment inflow definitely affects the magnitude of aggradation and degradation, but it is not the dominant variable driving the current and future trends.

Figure 61. Ohio River measured suspended sediment at Louisville (1978–1982) and Dam 53 (1973–2014).

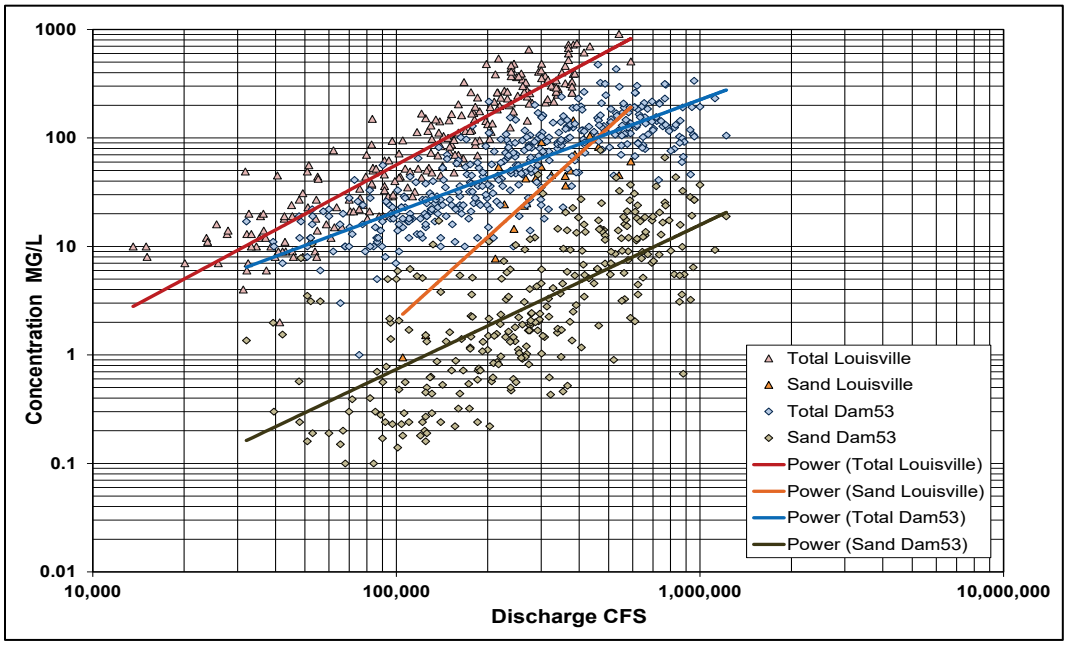

Figure 62. Difference in Project Flood peak water-surface elevations after 50 years of sediment aggradation/degradation for various Middle Mississippi and Ohio River sediment inflow conditions.

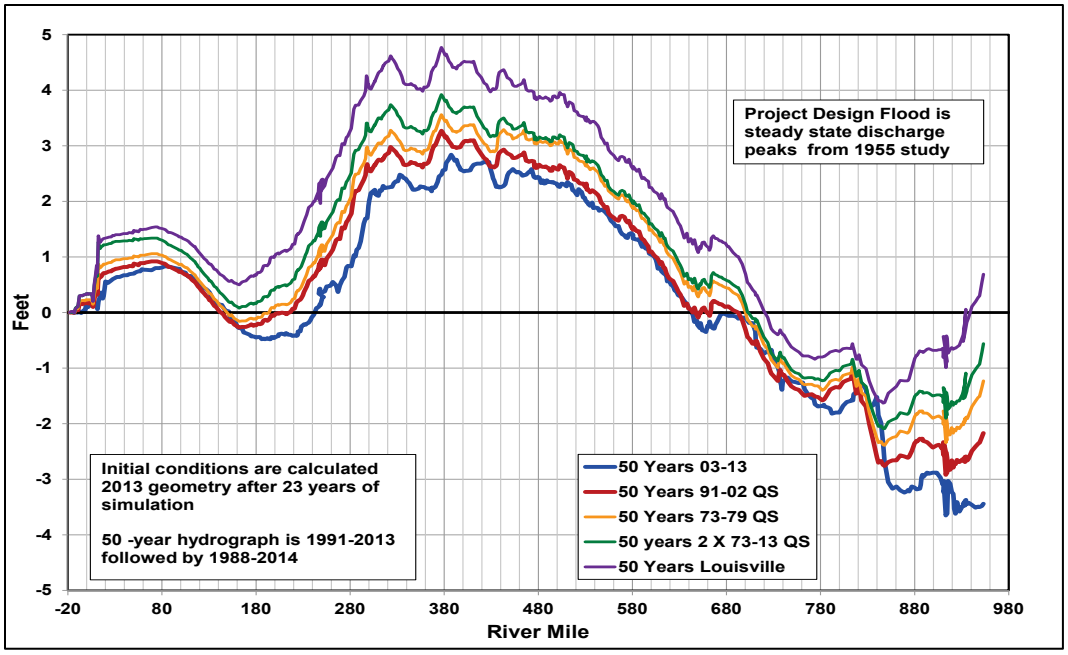

Effect of dikes

Dikes constructed throughout the length of the Lower Mississippi River have constricted the river and increased sediment transport capacity especially at lower flows. Dike locations and construction dates are listed in Tables 2–4. The numerical model was used to predict the effect of dike construction on long-term aggradation and degradation. Dikes were removed from the numerical model geometry, and the calculated differences in Project Flood peak water-surface elevations after 50 years were compared. The first test was conducted by removing all the dikes constructed after 1991. The initial geometry from the Regional Model was used for this test. All the dikes were removed from the initial geometry in the second test. Removing the dikes constructed before 1991 does not adequately define pre-dike conditions because the hydrographic survey data reflects bed changes induced by the dikes. The 50-year calculated dike effect is shown in Figure 63. It is concluded that the constrictions caused by dikes do affect degradation, but they are not the primary driving variable responsible for the long-term morphologic changes.

Figure 63. Difference in Project Flood peak water-surface elevations after 50 years of sediment aggradation/degradation with and without dikes.

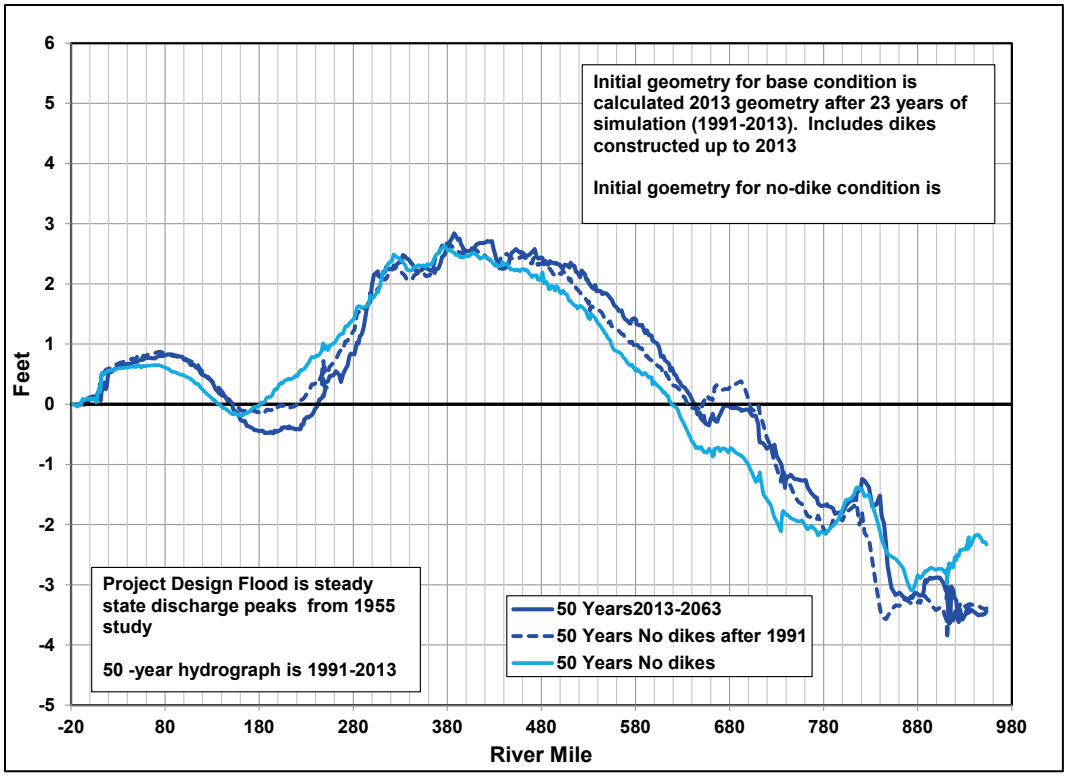

Effect of flow diversion percentage

The distributary flow diversion percentages in the numerical model were assigned using measured data as much as possible. Outflow rating curves were developed taking diversion percentage to be a function of the upstream Mississippi River discharge. It is clear from the data measurements that a combination of measurement error and variable boundary conditions make it difficult to predict diversion percentages at any specific point in time. Fortunately, in a long-term sedimentation assessment, it is the average condition that is important, and this can be reliably determined from the measured data. However, it is important to quantify the uncertainty associated with the assignment of flow diversion percentages.

The influence of diversion percentages on the predicted long-term PDF water-surface elevation change due to sedimentation was demonstrated by increasing and decreasing diverted flow by 10% in the 50-year simulation. The assigned flow diversion percentages were changed at all of the natural distributary outlets in the model. The distributaries controlled by structures were not changed. The controlled outlets include Caernarvon, Davis Pond, Bonnet Carré, Morganza, and the Old River Control Complex.

Also not changed were the backwater and floodway diversions at the Yazoo River and the New Madrid Floodway. The calculated differences in PDF water-surface elevation after 50 years of sedimentation are shown in Figure 64. The effect of flow diversion percentage on PDF water-surface change due to sedimentation is negligible. In this figure, only the effects due to sedimentation are being compared. A comparison of water-surface elevations calculated using the different diversion percentages would show a more significant difference.

Figure 64. Difference in Project Flood peak water-surface elevations after 50 years of sediment aggradation/degradation—effect of 10% change in natural flow diversions.

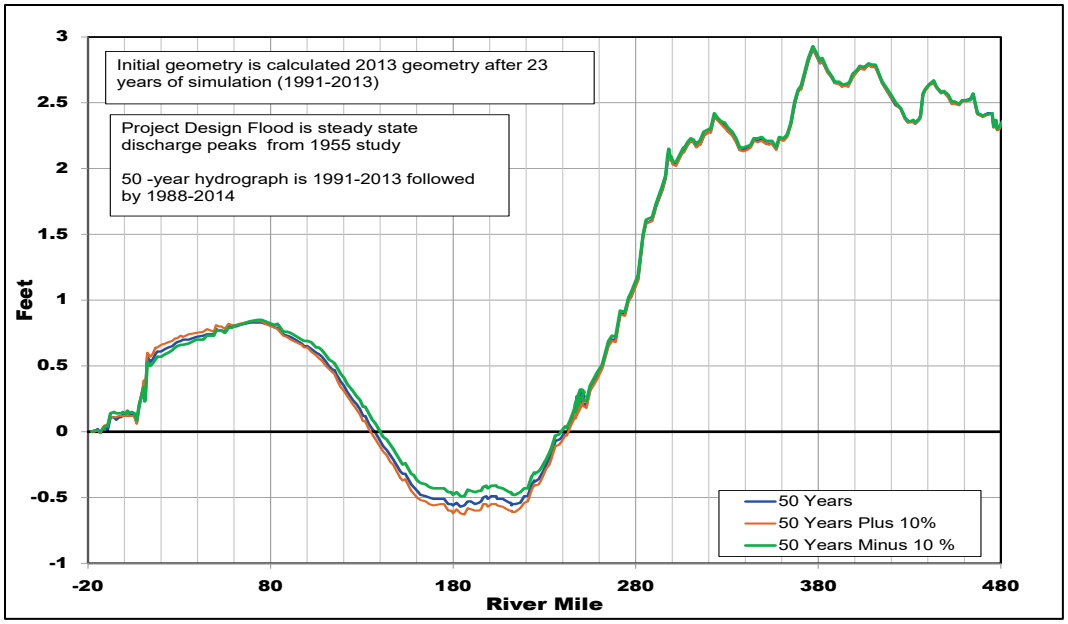

Effect of restoring cutoff mileage

The 1930–1940 cutoff program had a significant impact on the geomorphology of the Lower Mississippi River. One hypothesis is that the river is still in the process of responding to these cutoffs. Lacking 1930 cross-section data, it is not possible to build a HEC-6T model to test this hypothesis. However, inverse logic can be applied. Historic data show that when the river's base level is lowered, as it was with the cutoff program, then head cutting will occur upstream. Specific gage plots and model results show a long-term degradation trend in the Memphis District. Using inverse logic, it can be hypothesized that if the long-term degradation trend is actually a consequence of the cutoff program, then if the river's base level is returned to pre-cutoff elevations, the reversal of the degradation trend would be expected. This scenario can be tested with the numerical model.

The HEC-6T model was modified by increasing reach lengths between cross sections at the locations where cutoffs historically occurred. No additional cross sections were added. Hydraulic parameters in the restored reach were calculated from the upstream and downstream cross sections in the existing model. This change added 152 miles of river length to the Mississippi River. However, the cross-section geometry still reflects 1991 hydrographic survey elevations; therefore, degradation that has occurred due to the cutoffs has been neglected in this test. These simplifications introduce significant uncertainty relative to the absolute calculated water-surface elevations but provide useful insight with respect to long-term trends. Differences in Project Flood peak water-surface elevations after 50 years of aggradation and degradation are shown in Figure 65. Note that the river miles shown in the figure are 1962 RMs, which reflect distances after the cutoffs were completed. Hence, the sharp discontinuities shown for the *without cutoffs–initial* condition plot in the figure. The plot for the without cutoffs–initial condition reflects the increase in water-surface elevations due to the increase in reach length. This plot shows the difference between PDF water-surface elevations at time zero when reach lengths are instantaneously increased to reflect the hypothetical return of cutoff river miles. The without-cutoffs plots for 50 years and 100 years represent the water-surface elevation differences from the without cutoffs–initial condition. The effect of raising the base level is negligible upstream from RM 820. After 50 years of simulation, the without-cutoffs degradation upstream from RM 820 is similar to the with-cutoffs (base test) degradation. Without the cutoffs, the aggradation reach moves upstream to the vicinity of Helena and Memphis. The river-bed material scoured upstream from RM 820 is most likely responsible for the aggradation in the vicinity of Helena and Memphis. Downstream from this aggradation reach, the river shows significantly less difference in Project Flood water-surface elevations than the existing condition with cutoffs.

The conclusions from this test are that the cutoff program continues to have an effect on aggradation and degradation in this reach of the river and that its effects will continue to affect river geomorphology for the next 100 years. In addition, degradation and base level lowering due to cutoffs has moved upstream from the original reach lengths influenced by the cutoff program, and even if the original river length were returned to the cutoff reach, degradation would continue between Memphis and Cairo.

Figure 65. Difference in Project Flood peak water-surface elevations after 50 years of sediment aggradation/degradation with and without cutoffs.

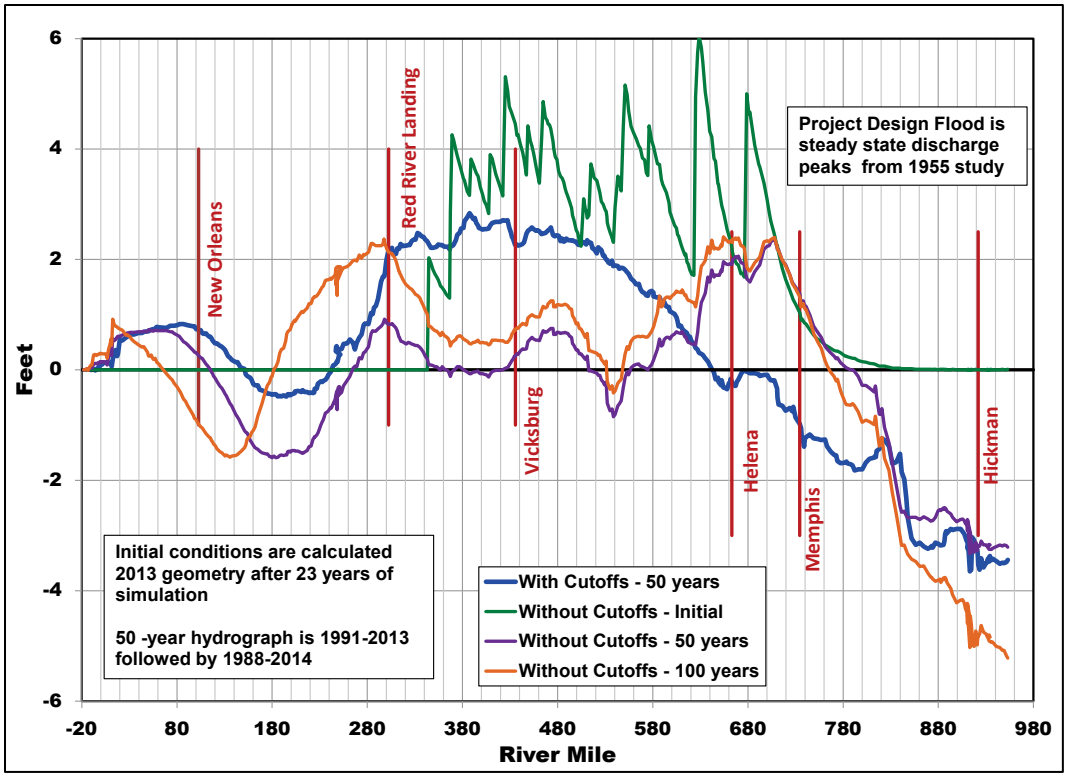

Effect of hypothetical new cutoffs

To get a sense of how the river would respond to a second round of shortening, a hypothetical cutoff program was simulated. The initial cross-section geometry for this test was taken from the 1991 hydrographic survey with all the dikes removed. Between RMs 340 and 680, reach lengths between cross sections were uniformly reduced so that the total length of river was reduced by 152 miles. The sediment inflow from the Middle Mississippi was taken from 1991–2002 data for 12 years and then 2003–2013 data for 111 years. The hydrograph was developed from historical annual hydrographs: 1991–2013, followed by 1991–2013, followed by 1988–2014, followed by 1991–2013, and finally, 1988–2014. The total simulation was 123 years. The differences in calculated Project Design peak water-surface elevations with the hypothetical new cut-off program and a base test run without the reduced reach lengths are compared in Figure 66.

This test should not be considered a simulation of the 1930–1940 cutoff program but rather a test to discern how the river responds to cutoffs in general. The 1991 geometry reflects river responses to the actual cutoffs and dikes constructed before 1991 instead of the 1930 geometry. The

152 miles of reduced channel length in the test represent only the neck cutoffs and do not account for the chute cutoffs in the actual program. The numerical model had to be modified to allow for significant deposition on overbanks in the cutoff reach and downstream. Dredging downstream from cutoffs was a significant consequence of the actual cutoff program but was not simulated in the numerical model. These simplifications introduce significant uncertainty relative to the absolute calculated water-surface elevations downstream from the cutoff reach but provide useful insight with respect to long-term trends upstream from the cutoff reach.

Though not a simulation of the 1930–1940 cutoffs, the figure plots are referenced to years after a base year, which is taken to be 1940. These references facilitate comparison to the historical time frame. The initial response to the hypothetical cutoffs was a 7 to 8 ft decrease in water-surface elevations between Vicksburg and Helena. Plots provided for 23, 73, and 123 years reflect changes in PDF water-surface elevations relative to the calculated water-surface elevations that would occur over the same time periods without the hypothetical cutoffs. After 23 years (1963), water-surface elevations continued to decline at Helena and Memphis but increased at Vicksburg. After 73 years (2013) the degradation trend reached Hickman. The aggradation and degradation trends continued through 123 years (2063). Even though this test is not a simulation of the historical cutoffs, river responses calculated in this test strongly support the hypothesis that the current and future aggradation and degradation trends in the Lower Mississippi River are a continuing response to the historical cutoffs.

Figure 66. Difference in Project Flood peak water-surface elevations due to sediment aggradation and degradation with new hypothetical cutoffs.

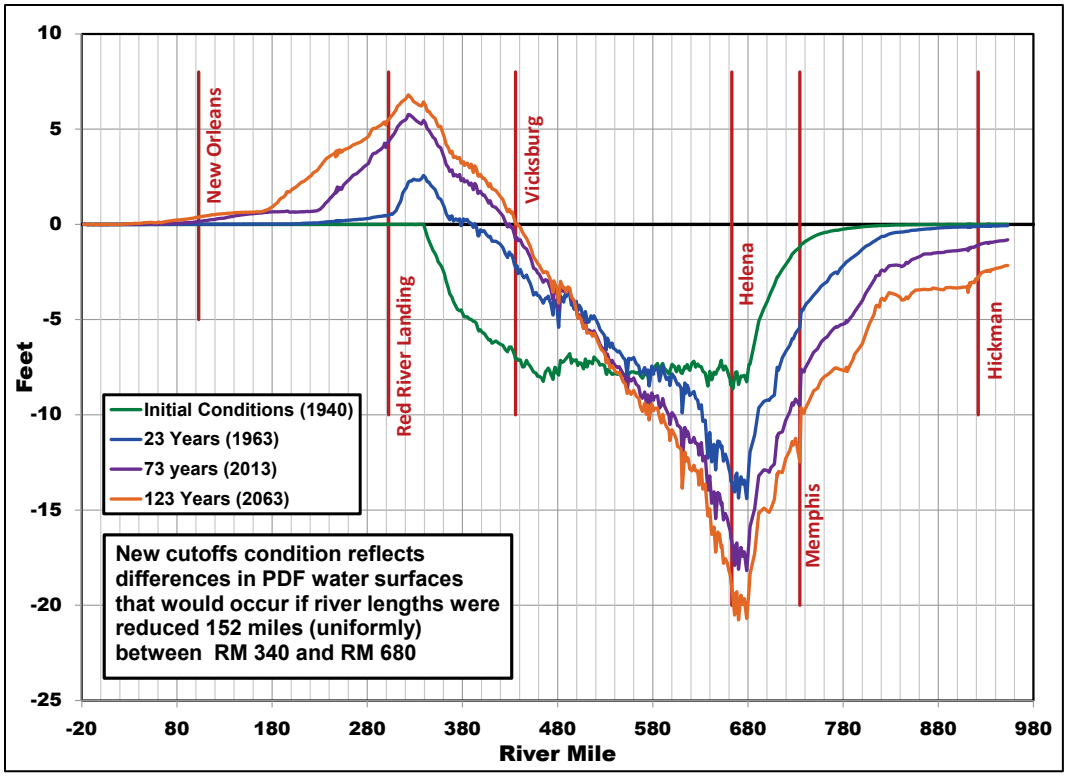

6 Sea-Level Rise (SLR) and Subsidence

The effects of SLR and subsidence on sedimentation and calculated water-surface elevations were determined using the HEC-6T numerical model. The water-surface elevation at the downstream boundary was increased by adding a sea-level rise component determined from Curve III of the National Research Council projection recommended in ER 1100-2-8162 (USACE 2013). Curve III provides a high estimate for sea-level rise. The downstream boundary elevation in HEC-6T was increased for each event during the 50-year simulation using the National Research Council equation as specified on the SLR options in the HEC-6T software. Subsidence values at each cross section up to RM 184 were taken from the ERDC MS-Hydro model LMR2_FWOPa_NRC1_R28.t5 (www.mvd.usace.army.mil/Missions/Mississippi-River-Science-Technology/Mississippi-River-Hydro/). Subsidence calculations, in which all elevations in the cross section were lowered at a constant rate, were made each October 1 in the HEC-6T model. Calculated water-surface elevations due to sea-level rise and subsidence do not include any changes to the elevation datum that might occur for whatever reason.

The difference in PDF peak water-surface elevations after 50 years of aggradation and degradation in the Mississippi River study reach is shown in Figure 67. Basically, the effects of sea-level rise and subsidence are negligible upstream from Vicksburg. The 50-year differences shown in Figure 67 represent the combined effect of sea-level rise, subsidence, and sedimentation.

There are several uncertainties associated with the calculations. There was no differentiation between overbank and channel subsidence. The numerical model simulation made no adjustment for flow diversion percentages out the distributaries. There was no adjustment made to the dredging template.

The results of this analysis should not be added to the flowline determined by the HEC-RAS flowline assessment due to sea-level rise as this would double count the effects of sea-level rise and subsidence.

Figure 67. Difference in PDF peak water-surface elevations after 50-years of sediment accumulation with subsidence and NRC Curve III sea-level rise.

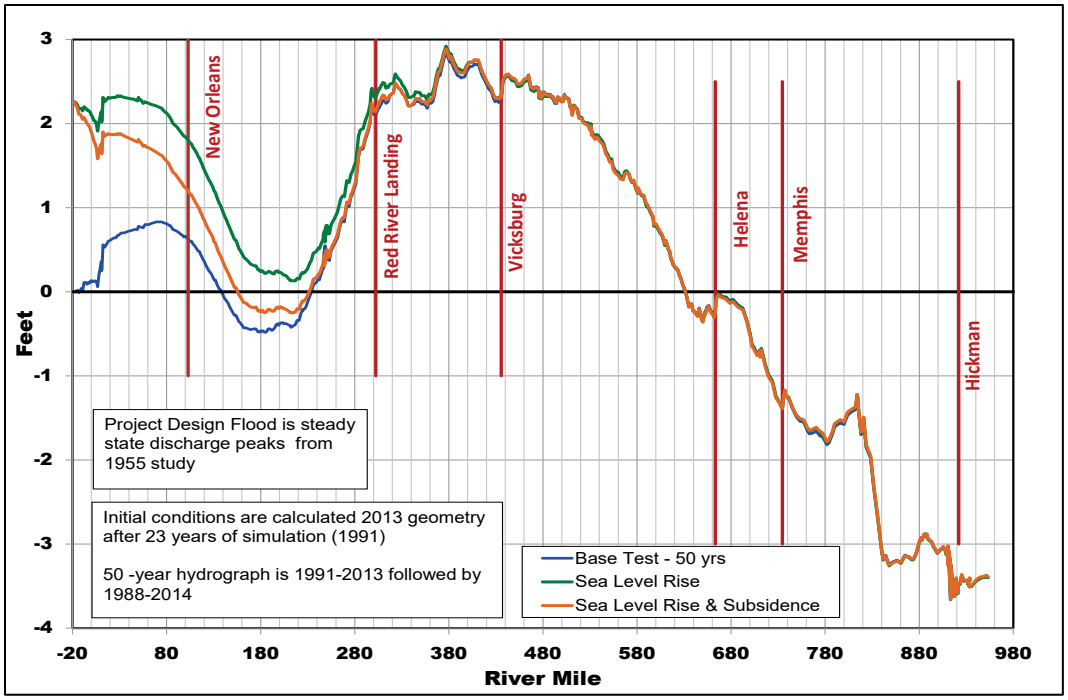

The increase in water-surface elevation differences shown in Figure 67 is primarily due to the increase in the downstream boundary elevation and not due to increased sedimentation due to sea-level rise and subsidence. To segregate the effects of sedimentation on the PDF peak water-surface elevations with respect to both sea-level rise and subsidence, the PDF peak water-surface elevations were calculated with the initial geometry conditions (2013) adjusted for 50-year subsidence and 50-year sea-level rise at the downstream boundary. Subtracting this value from the PDF peak water-surface elevations calculated after 50 years of sediment accumulation (with both sea-level rise and subsidence progressing with time) provided the segregated effect of sedimentation due to both sea-level rise and subsidence and is shown in Figure 68. The figure shows that the 50-year increase in water-surface elevation, due to sedimentation, for the PDF at New Orleans with both sea-level rise and subsidence is approximately 1.3 ft. Note from Figure 67 that the total effect of sea-level rise, subsidence, and sedimentation is an increase of only 1.2 ft. Increases in sedimentation due to subsidence is countered by decreases in water-surface elevations. If HEC-RAS water-surface elevations include the effects of subsidence and sea-level rise, the differences shown in Figure 68 can be used to account for 50 years of sediment accumulation.

Figure 68. Difference in PDF water-surface elevations after 50 years of sediment accumulation with NRC Curve III sea-level rise and subsidence — attributed to sedimentation.

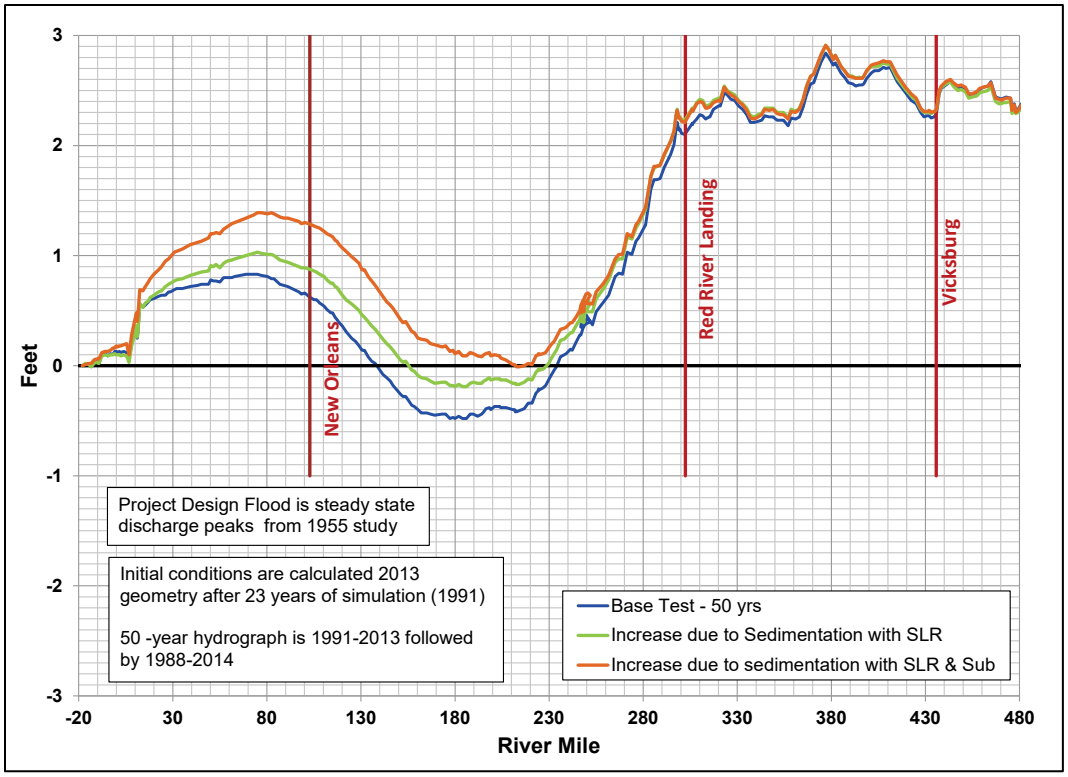

2016 Estimated Project Design hydrograph

The numerical model was used to determine the difference in maximum water-surface elevation due to 50 years of sedimentation for project design peaks of different magnitudes. The 1955 PDF and the estimated 2016 PDF peak discharges were compared in this assessment. The maximum calculated discharge for these two design floods is shown in Table 28. Predicted discharges for the PDF are considerably higher for the estimated 2016 PDF. Discharge is reduced at Hickman due to diversion into the New Madrid Floodway. Peak discharges increase again at Memphis due to inflow from the New Madrid Floodway and tributary inflow. The peak discharge at Helena is reduced due to diversion into the St. Francis Backwater. Peak discharge is reduced at Vicksburg due to diversion into the Yazoo Backwater. Peak discharge is reduced at Red River Landing due to diversion at Old River. Diversion at the Morganza Spillway is responsible for the reduction in peak discharge at Baton Rouge. The Bonnet Carré Spillway diversion is responsible for the decrease in peak discharge at New Orleans. The Bohemia Spillway and the Fort St. Philip distributaries are the primary diversions responsible for the decrease in peak discharge at the Venice Discharge Range.

Table 27. PDF peak discharges.

Mississippi River	1962 RM	2016 RM	1955 PDF 58A-EN Regulated (cfs)	2016 Estimated PDF 58A-R Existing Condition From HEC-RAS (cfs)
Chester	109.9	109.9	240,000	508,000
Thebes	43.7	43.7	410,000	520,000
Ohio Confluence	954.3	973.8	2,360,000	2,791,000
Hickman	922.0	941.2	1,810,000	1,973,000
Memphis	734.4	748.7	2,410,000	2,863,000
Helena	663.1	676.3	2,460,000	2,788,000
Arkansas City	554.1	562.2	2,890,000	3,264,000
Vicksburg	437.0	442.2	2,710,000	2,979,000
Natchez	363.3	368.4	2,720,000	2,977,000
Red River Landing	302.0	307.1	2,100,000	2,351,000
Baton Rouge	228.4	232.5	1,500,000	1,742,000
Donaldsonville	175.4	177.4	1,500,000	1,741,000
New Orleans	102.8	107.0	1,250,000	1,486,000
Venice Discharge Range	12.4	17.85	1,250,000	1,031,000

The approach was to calculate a steady-state water-surface profile for PDF peak discharges at the beginning of the simulation. The numerical model then calculated sedimentation changes for a 50-year period. Finally, another steady-state water-surface profile was calculated for PDF peak discharges at the end of the 50-year simulation. The difference in the two PDF water-surface profiles is the 50-year effect of sedimentation. These differences are shown in Figure 69. The figure shows that results using the 1955 PDF and 2016 estimated PDF are similar.

Figure 69. Difference in 1955 and 2016 estimated PDF peak water-surface elevations after 50 years of sedimentation.

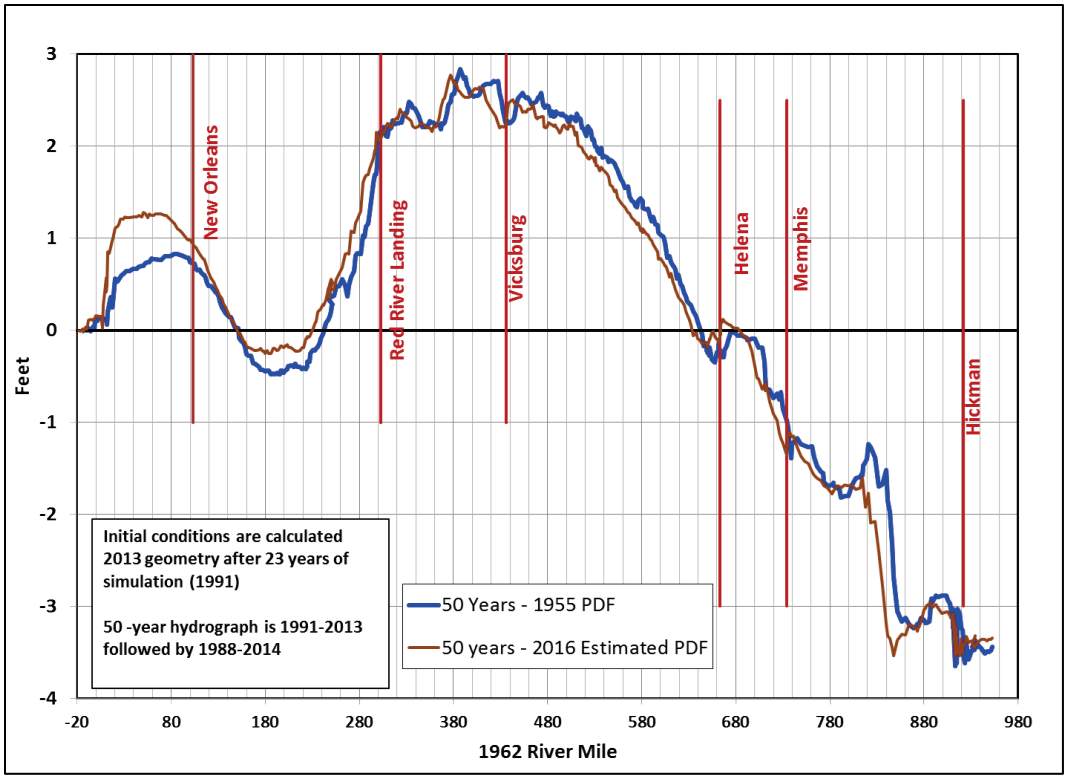

Channel geometry may change significantly during the rise of a major flood hydrograph. The channel change is not so much affected by the increase in bed sediment transport due to the increased discharge but by the difference in transport capacity between adjacent reaches. Thus, at any given time, the bed elevation of some cross sections may rise while others may decline. The numerical model was used to predict the difference in maximum PDF water-surface elevations due to channel changes during the rise of both the 1955 and 2016 estimated PDF hydrographs.

The approach was to first calculate a steady-state water-surface profile using only the peak discharges. This profile was compared to a maximum water-surface profile calculated by simulating the PDF hydrograph in the numerical model.

As shown in Figure 70, channel changes that occur as the flood rises result in maximum water-surface elevation differences of less than 1 ft. The 2016 estimated PDF has less channel change before the flood peak than the 1955 PDF. Less degradation occurs upstream from Old River because a higher percentage of the flood is diverted into floodways and backwaters

with the 2016 estimated PDF hydrograph. Less aggradation occurs downstream from Old River because a lower percentage of the flood is diverted through Old River, Morganza, and Bonnet Carré with the 2016 estimated PDF hydrograph.

Figure 70. Difference in PDF peak water surface elevation due to rising hydrograph.

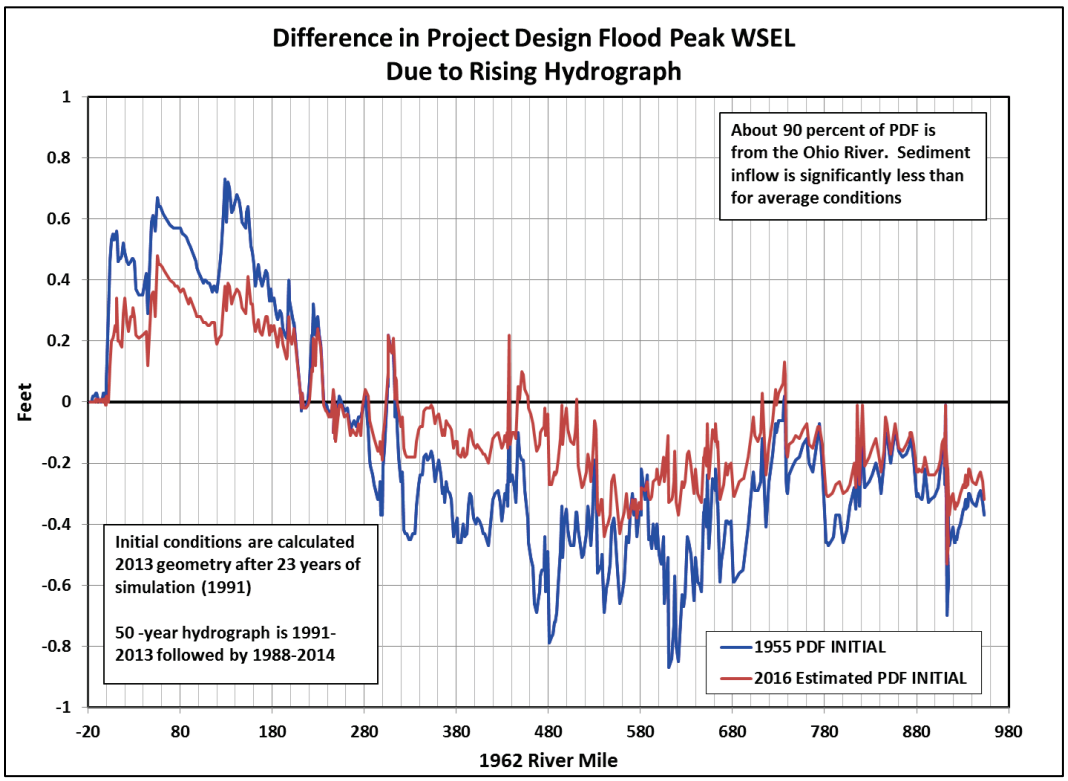

The combined difference in 2016 estimated PDF water-surface elevations accounting for both 50 years of sedimentation, and the rising of the flood hydrograph is shown in Figure 71.

Figure 71. Combined effect of 50 years of sedimentation and the rise of the hydrograph.

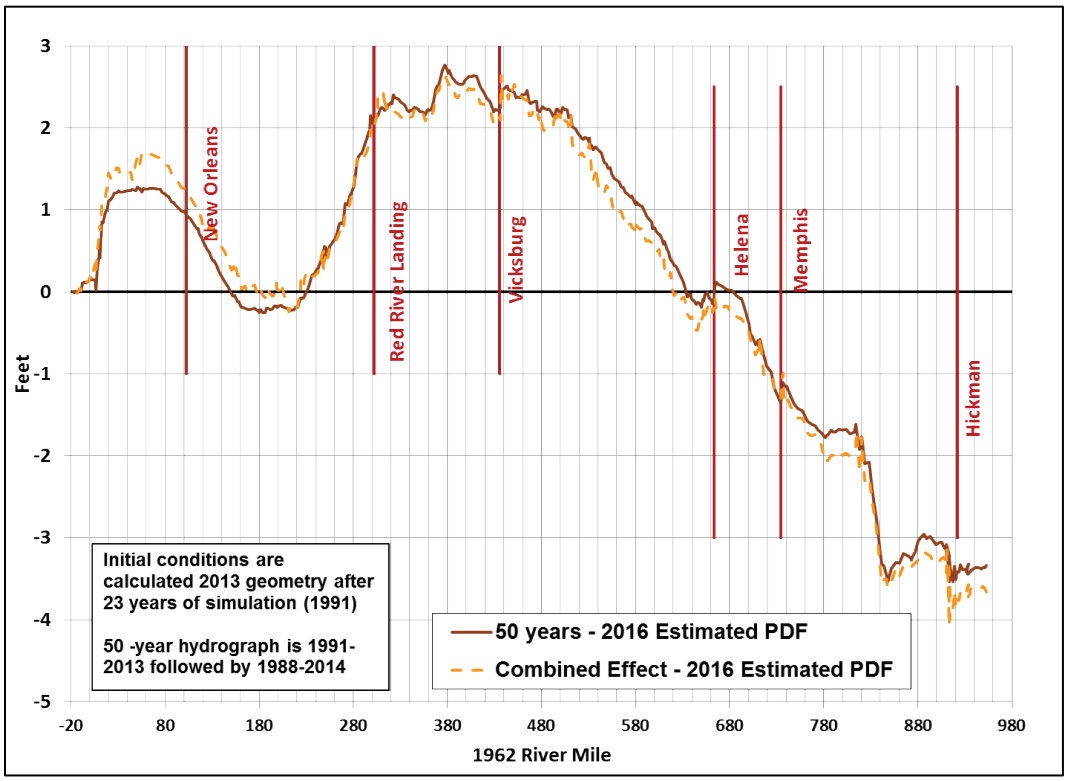

Since the PDF may occur at any time during the 50-year simulation, the differences in Project Flood water-surface elevations at every year during the 50-year simulation were calculated. The maximum difference is plotted in Figure 72. This was accomplished by inserting the 2016 estimated PDF peak discharges into the 50-year hydrograph on March 31 of each year. The time-step was set very small so that there was no bed change during the peak flows. As shown in Figure 72, the maximum differences in water-surface elevations between Head of Passes (RM 0) and RM 240 (upstream from Baton Rouge) occur before the end of the 50-year simulation. Likewise, the maximum water-surface elevations upstream from RM 640 (just downstream from Helena) occur before the end of the 50-year simulation. Upstream from Memphis, the maximum water-surface elevations occur near the very beginning of the simulation period.

Figure 72. Maximum difference in Project Flood peak water-surface elevation due to sediment aggradation/degradation over 50 years.

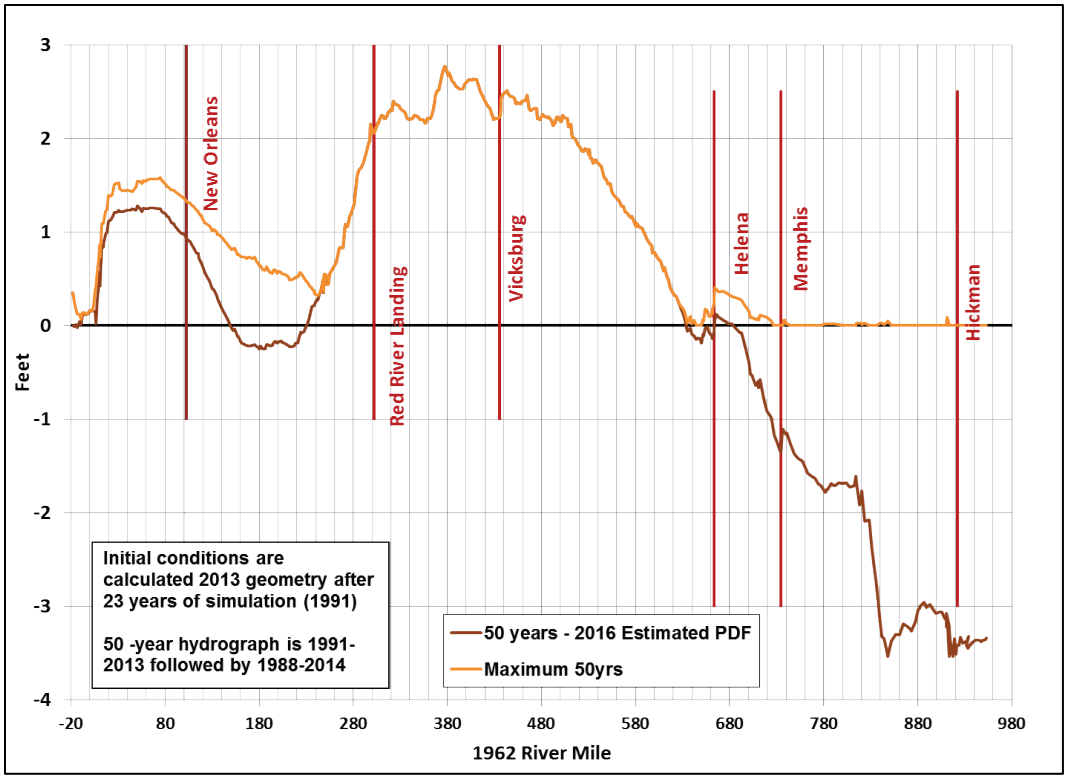

The calculated increase in the 2016 estimated PDF water-surface elevations to account for 50 years of sedimentation is shown in Figure 73 and Table 29. The preferred armoring algorithm used in the calculations is Exner 7. Figure 73 combines the calculated increase in water-surface elevation over the 50 years with the difference in water-surface elevation at the peak of the hydrograph related to sedimentation during the rise of the flood hydrograph using either Exner 5 or Exner 7. Calculated differences were determined every year during the 50-year period to account for the fact that the PDF could occur at any time during the 50-year simulation. Maximum water-surface elevations are less than zero at some stations because degradation occurs during the rise of the PDF hydrograph, and when the hydrograph results are compared with a steady state peak discharge at time zero, the result is negative. Calculated results using Exner 5 are also included. Conservative engineering practice would suggest using the highest calculated results for levee height design.

Figure 73. Maximum increase in 2016 Project Design water-surface elevations due to sedimentation, including the rise of the flood hydrograph, over a 50-year period. Calculated with Exner 7 and Exner 5.

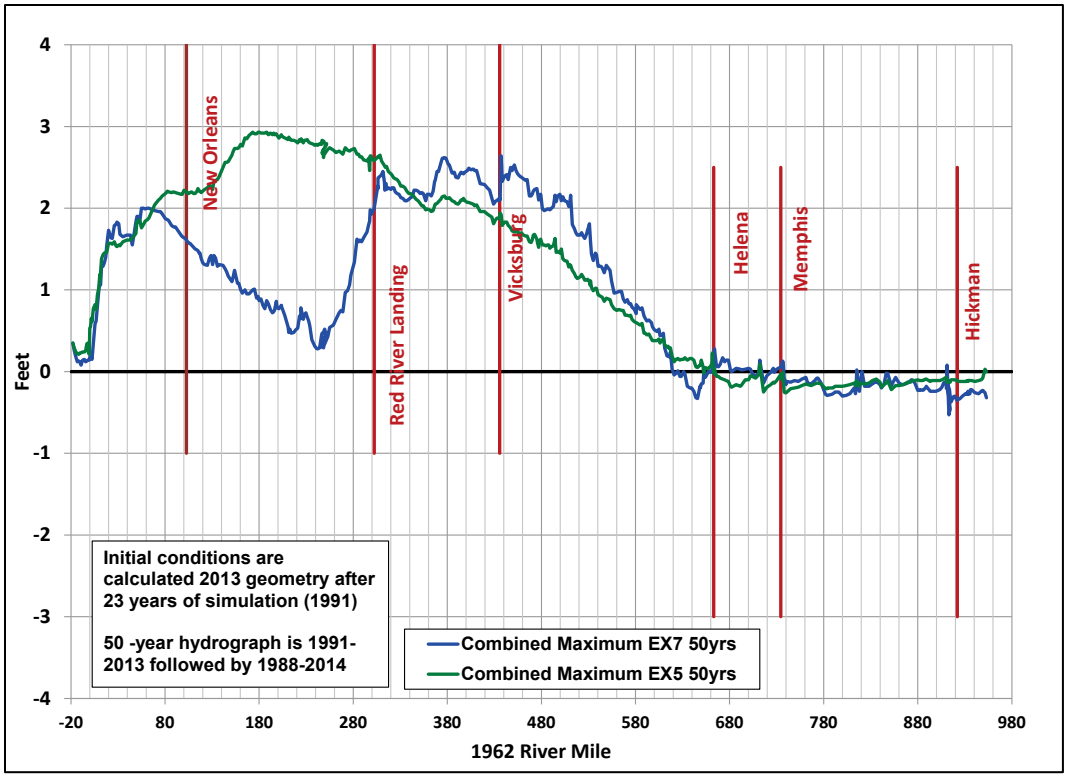

Table 28. Maximum PDF water-surface elevation difference.

River Station	50-Year Max and Hydrograph Combined Difference (feet)	
	EXNER7	EXNER 5
Cairo, IL		
953.03	-0.3	0.0
951.5	-0.3	0.0
949	-0.2	-0.1
947.4	-0.2	-0.1
944.75	-0.3	-0.1
940.79	-0.3	-0.1
937.2	-0.2	-0.1
936	-0.2	-0.1
Wolf Island Main (West) Channel		
935.4	-0.3	-0.1
933.4	-0.3	-0.1
931.53	-0.3	-0.1

River Station	50-Year Max and Hydrograph Combined Difference (feet)	
	EXNER7	EXNER 5
Wolf Island Secondary (East) Channel		
934.4	-0.3	-0.1
933.4	-0.2	-0.1
931.53	-0.3	-0.1
Downstream from Wolf Island		
930.8	-0.3	-0.1
927.5	-0.3	-0.1
925	-0.3	-0.1
923.46	-0.3	-0.1
Hickman, KY		
922	-0.3	-0.1
921.6	-0.4	-0.1
921	-0.3	-0.1
919.41	-0.3	-0.1
917.6	-0.3	-0.1
915.59	-0.4	-0.1
Island 8 Secondary (West) Channel		
914.6	-0.3	-0.1
913.8	-0.2	-0.1
913.21	-0.2	-0.1
911.2	-0.1	-0.1
910.54	-0.1	-0.1
Island 8 Main (East) Channel		
914.6	-0.5	-0.1
913.8	-0.5	-0.1
913.21	-0.5	-0.1
911.2	0.1	-0.1
910.54	-0.2	-0.1
Downstream from Island 8		
910	-0.1	-0.1
908.5	-0.1	-0.1
907.37	-0.1	-0.1

River Station	50-Year Max and Hydrograph Combined Difference (feet)	
	EXNER7	EXNER 5
905.6	-0.2	-0.1
903.45	-0.2	-0.1
899.27	-0.2	-0.1
Downstream from Island 8		
895	-0.2	-0.1
893.13	-0.2	-0.1
889.01	-0.2	-0.1
888.2	-0.2	-0.1
887.2	-0.2	-0.1
886.4	-0.2	-0.1
885.4	-0.2	-0.1
882.6	-0.2	-0.1
881.89	-0.2	-0.1
880	-0.2	-0.1
876.91	-0.1	-0.1
874.2	-0.1	-0.1
873.04	-0.1	-0.1
872.4	-0.1	-0.1
869.08	-0.1	-0.1
864.7	-0.2	-0.2
860.56	-0.2	-0.2
856.38	-0.1	-0.2
851.97	-0.2	-0.2
847.96	0.0	-0.1
846.4	0.0	-0.1
844.2	-0.2	-0.2
841.5	-0.2	-0.2
839.82	-0.2	-0.1
835.86	-0.1	-0.1
831.72	-0.2	-0.1
828.24	-0.2	-0.1
823.46	-0.2	-0.2

River Station	50-Year Max and Hydrograph Combined Difference (feet)	
	EXNER7	EXNER 5
820.8	0.0	-0.1
819.39	-0.1	-0.1
818	-0.2	-0.2
815.09	0.0	-0.1
814.4	-0.2	-0.1
813.8	-0.3	-0.2
Downstream from Island 8		
812.44	-0.2	-0.1
807.79	-0.3	-0.2
803.84	-0.3	-0.2
800.04	-0.3	-0.2
796.01	-0.3	-0.2
792.1	-0.2	-0.2
790	-0.3	-0.2
788.13	-0.3	-0.2
784	-0.3	-0.2
783.5	-0.3	-0.2
781.97	-0.3	-0.2
777.3	-0.1	-0.2
774	-0.1	-0.1
772.76	-0.1	-0.1
770.6	-0.1	-0.2
766.9	-0.1	-0.2
763.08	-0.1	-0.2
761.01	-0.1	-0.1
756.97	-0.1	-0.2
752.98	-0.1	-0.2
748.94	-0.1	-0.2
744.98	-0.1	-0.2
741	-0.1	-0.3
740	-0.2	-0.3
738.95	-0.1	-0.3

River Station	50-Year Max and Hydrograph Combined Difference (feet)	
	EXNER7	EXNER 5
738	-0.1	-0.3
737	0.1	-0.1
736.48	0.1	0.0
Memphis, TN		
735.9	0.1	-0.1
734.56	0.1	0.0
729.98	0.0	-0.1
727.6	0.0	-0.1
726.5	0.0	-0.1
Memphis, TN		
723.85	0.0	-0.2
719.67	-0.1	-0.2
716.06	-0.1	-0.3
712.12	0.1	0.1
711	0.0	0.0
710.6	0.0	0.0
707.79	-0.1	-0.1
704.08	0.0	-0.1
702.3	0.0	-0.1
700.28	0.0	-0.1
696.8	0.0	-0.1
692.43	0.0	-0.2
691.4	0.0	-0.2
687.09	0.0	-0.2
682.06	0.0	-0.2
681	0.0	-0.2
678.72	0.1	-0.1
676.2	0.1	-0.1
674.73	0.1	-0.1
672.61	0.2	-0.1
670	0.1	-0.1
668.22	0.1	-0.1

River Station	50-Year Max and Hydrograph Combined Difference (feet)	
	EXNER7	EXNER 5
667	0.1	-0.1
666.01	0.1	-0.1
663.93	0.3	0.0
663.6	0.2	0.0
Helena, AR		
663.11	0.1	0.0
662	0.1	0.2
661.68	0.1	0.2
661.25	0.0	0.1
659.95	0.0	0.1
658.06	0.0	0.0
656.21	0.0	0.0
Helena, AR		
654.23	-0.1	0.1
652.5	0.0	0.0
651.91	-0.1	0.1
649.89	-0.2	0.1
649	-0.2	0.1
648.47	-0.2	0.1
645.95	-0.3	0.1
644.23	-0.3	0.1
641.96	-0.2	0.1
639.73	-0.2	0.2
637.91	-0.2	0.2
635.11	-0.2	0.1
632.6	0.0	0.2
631.05	0.0	0.1
628.66	-0.1	0.2
627.1	-0.1	0.1
624.95	0.0	0.2
623.12	0.0	0.1
621.03	0.0	0.1

River Station	50-Year Max and Hydrograph Combined Difference (feet)	
	EXNER7	EXNER 5
618.93	0.0	0.2
617.09	0.2	0.3
616.07	0.2	0.3
614.58	0.2	0.3
613.6	0.2	0.3
610.94	0.3	0.3
609.68	0.5	0.4
607.17	0.4	0.4
606	0.4	0.3
604.92	0.5	0.4
602.95	0.5	0.4
600.1	0.5	0.4
598	0.6	0.4
597	0.6	0.4
594.21	0.6	0.5
Helena, AR		
591.99	0.6	0.4
590.4	0.6	0.5
589.07	0.7	0.5
587	0.8	0.6
584.86	0.8	0.6
580.8	0.8	0.6
580.8	0.7	0.6
578.8	0.8	0.6
576.21	0.8	0.6
574.8	0.8	0.7
573.15	0.8	0.7
571.4	0.9	0.7
569.03	0.8	0.7
567	0.9	0.8
565.19	1.0	0.8
562.4	1.0	0.8

River Station	50-Year Max and Hydrograph Combined Difference (feet)	
	EXNER7	EXNER 5
560	1.0	0.8
557.21	1.0	0.8
Arkansas City, AR		
554.59	1.1	0.8
553	1.2	0.9
551	1.3	0.9
549	1.3	0.9
546.83	1.2	0.9
544.72	1.3	0.9
543.21	1.3	0.9
540.38	1.3	0.9
538.56	1.4	1.0
537.25	1.4	1.0
535.17	1.4	1.0
533.13	1.4	1.0
532.2	1.6	1.1
531.7	1.7	1.1
531	1.8	1.1
Arkansas City, AR		
530.2	1.8	1.1
529.2	1.7	1.1
527.8	1.7	1.1
526	1.6	1.1
524.4	1.7	1.2
522.76	1.7	1.2
521.19	1.7	1.2
518.21	1.7	1.1
516.6	1.7	1.2
515.03	1.8	1.2
512.8	1.8	1.2
511.01	2.2	1.3
510	2.0	1.3

River Station	50-Year Max and Hydrograph Combined Difference (feet)	
	EXNER7	EXNER 5
509.2	2.0	1.3
507.29	2.1	1.3
504.66	2.1	1.4
502.8	2.1	1.4
501.2	2.1	1.5
499.59	2.2	1.5
497.2	2.2	1.5
495.59	2.1	1.5
494.59	2.2	1.6
492.69	2.0	1.5
490.8	2.0	1.5
489	2.0	1.5
487.8	2.0	1.6
486.4	2.0	1.5
484.8	2.0	1.5
483	2.0	1.6
481.06	2.0	1.6
479.21	2.2	1.6
478	2.1	1.6
477.2	2.1	1.5
476	2.2	1.6
Arkansas City, AR		
475.2	2.2	1.6
472.8	2.2	1.7
471.4	2.2	1.7
470.13	2.2	1.6
468.97	2.2	1.6
467.2	2.1	1.6
464.79	2.4	1.7
463.2	2.3	1.7
460.8	2.4	1.7
458.79	2.4	1.7

River Station	50-Year Max and Hydrograph Combined Difference (feet)	
	EXNER7	EXNER 5
457.21	2.4	1.6
454.77	2.4	1.7
453	2.5	1.7
451.2	2.5	1.7
448.8	2.5	1.7
447.2	2.5	1.8
444.79	2.3	1.8
443.2	2.4	1.8
440.8	2.4	1.8
438.39	2.3	1.8
437.28	2.6	1.9
436	2.1	1.9
Vicksburg, MS		
435.37	2.1	1.9
434.6	2.1	1.9
433	2.1	1.9
432	2.1	1.9
431	2.1	1.8
429.2	2.1	1.8
427.4	2.1	1.9
425.07	2.2	1.9
422.41	2.3	1.9
419.4	2.3	2.0
415	2.3	2.0
Vicksburg, MS		
411.2	2.5	2.0
409.03	2.5	2.0
407.62	2.5	2.1
405.18	2.5	2.1
402.8	2.5	2.1
401.21	2.5	2.1
398.8	2.4	2.1

River Station	50-Year Max and Hydrograph Combined Difference (feet)	
	EXNER7	EXNER 5
397.19	2.4	2.1
396.4	2.4	2.1
394.61	2.4	2.1
393	2.4	2.1
391.4	2.4	2.1
389.01	2.4	2.1
387.41	2.4	2.1
385.01	2.4	2.1
382.12	2.5	2.1
381	2.5	2.1
378.59	2.6	2.1
377	2.6	2.2
374.59	2.6	2.1
373.01	2.6	2.1
370.6	2.5	2.1
369	2.5	2.1
367.2	2.3	2.1
366.59	2.3	2.0
365	2.2	2.0
Natchez, MS		
363.01	2.1	2.0
361	2.2	2.0
358.63	2.2	2.0
357	2.1	2.0
354.58	2.2	2.0
352.98	2.2	2.0
351.12	2.2	2.1
Natchez, MS		
349	2.2	2.1
346.81	2.2	2.1
344.59	2.2	2.1
342.99	2.1	2.2

River Station	50-Year Max and Hydrograph Combined Difference (feet)	
	EXNER7	EXNER 5
341	2.1	2.2
339.02	2.1	2.2
337	2.1	2.2
335	2.1	2.3
332.8	2.1	2.3
330.61	2.1	2.3
328.6	2.2	2.3
326.6	2.2	2.4
324.6	2.2	2.4
323	2.3	2.4
321	2.3	2.4
320.1	2.2	2.4
317.3	2.3	2.4
315.4	2.2	2.5
315	2.3	2.5
314.2	2.3	2.5
313.7	2.2	2.5
313.2	2.3	2.5
311.6	2.5	2.6
310.1	2.4	2.6
308.4	2.4	2.7
306.3	2.4	2.6
306.3	2.2	2.6
306.1	2.3	2.6
Red River Landing, LA		
302.1	2.0	2.6
300.3	2.0	2.6
299.5	1.9	2.6
298.9	2.0	2.6
298.1	2.0	2.6
Red River Landing, LA		
297.45	1.8	2.5

River Station	50-Year Max and Hydrograph Combined Difference (feet)	
	EXNER7	EXNER 5
296.4	1.8	2.6
294.6	1.7	2.6
291.1	1.6	2.6
289	1.6	2.6
287	1.6	2.6
285.7	1.6	2.7
284	1.6	2.7
281.3	1.3	2.7
277.5	1.2	2.7
276.1	1.1	2.7
274	1.0	2.7
271.5	1.0	2.7
269	0.7	2.7
267	0.8	2.7
265.1	0.7	2.7
261.6	0.6	2.7
258.9	0.6	2.7
255	0.5	2.7
253	0.4	2.7
Profit Island Chute (East) Channel		
248.56	0.3	2.7
248.38	0.3	2.6
247.85	0.3	2.7
247.28	0.4	2.7
247	0.4	2.7
246.8	0.3	2.7
Profit Island Main (West) Channel		
251.8	0.5	2.8
250.6	0.5	2.8
249.6	0.5	2.8
248.6	0.5	2.8
248	0.5	2.8

River Station	50-Year Max and Hydrograph Combined Difference (feet)	
	EXNER7	EXNER 5
246.9	0.5	2.8
Downstream from Profit Island		
246.3	0.4	2.8
244.2	0.3	2.8
242.3	0.3	2.8
241.4	0.3	2.8
239.1	0.3	2.8
238	0.3	2.8
236	0.4	2.8
233.9	0.6	2.8
232.7	0.6	2.8
231	0.7	2.8
229.7	0.7	2.8
Baton Rouge, LA		
228.1	0.7	2.8
226.9	0.6	2.8
224.7	0.8	2.9
224.4	0.8	2.8
224.1	0.6	2.8
223	0.7	2.8
220.9	0.5	2.8
218.9	0.5	2.8
216.8	0.5	2.8
214	0.5	2.8
212.6	0.5	2.8
212.2	0.5	2.8
212	0.5	2.8
211.6	0.5	2.9
210.8	0.5	2.8
207.15	0.7	2.9
204.1	0.8	2.9
203.6	0.8	2.9

River Station	50-Year Max and Hydrograph Combined Difference (feet)	
	EXNER7	EXNER 5
201	0.8	2.9
199	0.8	2.9
198.2	0.9	2.9
196.4	0.8	2.9
Baton Rouge, LA		
195.3	0.7	2.9
194.2	0.7	2.9
192	0.8	2.9
189.75	0.8	2.9
188	0.9	2.9
186.1	0.8	2.9
184	0.8	2.9
181.9	0.9	2.9
179.9	0.9	2.9
179	0.9	2.9
177.3	0.9	2.9
175	1.0	2.9
173.2	1.0	2.9
169.2	0.9	2.9
166.9	0.9	2.9
165	1.0	2.9
162.1	1.0	2.8
160.3	1.0	2.8
158.3	1.1	2.7
157	1.1	2.7
153.8	1.2	2.7
152.3	1.2	2.7
151	1.1	2.7
147.1	1.2	2.6
145.6	1.2	2.6
143.7	1.3	2.6
141.6	1.3	2.5

River Station	50-Year Max and Hydrograph Combined Difference (feet)	
	EXNER7	EXNER 5
137.6	1.3	2.4
135.7	1.3	2.4
133.8	1.4	2.3
131.9	1.4	2.3
130.6	1.3	2.2
129	1.4	2.3
127.1	1.4	2.3
Baton Rouge, LA		
125	1.3	2.2
122.05	1.3	2.2
120.1	1.3	2.2
118.4	1.4	2.2
117.2	1.5	2.2
116.3	1.5	2.2
115	1.5	2.2
114	1.5	2.2
111.9	1.5	2.2
110.4	1.5	2.2
108.1	1.6	2.2
106.4	1.6	2.2
105	1.6	2.2
New Orleans, LA		
102.2	1.6	2.2
100.2	1.6	2.2
98.4	1.7	2.2
97	1.7	2.2
91.05	1.8	2.2
89	1.8	2.2
86.9	1.8	2.2
83.8	1.9	2.2
82.5	1.9	2.2
80.3	1.9	2.2

River Station	50-Year Max and Hydrograph Combined Difference (feet)	
	EXNER7	EXNER 5
77	1.9	2.2
75	2.0	2.1
73	2.0	2.1
69	2.0	2.0
62.9	2.0	1.9
61.3	2.0	1.9
58.8	2.0	1.8
57	2.0	1.8
55	2.0	1.8
53	1.8	1.9
New Orleans, LA		
51.6	1.9	1.8
50.2	1.9	1.8
49	1.8	1.7
45.2	1.6	1.6
43.2	1.7	1.6
39.3	1.7	1.6
35.1	1.7	1.6
32	1.7	1.5
30.8	1.8	1.6
28.8	1.8	1.5
27.8	1.8	1.5
26.1	1.8	1.6
24	1.6	1.6
22.4	1.6	1.6
20	1.7	1.6
18	1.5	1.5
17	1.4	1.5
15.4	1.3	1.5
14.1	1.3	1.4
12.5	1.3	1.4
11.5	1.1	1.2

River Station	50-Year Max and Hydrograph Combined Difference (feet)	
	EXNER7	EXNER 5
11.05	1.1	1.1
Venice, LA		
10.7	1.1	1.2
9.5	1.0	1.0
8.1	0.8	0.9
6.7	0.6	0.8
5.5	0.6	0.8
3.83	0.3	0.8
2.46	0.2	0.6
1.6	0.2	0.7
0.72	0.2	0.6
Southwest Pass		
-0.01	0.2	0.5
-0.5	0.1	0.2
-0.9	0.1	0.2
-1.9	0.1	0.4
-3.1	0.1	0.3
-4.5	0.1	0.3
-5.8	0.2	0.2
-7.7	0.1	0.2
-9.3	0.1	0.2
-10.7	0.1	0.2
-11.9	0.1	0.2
-13.3	0.1	0.2
-14.7	0.2	0.2
-16.5	0.3	0.3
-18	0.4	0.4

7 Conclusions

Sedimentation in the Mississippi River over the next 50 years is predicted to cause 2016 calculated peak water-surface elevations to increase up to 2.5 feet (ft) between Head of Passes (River Mile [RM] 0.0) and Helena (RM 663). During the 50-year period, peak water-surface elevations between Helena and Cairo (RM953) are predicted to decrease. The Project Flood could occur at any time during the 50-year period, so levee design heights need to account for design water-surface elevations should the flood occur today as well as 50 years in the future.

Results from the HEC-6T sedimentation assessment should be combined with results of the unsteady-flow HEC-RAS assessment to determine maximum PDF water-surface elevations along the Mississippi River between Cairo and Venice. The HEC-6T assessment predicted the maximum increase in water-surface elevation due to 50-years of sedimentation. The HEC-RAS assessment predicted the maximum increase in water-surface elevation due to other hydraulic factors.

Sedimentation effects due to the rise of the estimated 2016 Project Flood hydrograph are predicted to result in an increase in peak water-surface elevations of less than 0.5 ft between Head of Passes and RM 280 (upstream from Baton Rouge) and a decrease in peak water-surface elevations of less than 0.5 ft between RM 280 and Cairo.

There is a degree of uncertainty related to choice of the Exner equation in the numerical simulation, so a sensitivity analysis was performed. Based on experience gained from previous HEC-6T studies, results calculated using the Exner 7 algorithm are preferred. However, conservative design principles suggest using the higher increases in design water-surface elevation using Exner 5. Estimated 2016 Project Flood peak water-surface elevations are projected to increase up to 3.0 ft between Head of Passes (RM 0.0) and Helena (RM 663) with the Exner 5 algorithm.

The most significant driving variable causing the degradation trend upstream from Helena and the aggradation trend downstream is the long-term geomorphic response to the USACE cutoff program that shortened the river by approximately 152 miles in the 1930s and 1940s. Reduction in sediment inflow due to land use changes, reservoirs, locks and dams, and bank protection has affected the deposition patterns but not the long-term

trend. Likewise, constriction of the river by dike fields has affected sedimentation but not the long-term trend. The long-term trend does not appear to be significantly accelerated by individual flood years. Rather, the trend appears to be steady and continuous. The long-term trend continues past the 50-year assessment period for at least an additional 50 years.

These conclusions apply to engineering time scales. Over longer time scales, sedimentation processes could change due to changes in boundary variables. For example, sediment inflow from the Middle Mississippi River could change, or the composition of the bed sediment reservoir could change as the bed continues to degrade. The coarsest bed materials being supplied to the Lower Mississippi River are not transported all the way to the Gulf of Mexico. These coarse materials could eventually form an armor layer. In addition, if the finer sands are eventually exhausted from the bed sediment reservoir to the point where the volume of coarse material deposition exceeds fine material extraction, then the river response will be an increase in slope (and upstream stages). This change most likely would not be uniform in space or time.

Development of the HEC-6T numerical model of the Lower Mississippi River between Cairo and Pilots Station should not be considered complete. As additional data become available and as the river continues to adjust its geomorphic form, the model should be updated. For example, measurements taken during the January 2016 flood near Morganza, LA, indicated that the channel flow was less than two-thirds of the total flow of 1,300,000 cubic feet per second. Treatment similar to that conducted for Devils Swamp in this assessment should be considered in future studies for wide floodplains inside the flood control levees. Additional uncertainty exists related to the erosion rates of consolidated river beds that were treated as *hard bottoms* in this assessment. Such reaches exist at Hickman and in the Mississippi River below New Orleans. A field sampling program is recommended to collect data that can be used to determine critical shear and erosion rates for these bed materials. Gathering new sediment and bathymetric data will assist in improving the model sediment inflow predictions and model cross sections and will be beneficial for future studies. Using adaptive modeling techniques will enhance future model investigations.

Future studies related to specific diversions on the Mississippi River may require a more detailed treatment of the flow through the diversion or

diversions of interest. It is also critical to continue flow measurement programs to better define the outflow from distributaries and possible changes in outflow magnitudes with time.

The lack of sediment boundary condition data for the numerical model required that size-class percentages be estimated by calculation and/or judgment. A continuing sediment data collection program is essential to verify and enhance future sediment transport predictions.

Assessment results highlight the significant discrepancies in the measured sediment data for the Mississippi River system. The physical laws that govern the numerical model require that sediment continuity be maintained throughout the system. However, it is apparent that sediment continuity is not maintained in analyses of the measured data at various gages in the system. The most probable explanation for the discrepancies in the measured data is related to the differences in the sediment collection and laboratory methodologies and in the analytical methods used to calculate sediment concentrations from the sampled data. It is recommended that a comprehensive investigation of the sediment data gathering methods be undertaken and that consistent methodologies be incorporated for sediment data collection in the Mississippi Valley Division.

References

Abraham, David, Roger A. Kuhnle, and A. Jacob Odgaard. 2011. "Validation of Bed-Load Transport Measurements with Time–Sequenced Bathymetric Data." *Journal of Hydraulic Engineering* 137(7): 723–728.

Ariathurai, R., and R. B. Krone. 1976. "Finite Element Model for Cohesive Sediment Transport." *Journal of the Hydraulics Division, ASCE* 2(3): 323–338.

Biedenharn, D. S., M. A. Allison, C. D. Little, C. R. Thorne, and C. C. Watson. 2017. *Large-scale Geomorphic Change in the Mississippi River from St Louis, MO to Donaldsonville, LA, as Revealed by Specific Gage Records, Mississippi River Geomorphology and Potamology Program*. MRG&P Report No. 10. Vicksburg, MS: U.S. Army Engineer Research and Development Center. http://dx.doi.org/10.21079/11681/22744.

Catalyst-Old River Hydroelectric. 1999. *Lower Mississippi River Sediment Study, Volume 4 – HEC-6W Mississippi River Numerical Sedimentation Model Investigation, Vicksburg to Donaldsonville*. Vicksburg, MS: U.S. Army Corps of Engineers, Waterways Experiment Station. http://acwc.sdp.sirsi.net/client/en_US/default/search/detailnonmodal/ent:$002f$002fSD_ILS$002f0$002fSD_ILS:21073/one?qu=catalyst+old+river+hydroelectric+lower+mississippi+sediment.

Copeland, Ronald R. 1991. *Dredging Alternatives Study Cubits Gap, Lower Mississippi River, Report 1, TABS-1 Numerical Model Investigation*. TR HL-91-01. Vicksburg, MS: U.S. Army Corps of Engineers, Waterways Experiment Station.

Copeland, R. R., and W. A. Thomas. 1992. *Lower Mississippi River, Tarbert Landing to East Jetty, Sedimentation Study*. TR HL-92-6. Vicksburg, MS: U.S. Army Corps of Engineers, Waterways Experiment Station. http://www.dtic.mil/get-tr-doc/pdf?AD=ADA254685.

Copeland, Ronald R. 1993. *Numerical Modeling of Hydraulic Sorting and Armoring in Alluvial Rivers*. PhD thesis, University of Iowa, Iowa City, IA.

Copeland Ronald, R. 2002. *Red River below Denison Dam Texas, Oklahoma, Arkansas and Louisiana – Numerical Sedimentation Model*. ERDC/CHL TR-02-5. Vicksburg, MS: U.S. Army Engineer Research and Development Center.

Copeland, Ronald R. 2013. *Missouri River Sediment Modeling – Impact of Dredging Inputs, HEC-6T*. Study conducted as part of the Missouri river Recovery Program by Vicksburg District (CEMVK-EC-H) for the Omaha District (CENWO-ED-H), April 2013.

Ferguson, R. I. 1986. "River Loads Underestimated by Rating Curves." *Water Resources Research* 22(1): 74–76.

Hall, Brad, Andrey Shvidchenko, Rene Leclerc, Lea Adams, Ron Copeland, and Bryce Cruey. 2010. *Comprehensive Geomorphic and Sedimentation Analyses of Lower Sacramento River for Flood Management, Erosion Mitigation and Habitat Enhancement Design*, 2nd Joint Federal Interagency Conference, Las Vegas, NV, June 27–July 1, 2010, prepared for USACE, Sacramento District. https://acwi.gov/sos/pubs/2ndJFIC/Contents/7D_Hall%20_2-26_10.pdf.

Heath, Ronald E., Gary L. Brown, Charles D. Little; Thad C. Pratt, Jay J. Ratcliff, David D. Abraham, David W. Perkey, Naveen B. Ganesh, Keith Martin, and David P. May. 2015. *Old River Control Complex Sedimentation Investigation*. MRG&P Report No. 6. Vicksburg, MS: U.S. Army Engineer Research and Development Center.

Heimann, David C., Lori A. Sprague, and Dale W. Blevins. 2011. *Trends in Suspended-Sediment Loads and concentrations in the Mississippi River Basin 1950–2009*. National Water-Quality Assessment Program, Scientific Investigations Report 2011-5200. Reston, VA: U.S. Geological Survey.

Krone, R. B. 1962. *Flume Studies of the Transport of Sediment in Estuarial Shoaling Processes*. Berkeley, CA: Hydraulic Engineering Laboratory, University of California.

Little, Charles D., and David S. Biedenharn. 2014. *Mississippi River Hydrodynamic and Delta Management Study – Geomorphic Assessment*. ERDC/CHL TR-14-5. U.S. Vicksburg, MS: Army Engineer Research and Development Center.

Meyer-Peter, E. and R. Muller. 1948. "Formulas for Bed-Load Transport." *Second Meeting of the International Association for Hydraulics Research, Stockholm, Sweden*. Appendix 2, 39–64.

Parthenaides, E. 1965. "Erosion and Deposition of Cohesive Soils." *Journal of the Hydraulics Division, ASCE* 91(1): 105–139. http://cedb.asce.org/CEDBsearch/record.jsp?dockey=0013640.

Rouse, Hunter. 1937. "Modern Conceptions of the Mechanics of Fluids Turbulence." *Transactions, ASCE* 102(Paper No. 1965): 463–543.

Sharp, Jeremy A., Charles D. Little, Gary L. Brown, Thad C. Pratt, Ronnie E. Heath, Lisa C. Hubbard, C. Freddie Pinkard, Martin S. Keith; Nathan D. Clifton, David W. Perky, and Naveen B. Ganesh. 2013. *West Bay Sediment Diversion Effects*. ERDC/CHL TR-13-15. Vicksburg, MS: U.S. Army Engineer Research and Development Center.

Thomas, W. A., and H. Chang. 2008. *Computational Modeling of Sedimentation Processes, Sedimentation Engineering, ASCE Manuals and Reports on Engineering Practice No. 110,* Chapter 14. Edited by Marcelo H. Garcia. Reston, VA: American Society of Civil Engineers.

Thomas, W. A., R. E. Heath, J. P. Stewart, and D. G. Clark. 1988. *The Atchafalaya River Delta, Report 5: The Atchafalaya River Delta Quasi-Two-Dimensional Model of Delta Growth and Impacts on River Stages*. Technical Report HL-82-15, Report 5. Vicksburg, MS: U.S. Army Corps of Engineers, Waterways Experiment Station.

Thomas, W. A. 2012. *Allocation of Water and Sediment Resources – Myrtle Grove Diversion for Land Building*. Prepared for Coastal Protection and Restoration Authority, Office of Coastal Protection and Restoration, State of Louisiana, by Mobile Boundary Hydraulics PLLC, Clinton, MS.

Thomas, W. A. 2016. *Sedimentation in Stream Networks (HEC-6T), User Manual*. Clinton, MS: Mobile Boundary Hydraulics.

Toffaleti, Fred B. 1968. A procedure for computation of the total river sand discharge and detailed distribution, bed to surface, Technical Report No. 5, Committee on Channel Stabilization, U.S. Army Corps of Engineers, Vicksburg, MS. <http://libweb.wes.army.mil/uhtbin/hyperion/TR-5-1968.pdf>

U.S. Army Corps of Engineers (USACE). 2013. *Incorporating Sea Level Change in Civil Works Programs*. ER 1100-2-8162. Washington, DC: U.S. Army Corps of Engineers.

USACE. 2009. *Performance Evaluation of the New Orleans and Southeast Louisiana Hurricane Protection System*. Final Report of the Interagency Performance Evaluation Task Force (IPET). https://biotech.law.lsu.edu/katrina/ipet/Volume%20I%20FINAL%2023Jun09%20mh.pdf.

USACE, HEC. 1992. *Guidelines for the Calibration and Application of Computer Program HEC-6, Training Document No. 13*. Davis, CA: Hydrologic Engineering Center.

USACE, MVN. 1980. *Mississippi River and Tributaries, Old River Control, LA, Auxiliary Structure*. Design Memorandum No. 17, Hydraulic Design, New Orleans, LA, November. https://erdc-library.erdc.dren.mil/xmlui/handle/11681/3188.

USACE, SPN. 2014. *San Lorenzo River Project Performance Evaluation*. FINAL. San Francisco, CA: USACE, San Francisco District. www.cityofsantacruz.com/home/showdocument?id=40594.

REPORT DOCUMENTATION PAGE

Form Approved
OMB No. 0704-0188

1. REPORT DATE	2. REPORT TYPE	3. DATES COVERED *(From - To)*
December 2018	Report 4 of a series	

4. TITLE AND SUBTITLE

Mississippi River and Tributaries Flowline Assessment: Mississippi River Sedimentation Report

5a. CONTRACT NUMBER

5b. GRANT NUMBER

5c. PROGRAM ELEMENT NUMBER

6. AUTHOR(S)

Ronald R. Copeland

5d. PROJECT NUMBER

449963

5e. TASK NUMBER

5f. WORK UNIT NUMBER

7. PERFORMING ORGANIZATION NAME(S) AND ADDRESS(ES)

Mississippi Valley Division
U.S. Army Corps of Engineers
1400 Walnut Street
Vicksburg, MS 39180

8. PERFORMING ORGANIZATION REPORT NUMBER

MRG&P Report No. 24; Volume 4

9. SPONSORING/MONITORING AGENCY NAME(S) AND ADDRESS(ES)

U.S. Army Corps of Engineers, Mississippi Valley Division
1400 Walnut Street
Vicksburg, Mississippi 39180

10. SPONSOR/MONITOR'S ACRONYM(S)

USACE MVD

11. SPONSOR/MONITOR'S REPORT NUMBER(S)

12. DISTRIBUTION/AVAILABILITY STATEMENT

Approved for public release; distribution is unlimited.

13. SUPPLEMENTARY NOTES

14. ABSTRACT

A numerical sedimentation model assessment was conducted to determine the effects of long-term sedimentation processes on the Project Design Flood (PDF) flowline for the Mississippi River. The assessment reach was between Pilots Station, which is located at the end of Southwest Pass in Louisiana, and Cairo, IL, which is located at the confluence of the Ohio River. In addition, the assessment determined the effects of scour and deposition, which occur during the passage of the PDF hydrograph, on maximum water-surface elevations. The HEC-6T numerical sedimentation model was used in this assessment.The assessment identified a long-term degradation trend between Helena, AR, and Cairo, IL, and a long-term aggradation trend between Helena, AR, and Red River Landing, Louisiana. The numerical model was used to evaluate the effects of several driving variables on the long-term sedimentation trends. These variables included the effects of floods, sediment inflow, dikes, historical cutoffs, sea-level rise, and subsidence.The assessment results provide 50-year increases in PDF water-surface elevations attributed to sedimentation in the Mississippi River. These results are to be added to water-surface elevations calculated using an unsteady flow HEC-RAS model that uses current surveys to define the HEC-RAS geometry.

15. SUBJECT TERMS

Flood control, Hydraulic measurements, Mississippi River, Numerical analysis, Sedimentation and deposition, Sediment transport

16. SECURITY CLASSIFICATION OF:			17. LIMITATION OF ABSTRACT	18. NUMBER OF PAGES	19a. NAME OF RESPONSIBLE PERSON
a. REPORT	b. ABSTRACT	c. THIS PAGE			Ronald R. Copeland
Unclassified	Unclassified	Unclassified	SAR	168	19b. TELEPHONE NUMBER *(Include area code)* 601-613-2133